# ENERGY-EFFICIENT CHEMICAL RECYCLING OF POLYETHYLENE TEREPHTHALATE (PET)

By

Zahra Aayanifard

# A DISSERTATION

Submitted to
Michigan State University
in partial fulfillment of the requirements
for the degree of

Chemistry—Doctor of Philosophy Packaging—Dual Major

2025

#### **ABSTRACT**

Energy-efficient recycling of post-consumer polyethylene terephthalate (PET) is a persisting challenge in the field of plastic circular economy. Today, the major method for PET recycling is mechanical recycling, in which the quality of the recycled PET decreases with each cycle. To address this, chemical recycling methods have been developed where PET is depolymerized to its parent monomers that can be repolymerized to yield virgin PET.

This Ph.D. thesis is primarily focused on an energy-efficient chemical recycling method to convert discarded PET into its parent monomers for remanufacturing virgin PET. For this purpose, the impact of different catalysts, diols, and melt-pretreatment on depolymerization rates of PET has been investigated. Initially, pretreatment was effective in eliminating the crystalline regions that hinder the depolymerization process. Furthermore, the addition of catalyst and diol during the melt-pretreatment process could reduce the chain length of the polymer while active sites were created to accelerate the rate of depolymerization within the chunk of polymer. PET samples were subjected to methanolysis at temperatures ranging from 140 °C to 200 °C, and results revealed that the time for full depolymerization for pretreated and control (without pretreatment) samples were significantly different. For the optimized meltpretreatment process and reaction condition, in the case of methanolysis, at 200°C, the time of full depolymerization shortened from 166 min to 7 min yielding >99% dimethyl terephthalate (DMT), while a minimum of 8-fold decrease in the energy demand for the depolymerization of melt-pretreated PET in comparison to the untreated PET was achieved. In the case of PET glycolysis, the optimal pretreatment could reduce the depolymerization time from 181 min to 9 min (under the same optimal reaction conditions) at 180 °C and yielded ~85% monomer. The scope of the research was further expanded and two organic catalysts, were employed as

alternatives for zinc-based catalysts. The addition of 0.5 mol% of catalyst and diol during melt-pretreatment confirmed the striking effect of this extrusion-quench pretreatment on the organocatalytic depolymerization at 190 °C enabling full conversion of PET within 30 to 32 minutes in the presence of either organic catalyst, while conserving at least 38.5% of the required energy. With the growing production and consumption of PET, this project can help to convert billion tons/year of waste PET bottles into valuable materials and save resources.

In a separate study, a technoeconomic analysis (TEA) was performed for a novel ionic polybutylene adipate-co-terephthalate (CPBAT) as a paper coating material with excellent water-in-oil resistance. The TEA determined the total capital investment for a production capacity of 1 ton of CPBAT per day. The minimum selling prices of CPBAT coated on Kraft paper (CPBAT-K) and CPBAT coated on starch-coated paper (CPBAT-S) are estimated to be \$1.327/m² and \$1.864/m², respectively. Additionally, the results of a sensitivity analysis show that the production of CPBAT-K and CPBAT-S is highly sensitive to the plant production capacity, raw material costs, the energy efficiency of the coating process, and reaction energy, as well as reaction yield. Additionally, recovery of the ionization solvent only marginally increases the selling prices of CPBAT-K and CPBAT-S, hence it is highly suggested.

In the base case scenario, the price of CPBAT-K is ~40%, and CPBAT-S is ~96% more than that of commercial polyethylene-coated paper (PE Paper). With increased production capacity, lower cost of raw material, use of more energy-efficient coating machines, and partial recovery of the energy produced from the reactions, the MSPs will reduce to 0.588 and \$0.914/m², for CPBAT-K and CPBAT-S respectively. Conclusively, with comparable mechanical and barrier properties to PE paper and the added benefit of biodegradability and recyclability, the CPBAT offers an economically feasible and sustainable alternative to current coated paper packaging.

Copyright by ZAHRA AAYANIFARD 2025

dream and strive toward	ed to my sister, Sahar, v l it, to my mother, Mehr	i Mirzaei, who cher	ished her dream of	becoming a
	et it aside so that we co pirations now lie benea			Qaza whose

#### ACKNOWLEDGEMENTS

I would like to express my deepest gratitude to my Ph.D. supervisor Prof. Muhammad Rabnawaz. I believe he has changed my life not only through his personalized mentorship but also his consistent support. He has always been understanding and caring about me throughout my Ph.D. and has put every effort to empower me academically, professionally, and personally.

My special thanks also go to Prof. Christopher Saffron for his guidance on the TEA project. I have learned a lot from him and have enjoyed our collaboration and meaningful conversations. I would also like to thank my committee members Prof. Gary Blanchard, Prof. Babak Brohan, Prof. James Jackson, and Prof. Rafael Auras for their constant aid, valuable comments, questions, and suggestions on my research work.

I want to specifically thank Prof. Gary Blanchard for supporting my career by giving continuous financial and academic support through a teaching assistant position. I would also like to thank NSF for financially supporting my RA for the TEA project. I am very thankful of all the staff members of the Department of Chemistry and School of Packaging, more specifically, Anna Osborn, Cathie Allison, and Amy Radford Popp, who have always been willing to help me.

I also want to acknowledge the impactful role of my colleagues, Dr. Ajmir Khan, and Dr. Shumaila Hamdani, Ash and Vikash for generously helping me throughout my Ph.D. Journey. I have enjoyed being a member of our research group and spending time with my lab mates.

I would like to extend my gratitude and love to my family who have been very supportive in the ups and downs of this windy road. Most importantly, I would like to thank my cousin, Mahdieh, whose generous support enabled me to be here today, and my amazing friends, Elham, Mina, Saman, Negin, Behdad, Shadi, Audra, Behnoosh, and my partner, Babak, who were always there for me and inspired me all these years of hectic studies and immigration challenges.

# **TABLE OF CONTENTS**

LIST OF ABBREVIATIONS	ix
Chapter 1. INTRODUCTION	1
1.1 Background and Motivation	1
1.2 Goal and Objectives	7
REFERENCES	
Chapter 2. LITERATURE REVIEW	15
2.1 Chemical Recycling of PET	
2.2 Paper Coating	
REFERENCES	
Chapter 3. MATERIALS AND METHODS	41
3.1 Materials	
3.2 Pretreatment Process	
3.3 Depolymerization Process	43
3.4 Characterization	
3.5 Energy Requirement Calculation	
3.6 Technoeconomic analysis (TEA) of ionic polybutylene adipate-co-terephthalate	
(CPBAT) for paper coating applications	51
REFERENCES	53
Chapter 4. EFFICIENT CHEMICAL RECYCLING OF POLYETHYLENE	55
TEREPHTHALATE (METHANOLYSIS)	
4.1 Summary	
4.3 Results and Discussion.	
4.4 Conclusions	
REFERENCES	
KLI LKLIVCLS	70
Chapter 5. EFFICIENT CHEMICAL RECYCLING OF POLYETHYLENE	70
TEREPHTHALATE (GLYCOLYSIS)	
<ul><li>5.1 Summary</li><li>5.2 Materials and Methods</li></ul>	
5.3 Results and Discussion.	
5.4 Conclusions	
REFERENCES	112
Chapter 6. BIODEGRADABLE PAPER COATED WITH SYNTHETIC IONIC PBAT F	
PACKAGING APPLICATION: A TECHNOECONOMIC ANALYSIS	
6.1 Summary	
6.2 Methods	
6.3 Results and Discussions	
6.4 Conclusions	129

Chapter	7. CONCLUSIONS AND FUTURE DIRECTIONS	133
7.1	Conclusions	133
7.2	Future Directions	135
APPEN	DIX A: ENERGY REQUIREMENT ASSESSMENT FOR DEPOLYMERIZATION	OF
POLYE	THYLENE TEREPHTHALATE (PET)	137
APPEN	DIX B: ANALYSIS OF GLYCOLYSIS PRODUCTS OF POLYETHYLENE	
TEREPI	HTHALATE (PET)	147
APPEN	DIX C: TECHNOECONOMIC ANALYSIS CALCULATIONS	151

#### LIST OF ABBREVIATIONS

ACN Acetonitrile

AIBN Azobisisobutyronitrile

APR Association of Plastic Recyclers

ASTM American Society for Testing and Materials

BDO 1,4-Butanediol

BHET Bis (2-hydroxyethyl) terephthalate

BHTD 4,8-Bis(hydroxymethyl)tricyclo[5.2.1.0<sup>2,6</sup>]decane

<sup>13</sup>C NMR Carbon (13) Nuclear Magnetic Resonance

CFT Capillary flow technology

CHDM 1,4-Cyclohexanedimethanol

CPBAT Ionic polybutylene adipate-co-terephthalate

CPBAT-K Ionic polybutylene adipate-co-terephthalate coated on Kraft paper

CPBAT-S Ionic polybutylene adipate-co-terephthalate coated on starch-coated paper

CSTR Continuous stirred tank reactor

DBU 1,8-Diazabicyclo[5.4.0]undec-7-ene

DCM Dichloromethane

DMAP 4-Dimethylaminopyridine

DMC Dimethyl carbonate

DMC Dimethyl carbonate

DMIAC 1,3-Dimethylimidazolium-2-carboxylate

DMSO Deuterated Dimethyl sulfoxide-d6

DMT Dimethyl terephthalate

DSC Differential Scanning Calorimetry

EDX Dispersive X-ray Spectroscopy

EG Ethylene glycol

EM Electron Multiplier

GC-MS Gas Chromatography-Mass Spectrometry

<sup>1</sup>H NMR Hydrogen (1) Nuclear Magnetic Resonance

HED Triple-Axis High Energy Diode

HTBD 1,5,7-Triazabicyclo[4.4.0]dec-6-ene

IBM Business Machine Corporations

IPA Isopropyl alcohol

IRR Internal rate of return

LC-MS Liquid Chromatography-Mass Spectrometry

LDPE Low-density polyethylene

MBTCA Meso-butane-1,2,3,4-tetracarboxylic dianhydride

MHET 2-Hydroxyethyl terephthalic acid

MIA 1-Methylimidazole

MSA Methane sulfonic acid

MSD Mass Selective Detector

MSP Minimum selling price

MTBSTFA N-methyl-N-tertbutyldimethylsilyltrifluoroacetamide

M<sub>w</sub> Weight average molecular weight

NAPCOR National Association for PET Container Resources

NIST National Institute of Standards and Technology

NMR Nuclear Magnetic Resonance

OPA Orange peel ash

PBAT Polybutylene adipate-co-terephthalate

PDA Photodiode array

PE Polyethylene

PET Polyethylene terephthalate

PFAS Per- and polyfluoroalkyl compounds

PFD Process flow diagram

PHA Polyhydroxyalkanoate

PIL Polyionic liquid

PLA Polylactic acid

Poly Polyethylene

POSS<sub>(epoxy)8</sub> Polyhedral oligomeric silsesquioxanes

PVOH Polyvinyl alcohol

SEM Scanning Electron Microscopy

STR-FTIR Attenuated Total Reflection-Fourier Transform Infrared

TA Thermal analysis

TBD 1,5,7-Triazabicyclo[4.4.0]dec-5-ene

TBDMS Tert-Butyldimethylsilyl

TBDMSCl Tert-butyldimethylsilyl chloride

TBHDPB Tributylhexadecylphosphonium bromide

TBHDPB Tributylhexadecylphosphonium bromide

TEA Technoeconomic analysis

TPA Terephthalic acid

USA United States

Zn-EH Zinc 2-ethylhexnoate

#### Chapter 1. INTRODUCTION

### 1.1 Background and Motivation

#### 1.1.1 Polyethylene terephthalate (PET)

In the past few decades, plastics have played a significant role in our daily lives owing to their unequaled performance, simple processability, and low-cost [1], [2]. Estimates show that plastic production is more than 395 million tons/year, a high percentage of which ends up in the environment or landfill [3], [4]. Polyethylene terephthalate (PET) is one of the most widely used plastics, with an approximate worldwide production of 70 million tons/year in the packaging and apparel industry [5]. The high application of lies PET in its outstanding properties such as low weight, incredible barrier properties, high chemical stability, durability, and superior thermal properties compared to many other polymers [6]. Its cost-effectiveness and transparency have further elevated its employment in various applications [7].

A joint study released in November 2018 by NAPCOR¹ and APR² revealed that approximately 4 million tons of PET bottles were sold in the U.S. in only one year in 2017; however, only 29.2% found their way to be recycled, while the rest were exported, landfilled, incinerated, or accumulated in the ocean. The collected and sorted post-consumer PET bottles were primarily used in the production of lower-quality products such as fibers, films, and strapping, and a mere ~21% were recycled back into bottles, which equaled around 6.1% of the overall quantity [8]. This fast consumerization of plastics, along with pressure on building more and more waste management infrastructure, has created an environmental dilemma. Therefore, development of an effective solution to handle plastic waste is of dire necessity [9], [10].

Various methods for plastic waste treatment are available, including suboptimal choices

1

<sup>&</sup>lt;sup>1</sup> National Association for PET Container Resources

<sup>&</sup>lt;sup>2</sup> the Association of Plastic Recyclers

like incineration for energy retrieval, which offers limited energy efficiency and produces considerable greenhouse gas emissions. Crucially, the challenge of plastic waste, particularly polyethylene terephthalate (PET) waste, is a global issue that transcends the capabilities of individual nations and necessitates collective policy intervention [11]. At present, the export of plastic waste is a significant aspect for developed countries, often perceived by governments as a resolution to their plastic waste management dilemmas [12]. This perception stems from the reality that many developed nations lack adequate recycling infrastructure to handle their generated plastic waste. With the advent of more ecologically responsible policies, such waste management tactics will likely see modification [13].

Potential policies for immediate implementation encompass measures such as promoting the use of single-material over mixed-material plastics, encouraging product reuse and refill schemes [14], and ensuring end-users bear responsibility for the accurate segregation of plastic varieties destined for recycling processes [15]. Of paramount importance is the imperative to enhance both the capacity and efficiency of recycling by fostering the development of advanced recycling infrastructures and technological solutions [16].

One of the major drawbacks of PET is non-biodegradability and by exposure to the environment, it breaks into microplastics and creates hard-to-tackle environmental problems [17], [18]. On the other hand, some analyses have revealed that replacing plastic packaging with more environmentally sound materials may increase energy requirements and elevate the environmental footprint. Thus extension of the life cycle of plastics using efficient recycling pathways is the key answer to this worldwide environmental crisis [10].

Plastic recycling encompasses a spectrum from primary to quaternary methods, with the secondary (post-consumer) recycling pathway, employing thermomechanical processing, being

predominantly utilized to prolong the lifecycle of post-consumer plastics in an economically feasible manner [19]. However, the drawbacks of the mechanical recycling (secondary recycling) of PET include but are not limited to the decreased molecular weight ( $M_w$ ) of the polymer and viscosity drop due to polymer chain scissions during the extrusion process, which lead to deteriorated mechanical and thermal properties of waste PET [20]–[22]. Although the incorporation of chain extenders, solid-state polymerization strategies, and the addition of virgin petrochemical-based PET have improved the mechanical properties of recycled PET, 79% of all post-consumer PET are still downcycled to lower-quality products (e.g., fiber), the destination of which will be landfilling or incineration (linear economy) [23], [24].

On the other hand, tertiary recycling, known as chemical recycling, of PET has superiority with benefits such as enabling a circular economy through unlimited cycles of bottle-to-bottle recycling by yielding highly pure monomers compared to virgin PET building blocks that can be reused in food packaging applications [25]–[28]. Albeit producing monomers through the existing chemical recycling methodologies is more expensive than those derived from fossil-based resources which then cannot be competitive to mechanical recycling. The high costs of chemical recycling approaches majorly stem from the energy-intensive depolymerization processes at high temperatures and for extended period of time [27], [29]–[31].

The chemical depolymerization of PET varies based on the specific depolymerization reagent employed [32]. This process can occur through hydrolysis, methanolysis, glycolysis or ammonolysis. Through hydrolysis reaction, PEG is depolymerized to the parent monomers, terephthalic acid (TPA) and ethylene glycol (EG) in the presence of water [24]. Methanolysis reaction occurs in presence of methanol to convert PET into dimethyl terephthalate (DMT) and ethylene glycol (EG) monomers [24], while glycolytic depolymerization of PET yields bis (2-

hydroxyethyl) terephthalate (BHET) as another monomer of PET using a glycol, mostly ethylene glycol, as the reagent [33]. Ammonolysis, as the least widely researched polymerization route of PET, produces 1,4-benzene dicarboxamide, commonly known as terephthalamide in the presence of liquid ammonia [33].

Investigations show that Zn<sup>+2</sup>-based acetate have higher capability among all the compounds (e.g. Pb<sup>+2</sup>, Mn<sup>+2</sup>, and Co<sup>+2</sup> acetates) that have been used in the depolymerization of PET. As a result, zinc-containing catalysts have been broadly investigated and commercialized thanks to their outstanding stability and activity, as well as cost-effectiveness [34]–[36]. Very recently, some modifications were applied either into the depolymerization process or the development of new complex catalysts to enhance the zinc-based catalytic depolymerization of PET [33], [37]–[39]. Although some of these efforts could improve the rate of depolymerization, they majorly relied on bench-top-scale-produced catalysts or complicated techniques.

Furthermore, a wide range of organocatalysts have been investigated as greener alternatives to metallic catalysts [40], [41]. International Business Machines Corporation (IBM) researched a myriad of volatile organocatalysts from 2008 to 2013. In their initial study, the most effective catalyst introduced was 1,5,7-triazabicyclo[4.4.0]dec-5-ene (TBD) that depolymerized PET at 190 °C within 325 min and 10 min at catalyst concentrations of 0.5 mol% and 10 mol%, respectively [42]. In subsequent research, 1,8-diaza-bicyclo[5.4.0]undec-7-ene (DBU) was deployed to depolymerize PET at 190 °C within 220 min and 7 min with 0.5 mol% and 10 mol% of catalyst, respectively [35]. Subsequent research efforts aimed to enhance the performance of TBD- and DBU-catalyzed depolymerization of PET. These studies include, but are not limited to: conjugation of TBD with methane sulfonic acid (MSA) [36], incorporation of Zn(OAc)<sub>2</sub> with TBD [43], and DBU [44], functionalizing TBD with dimethyl terephthalate (DMT) [45], and using TBD

with oxoacid protic ionic salts as ligands [46]. Despite their improved performance, each of these methods presents certain drawbacks. These include environmental pollution resulting from the high reactivity of MSA [46], the environmental impact associated with zinc usage, the lab-scale production of functionalized TBD with DMT, and the limited bench-top scale when combining TBD with oxoacids.

In this thesis, a melt treatment process is combined with catalysts and diols for PET depolymerization. This innovative approach hastened the chemical breakdown of PET by thermally targeting hard-to-depolymerize crystalline regions and creating active catalytic sites where diols, in tandem with the catalyst, initiated the depolymerization from within the PET bulk. This process led to a considerably faster methanolysis of PET with significant energy savings compared to a non-pretreated sample. Subsequently, glycolysis of PET was executed using a similar methodology but in a reduced timeframe and with a decreased quantity of catalyst.

Furthermore, zinc-containing catalysts were replaced with organic catalysts to create a metal-free depolymerization process. TBD and DBU were used combined with the pretreatment process using a minimal catalyst amount of 0.5 mol%. The outcomes surpassed the prior results where zinc 2-ethyl hexanoate was used as the catalyst during melt pretreatment. Although existing research suggests that organocatalytic processes typically underperform compared to metallic-based methods regarding degradation factors, integration with the melt-pretreatment phase shows great promise in efficiently and simply breaking down PET into the valuable monomer, bis(2-hydroxyethyl) terephthalate (BHET).

#### 1.1.2 Technoeconomic analysis of CPBAT as coating materials

Polybutylene adipate-co-terephthalate (PBAT) is a hydrophilic polymer that has been commercialized for several decades as a substitute for non-degradable material with wide

application in packaging. Its full biodegradability in soil, thermoplastic behavior, excellent elongation, and ease of processing are key reasons for its potential applicability as a coating material. However, it has low modulus and thermal resistance that limits its mass application as a solo materials [47], [48].

To overcome these limitations, several co-blends, such as starch, and bio-fillers, including chitin, cellulose, and lignin, are often deployed into PBAT blends to enhance their properties while preserving biodegradability [49], [50]. The addition of lignin has several limitations including thermal degradability, the tendency to agglomerate within host matrices, and variability in chemical structure depending on the feedstock source [51]. However, blending polylactic acid (PLA) with PBAT holds promise due to the combination of PLA's mechanical strength and PBAT's toughness. However, challenges arise from low adhesion to interfaces and macro-separation between the blend of polymers, potentially leading to immiscibility despite the similarity in carbonyl groups between PLA and PBAT [52]. There have been attempts to address this issue, such as the addition of corn stover as biomass filler [53], the addition of potato fruit juice in glycerol and then extrusion-coated with a blend of PLA and PBAT in a multilayer coating [54], or compounding with polyhedral oligomeric silsesquioxanes (POSS<sub>(epoxy)8</sub>) as an additive [55].

Recently, our group synthesized an ionized PBAT (CPBAT) from commercially available PBAT, followed by neutralization using ammonium hydroxide to generate waterborne coating material. The obtained waterborne coating/emulsion was applied to Kraft paper and starch-coated paper. CPBAT has shown improved water and oil resistance with prospects of recyclability and biodegradability. Herein, we report, for the first time, a detailed technoeconomic analysis of CPBAT production and the coating onto uncoated Kraft paper and starch-coated paper. No comprehensive TEA is performed on PBAT or modified CPBAT-coated paper. This TEA

determines total capital investment for a production capacity of 1 ton of CPBAT per day and also estimates the minimum selling prices of CPBAT-K and CPBAT-S. Additionally, sensitivity analysis for the production of CPBAT-K and CPBAT-S are performed. Furthermore, the price of CPBAT-K and CPBAT-S are compared with PE-Paper.

#### 1.2 Goal and Objectives

#### 1.2.1 Goal 1 and Objectives

**Goal 1.** The overall goal is to develop an energy-efficient method for the depolymerization of PET under mild conditions without using any organic solvent. Goal 1 is accomplished by following objectives:

Objective 1.1. Investigating the effect of zinc-containing catalysts and diols during melt-pretreatment of PET properties and their effect on the depolymerization of PET in methanol: The hypothesis was that melt-pretreatment of post-consumer PET in the presence of metallic catalysts could eliminate crystallized region in PET while trapping catalysts within the structure of PET. To investigate the hypothesis, two zinc-containing catalysts were added during melt-extrusion along with three different diols. In this study, catalysts were added both during melt-pretreatment and depolymerization reactions. The impact of catalysts alone and the combination of catalysts and diols on the properties of treated PET, depolymerization reaction, and products were studied. The energy demand of this two-step process was compared to that of depolymerization without pretreatment.

**Objective 1.2.** Extending the research to the faster glycolytic depolymerization due to high-pressure reaction requirement in the case of methanolysis [56]: To explore the glycolysis of the melt-pretreated samples, ethylene glycol was used as the reagent. The same catalysts were used during the melt-extrusion process; however, owing to faster depolymerization in glycolysis, the

use of catalysts during depolymerization was eliminated. The properties of treated samples and products as well as varying reaction conditions were studied. As with methanolysis, the required energy for pretreated versus non-pretreated PET was calculated and compared.

**Objective 1.3.** Replacing metallic catalysts with organo-catalysts in glycolysis of PET: Based on previous investigations, volatile catalysts, 1,5,7-triazabicyclo[4.4.0]dec-5-ene (TBD) and 1,8diazabicyclo[5.4.0]undec-7-ene (DBU) 40,41 were used to replace the metallic catalyst and the results were analyzed. In this study minimal amount of catalyst, (0.5 and 1 mol%) was deployed only during melt-pretreatment, and the energy properties of pretreated samples and products were analyzed in addition to the role of reaction conditions.

#### 1.2.2 Goal 2 and Objectives

**Goal 2.** The secondary goal is performing a technoeconomic analysis (TEA) for a biodegradable paper coating material. Goal 2 is accomplished by following objectives:

Objective 2.1. TEA analysis of ionic PBAT (CPBAT) at an industrial production of 1 ton per day: Synthesis and utilizing of CPBAT as a coating material on Kraft paper and starch-coated paper were carried out and the results revealed high water-oil resistance as well as enhanced mechanical properties. To explore the economic feasibility and commercialization potential of CPBAT for coating application, the bench-top experiment was scaled up to an industrial scale of production of 1 ton CPBAT per day. A process flow diagram was developed, and the equipment was designed using Aspen HYSYS software and literature.

**Objective 2.1.** Finding the total capital investment and minimum selling price of CPBAT coated Kraft paper: To calculate the capital investment costs, equipment costs were estimated and multiplied by factors encompassing direct and indirect expenses. The direct operating costs were estimated by combining calculated process flow rates with unitary costs of raw materials and

utilities as well as indirect operating expenses, including labor and benefits, insurance, depreciation, etc. that were derived from operating costs and capital investment values. Based on these costs, and the internal rate of return, the minimum selling price was calculated.

**Objective 2.3.** Exploring the sensitivity of costs and minimum selling price of CPBAT-K and CPBAT-S to various parameters: To investigate how sensitive the costs are to various parameters; three variables were chosen for sensitivity analysis. By altering the recovery rate of neutralization solvent, reaction energy requirement, and energy efficiency of the coating process, the most and least sensitive parameters were identified, and suggestions for cost-effectiveness and environmental sustainability were discussed.

#### REFERENCES

- [1] A. Khan, N. Ahmed, and M. Rabnawaz, "Covalent adaptable network and self-healingmaterials: Current trends and future prospects in sustainability," *Polymers (Basel).*, vol. 12, no. 9, 2020.
- [2] A. L. Andrady and M. A. Neal, "Applications and societal benefits of plastics," *Philos. Trans. R. Soc. B Biol. Sci.*, vol. 364, no. 1526, pp. 1977–1984, 2009.
- [3] R. Geyer, J. R. Jambeck, and K. L. Law, "Production, use, and fate of all plastics ever made," *Sci. Adv.*, vol. 3, no. 7, pp. 25–29, 2017.
- [4] V. Kumar, A. Khan, and M. Rabnawaz, "Efficient Depolymerization of Polystyrene with Table Salt and Oxidized Copper," *ACS Sustain. Chem. Eng.*, vol. 10, no. 19, pp. 6493–6502, 2022.
- [5] V. Tournier *et al.*, "An engineered PET depolymerase to break down and recycle plastic bottles," *Nature*, vol. 580, no. 7802, pp. 216–219, 2020.
- [6] G. Lonca, P. Lesage, G. Majeau-Bettez, S. Bernard, and M. Margni, "Assessing scaling effects of circular economy strategies: A case study on plastic bottle closed-loop recycling in the USA PET market," *Resour. Conserv. Recycl.*, vol. 162, no. December 2019, p. 105013, 2020.
- [7] R. Zhang *et al.*, "PET bottles recycling in China: An LCA coupled with LCC case study of blanket production made of waste PET bottles," *J. Environ. Manage.*, vol. 260, no. January, p. 110062, 2020.
- [8] R. D. Allen and M. I. James, "Chemical Recycling of PET," *ACS Symp. Ser.*, vol. 1391, pp. 61–80, 2021.
- [9] T. Galloway, M. Haward, S. A. Mason, B. D. Hardesty, and S. Krause, "Science-Based Solutions to Plastic Pollution," *One Earth*, vol. 2, no. 1, pp. 5–7, 2020.
- [10] R. A. Sheldon and M. Norton, "Green chemistry and the plastic pollution challenge: Towards a circular economy," *Green Chem.*, vol. 22, no. 19, pp. 6310–6322, 2020.
- [11] M. Kusenberg *et al.*, "Towards high-quality petrochemical feedstocks from mixed plastic packaging waste via advanced recycling: The past, present and future," *Fuel Processing Technology*, vol. 238. Elsevier B.V., 15-Dec-2022.
- [12] J. Chu, Y. Cai, C. Li, X. Wang, Q. Liu, and M. He, "Dynamic flows of polyethylene terephthalate (PET) plastic in China," *Waste Manag.*, vol. 124, pp. 273–282, 2021.
- [13] A. Chandra and S. Siddiqua, "Sustainable utilization of chemically depolymerized polyethylene terephthalate (PET) waste to enhance sand-bentonite clay liners," *Waste Manag.*, vol. 166, no. April, pp. 346–359, 2023.

- [14] B. Madden, M. Jazbec, and N. Florin, "Increasing packaging grade recovery rates of plastic milk bottles in Australia: A material flow analysis approach," *Sustain. Prod. Consum.*, vol. 37, pp. 65–77, May 2023.
- [15] S. Schmidt and D. Laner, "The multidimensional effects of single-use and packaging plastic strategies on German household waste management," *Waste Manag.*, vol. 131, pp. 187–200, Jul. 2021.
- [16] I. S. Lase *et al.*, "Material flow analysis and recycling performance of an improved mechanical recycling process for post-consumer flexible plastics," *Waste Manag.*, vol. 153, pp. 249–263, Nov. 2022.
- [17] A. Khan, M. Naveed, and M. Rabnawaz, "Melt-Reprocessing of Mixed Polyurethane Thermosets," *Green Chem.*, 2021.
- [18] E. Nikolaivits *et al.*, "Progressing Plastics Circularity: A Review of Mechano-Biocatalytic Approaches for Waste Plastic (Re)valorization," *Front. Bioeng. Biotechnol.*, vol. 9, no. June, pp. 1–31, 2021.
- [19] N. Vora *et al.*, "Leveling the cost and carbon footprint of circular polymers that are chemically recycled to monomer," 2021.
- [20] I. Vollmer *et al.*, "Beyond Mechanical Recycling: Giving New Life to Plastic Waste," *Angew. Chemie Int. Ed.*, vol. 59, no. 36, pp. 15402–15423, 2020.
- [21] M. Del Mar Castro López, A. I. Ares Pernas, M. J. Abad López, A. L. Latorre, J. M. López Vilariño, and M. V. González Rodríguez, "Assessing changes on poly(ethylene terephthalate) properties after recycling: Mechanical recycling in laboratory versus postconsumer recycled material," *Mater. Chem. Phys.*, vol. 147, no. 3, pp. 884–894, 2014.
- [22] D. Dimonie *et al.*, "Overview on Mechanical Recycling by Chain Extension of POSTC-PET Bottles," *Mater. Recycl. Trends Perspect.*, no. March, 2012.
- [23] Damayanti and H. S. Wu, "Strategic possibility routes of recycled pet," *Polymers (Basel)*., vol. 13, no. 9, pp. 1–37, 2021.
- [24] S. Ügdüler *et al.*, "Towards closed-loop recycling of multilayer and coloured PET plastic waste by alkaline hydrolysis," *Green Chem.*, vol. 22, no. 16, pp. 5376–5394, 2020.
- [25] M. Khoonkari, A. H. Haghighi, Y. Sefidbakht, K. Shekoohi, and A. Ghaderian, "Chemical Recycling of PET Wastes with Different Catalysts," *Int. J. Polym. Sci.*, vol. 2015, 2015.
- [26] T. S. Daniel Paszun, "Chemical Recycling of Poly Ethylene Terephthalate Wastes," vol. 8, no. 7, pp. 839–846, 2010.
- [27] L. Bartolome, M. Imran, B. Gyoo, W. A., and D. Hyun, "Recent Developments in the Chemical Recycling of PET," *Mater. Recycl. Trends Perspect.*, no. March 2012, 2012.

- [28] J. Payne and M. D. Jones, "The Chemical Recycling of Polyesters for a Circular Plastics Economy: Challenges and Emerging Opportunities," *ChemSusChem*, vol. 14, no. 19, pp. 4041–4070, 2021.
- [29] V. Sinha, M. R. Patel, and J. V. Patel, "Pet waste management by chemical recycling: A review," *J. Polym. Environ.*, vol. 18, no. 1, pp. 8–25, 2010.
- [30] D. S. Achilias and G. P. Karayannidis, "The chemical recycling of PET in the framework of sustainable development," *Water, Air, Soil Pollut. Focus*, vol. 4, no. 4–5, pp. 385–396, 2004.
- [31] E. Barnard, J. J. Rubio Arias, and W. Thielemans, "Chemolytic depolymerisation of PET: A review," *Green Chem.*, vol. 23, no. 11, pp. 3765–3789, 2021.
- [32] A. Sheel and D. Pant, "Chemical Depolymerization of PET Bottles via Glycolysis," in *Recycling of Polyethylene Terephthalate Bottles*, Elsevier, 2019, pp. 61–84.
- [33] L. Deng, R. Li, Y. Chen, J. Wang, and H. Song, "New effective catalysts for glycolysis of polyethylene terephthalate waste: Tropine and tropine-zinc acetate complex," *J. Mol. Liq.*, vol. 334, p. 116419, 2021.
- [34] P. Fang *et al.*, "High-efficiency glycolysis of poly(ethylene terephthalate) by sandwich-structure polyoxometalate catalyst with two active sites," *Polym. Degrad. Stab.*, vol. 156, pp. 22–31, Oct. 2018.
- [35] K. Fukushima *et al.*, "Unexpected efficiency of cyclic amidine catalysts in depolymerizing poly(ethylene terephthalate)," *J. Polym. Sci. Part A Polym. Chem.*, vol. 51, no. 7, pp. 1606–1611, 2013.
- [36] C. Jehanno, I. Flores, A. P. Dove, A. J. Müller, F. Ruipérez, and H. Sardon, "Organocatalysed depolymerisation of PET in a fully sustainable cycle using thermally stable protic ionic salt," *Green Chem.*, vol. 20, no. 6, pp. 1205–1212, 2018.
- [37] A. C. Fernandes, "Reductive Depolymerization of Plastic Waste Catalyzed by Zn(OAc)2 · 2H2O," *ChemSusChem*, vol. 14, no. 19. pp. 4228–4233, 2021.
- [38] Y. Li, K. Li, M. Li, and M. Ge, "Zinc-doped ferrite nanoparticles as magnetic recyclable catalysts for scale-up glycolysis of poly(ethylene terephthalate) wastes," *Adv. Powder Technol.*, vol. 33, no. 3, p. 103444, 2022.
- [39] M. Li, Y. Huang, T. Yu, S. Chen, A. Ju, and M. Ge, "Chemical recycling of waste poly(ethylene terephthalate) fibers into azo disperse dyestuffs," *RSC Adv.*, vol. 4, no. 87, pp. 46476–46480, 2014.
- [40] C. Jehanno, M. M. Pérez-Madrigal, J. Demarteau, H. Sardon, and A. P. Dove, "Organocatalysis for depolymerisation," *Polym. Chem.*, vol. 10, no. 2, pp. 172–186, 2019.
- [41] P. Mckeown et al., "Organocatalysis for versatile polymer degradation," Green Chem., vol.

- 22, no. 12, pp. 3721–3726, 2020.
- [42] K. Fukushima *et al.*, "Organocatalytic depolymerization of poly(ethylene terephthalate)," *J. Polym. Sci. Part A Polym. Chem.*, vol. 49, no. 5, pp. 1273–1281, Mar. 2011.
- [43] K. R. Delle Chiaie, F. R. McMahon, E. J. Williams, M. J. Price, and A. P. Dove, "Dual-catalytic depolymerization of polyethylene terephthalate (PET)," *Polym. Chem.*, vol. 11, no. 8, pp. 1450–1453, Feb. 2020.
- [44] W. Chen, M. Li, X. Gu, L. Jin, W. Chen, and S. Chen, "Efficient glycolysis of recycling poly(ethylene terephthalate) via combination of organocatalyst and metal salt," *Polym. Degrad. Stab.*, vol. 206, Dec. 2022.
- [45] E. B. S. Nica, M. Duldner M, A. Hanganu, S. Iancu, B. Cursaru, A. Sarbu, P Filip, "Functionalized 1,5,7-triazabicyclo [4.4.0] dec-5-ene (TBD) as Novel Organocatalyst for Efficient Depolymerization of Polyethylene Terephthalate (PET) Wastes," vol. 6, no. 70, pp. 2–6, 2018.
- [46] C. Zhu, L. Yang, C. Chen, and G. Zeng, "Metal-free recycling of waste polyethylene terephthalate mediated by TBD protic ionic salts: the crucial role of anionic ligands †," pp. 27936–27941, 2023.
- [47] D. K. Debeli, L. Wu, and F. Huang, "PBAT-based biodegradable nanocomposite coating films with ultra-high oxygen barrier and balanced mechanical properties," *Polym. Degrad. Stab.*, vol. 216, no. July, p. 110489, 2023.
- [48] S. Shankar and J. W. Rhim, "Effects of poly(butylene adipate-co-terephthalate) coating on the water resistant, mechanical, and antibacterial properties of Kraft paper," *Prog. Org. Coatings*, vol. 123, no. April, pp. 153–159, 2018.
- [49] S. J. Xiong *et al.*, "Economically Competitive Biodegradable PBAT/Lignin Composites: Effect of Lignin Methylation and Compatibilizer," *ACS Sustain. Chem. Eng.*, vol. 8, no. 13, pp. 5338–5346, 2020.
- [50] S. J. Xiong *et al.*, "A strong, tough and cost-effective biodegradable PBAT/lignin composite film via intrinsic multiple noncovalent interactions," *Green Chem.*, vol. 25, no. 8, pp. 3175–3186, Mar. 2023.
- [51] R. Shorey and T. H. Mekonnen, "Sustainable paper coating with enhanced barrier properties based on esterified lignin and PBAT blend," *Int. J. Biol. Macromol.*, vol. 209, no. PA, pp. 472–484, 2022.
- [52] Y. Ding, B. Lu, P. Wang, G. Wang, and J. Ji, "PLA-PBAT-PLA tri-block copolymers: Effective compatibilizers for promotion of the mechanical and rheological properties of PLA/PBAT blends," *Polym. Degrad. Stab.*, vol. 147, pp. 41–48, Jan. 2018.
- [53] R. Li, X. Zhu, F. Peng, and F. Lu, "Biodegradable, Colorless, and Odorless PLA/PBAT Bioplastics Incorporated with Corn Stover," *ACS Sustain. Chem. Eng.*, Jun. 2023.

- [54] S. Poulose, J. Toriseva, J. Lahti, I. Jönkkäri, M. S. Hedenqvist, and J. Kuusipalo, "A Green High Barrier Solution for Paperboard Packaging based on Potato Fruit Juice, Poly(lactic acid), and Poly(butylene adipate terephthalate)," *ACS Appl. Polym. Mater.*, vol. 4, no. 6, pp. 4179–4188, 2022.
- [55] S. Qiu, Y. Zhou, I. N. Waterhouse, R. Gong, J. Xie, and K. Zhang, "Optimizing interfacial adhesion in PBAT / PLA nanocomposite for biodegradable packaging fi lms," vol. 334, no. June 2020, 2021.
- [56] J. Xin *et al.*, "Progress in the catalytic glycolysis of polyethylene terephthalate," *J. Environ. Manage.*, vol. 296, Oct. 2021.

#### Chapter 2. LITERATURE REVIEW

This chapter is mainly focused on the overview of potential pathways for recycling polyethylene terephthalate (PET), with emphasis on two chemical recycling methods-methanolysis and glycolysis. Additionally, it gives insights into the importance of the economic feasibility of biodegradable, recyclable coated papers.

# 2.1 Chemical Recycling of PET

As revealed in the report by NAPCOR<sup>3</sup> and the APR<sup>4</sup> out of approximately 4 million tons of PET bottles sold in the U.S. in 2017, only about 29.2% were recycled while the rest were exported, landfilled, incinerated, or left in the oceans. More importantly, a significant portion of this 29.2% of post-consumer PET bottles the majority were downcycled into fibers, films, and strapping and 21% were recycled back into bottles, accounting for approximately 6% of the total PET bottle sales volume [1].

Despite the economic and technical benefits of today's PET mechanical recycling routes [2], they present significant disadvantages, such as dependency on transparent bottles and the deterioration of mechanical properties during the extrusion process. [3]. Additionally, mechanical recycling is limited by the high cost and efforts linked to sorting [4]. As a result, there is an urgent need for more sustainable solutions aligned with the principles of a circular economy.

Chemical depolymerization is a promising avenue, as it converts PET into its foundational monomers. These monomers can then be purified and reintegrated as components equivalent to virgin fossil-derived inputs, being a significant step towards achieving a more circular economy [5].

Three routes that are extensively studied in the depolymerization of PET are reviewed in

2

<sup>&</sup>lt;sup>3</sup> National Association for PET Container Resources

<sup>&</sup>lt;sup>4</sup> Association of Plastic Recyclers

the following sections. A selection of the most recent studies on the chemical recycling of PET are summarized in *Table 2-1*.

### 2.1.1 Hydrolysis

During hydrolysis chemical reaction chain scission occurs in PET polymer through either acidic or basic aqueous processes to yield terephthalic acid (TPA) and ethylene glycol (EG) [6]. Various methods are studied for the hydrolysis of PET. The hydrolytic depolymerization reaction of PET is derived from a publication and is depicted in *Figure 2-1*.

Alkaline hydrolysis for recycling PET includes various advantages such as easy separation of highly pure products, particularly well-suited for bottle-to-bottle recycling. However, this process requires concentrated alkaline solutions (1–5 M NaOH) so that separating the products necessitates a significant amount of acid to neutralize to precipitate TPA from the solution [7].

**Figure 2-1.** Hydrolysis reaction of PET for full degradation to terephthalic acid and ethylene glycol.

In a recent study, alkaline hydrolysis was presented for PET depolymerization, conducted under mild temperatures of 80 to 100 °C and atmospheric pressure.

Tributylhexadecylphosphonium bromide (TBHDPB), was utilized as a catalyst. PET conversion rates reached up to 99.9%, with a maximum TPA yield of 93.5% when the catalyst mass ratio of TBHDPB to PET ranged from 0 to 20%. Optimal results were obtained within 4 hours at 100 °C, with a 20 weight% of TBHDPB [8].

In another recent investigation, hydrolysis of PET occurred utilizing novel catalysts such as NaCl, CaCl<sub>2</sub>, NaHCO<sub>3</sub>, KHCO<sub>3</sub>, and marine water. Reaction happened within 2 hours in the presence of 2 weight percent of the catalyst under nitrogen, to increase the internal pressure to over 3 MPa to maintain water in liquid state at temperatures of 190 to 215 °C. The maximum TPA yield of 95.7% was obtained in the presence of 40 weight% NaHCO<sub>3</sub> + KHCO<sub>3</sub> (1:1) at 195 °C within 120 minutes. TPA recovery initially involved a filtration step for separation of the precipitate that was formed, followed by treating the liquid that was separated in the prior steps with a 2N H<sub>2</sub>SO<sub>4</sub> solution to isolate TPA from the sodium terephthalate solution through precipitation. Finally, the recovered TPA was washed, dried, and weighed [9].

Another study was focused on the depolymerization of PET textiles, both with and without the presence of zinc acetate as catalyst, at a temperature range of 180 to 250 °C and 39 bar within 6 h. Initially, complete depolymerization was achieved with an 85% yield of terephthalic acid (TPA). Subsequently, PET oligomers were treated with an enzyme solution, followed by an incubation period of 24 hours at 50 °C and 600 rpm, resulting in a 97% yield of TPA [10].

In an investigation, waste PET was subjected to depolymerization using excess supercritical water in the absence of catalysts. The drastic reaction conditions could form secondary products such as benzoic acid, 1,4-dioxane, and acetaldehyde. High yields of terephthalic acid (TPA) of 93.46% were achieved at 300 °C and 30 bar within 1 min. Once the reaction was finished, the treatment with sodium hydroxide was performed to produce the water-

soluble sodium salt of terephthalic acid, followed by filtration to separate any unreacted PET. The filtrate was then subjected to acidification using concentrated hydrochloric acid to precipitate TPA [11].

Enzymatic hydrolytic methods have also gained attention recently. A very recent publication summarizing the research on enzymatic hydrolysis of PET shows that PET depolymerization can occur at mild temperatures of 30 to 86 °C within 9 h to 30 days [12]. Some of the recent studies on enzymatic hydrolysis are highlighted below.

In a recent investigation, four PET hydrolases were discovered using a standardized enzymatic PET hydrolysis protocol, two of which showed promising results with depolymerization of PET into monomeric products within 24 hours with 80% and 98% yields. The reaction conditions for one of them were optimized for economic viability, reducing enzyme usage (3 times less) and lowering the temperature from 72 °C to 68 °C [3].

In another study, a pretreatment process was employed, utilizing an engineered transselective variant in conjunction with the resulting trans-oligomeric substrate. This approach facilitated the alignment of enzyme and substrate conformations that enhanced biocatalysis. The PET film underwent incubation with 100 nM PETase for 72 hours at 30 °C and 100 rpm in phosphate buffer with a pH of 7.2 for full depolymerization to TPA [13].

In the case of hydrolysis, the degradation process faces significant challenges because of harsh reaction conditions, such as high temperatures (200 °C to 300 °C), pressures between 1.4 to 3 MPa, prolonged reaction times, and the expenses to purify TPA from the reaction medium. Additionally, to mitigate harsh conditions, such as high pressure and temperature, an acid catalyst, mostly concentrated sulfuric acid, is commonly employed in the hydrolysis reaction. These factors have decreased the commercial viability of using this technique to produce food-grade applications

[14].

Furthermore, despite the efforts of small biotech companies such as the French company Carbios and Novozymes that commercialized hydrolase enzymes [15], enzymatic hydrolysis still faces challenges such being sensitive to pH and temperature, as well as low efficiency of degradation process for crystalline polymers due to difficulty of solvent access to crystalline regions unless a pretreatment process is deployed [16], [12], [13], [17]. Even with highly efficient enzymatic methods, it takes at least 1 to a few days to fully depolymerize PET at 70 °C, which is both time- and energy-inefficient.

#### 2.1.2 Methanolysis

PET methanolysis produces dimethyl terephthalate (DMT) and ethylene glycol (EG) as reaction products. Liquid methanolysis occurs at temperatures of 180 to 280 °C and pressures between 20 to 40 atm. Typically, transesterification catalysts including zinc acetate, magnesium acetate, cobalt acetate, and lead dioxide are employed for the reaction acceleration. The high pressure is necessary to maintain methanol in a liquid state during the reaction. The methanolysis products are mostly separated and/or purified either through distillation or crystallization processes. [18]. The reaction equation for methanolytic depolymerization of methanol to the monomers with no byproducts is derived from article [19] and depicted in *Figure 2- 2*.

Figure 2- 2. Full methanolytic depolymerization of PET to its parent monomers.

Superheated vapor methanolytic path for depolymerization of PET is an alternative to liquid methanol occurring at lower pressures than required to maintain the liquid state for methanol while facilitating the removal of resultant DMT as a vapor. This process tolerates more contamination in PET than conventional methods of liquid methanolysis by eliminating vapor esters and alcohols Consequently, vapor methanolysis typically exhibits higher reaction yields compared to liquid-phase methanolysis [20], [21].

PET can be depolymerized in supercritical methanolysis conditions (300 °C and pressures higher than 80 atm) as fast as within 30 minutes. However, the high pressure and temperature of both liquid and vapor methanolysis elevate operational costs, leading to low economic feasibility as an industrial PET depolymerization technique. Additionally, the reaction products of supercritical methanolysis can include BHET, methyl-2-hydroxy ethylene terephthalate in addition to DMT, and, with DMT yielding approximately 80% [22]–[26].

Despite the disadvantages of conventional methanolytic depolymerization of PET, it has the advantage of treating low-quality feedstocks, as it is more tolerant of contamination compared to other recycling processes [18]. Some of the recent studies on methanolysis of PET

are summarized below to give more insights about this depolymerization route.

In a research study, a low-energy catalytic route has been developed for the methanolytic conversion of PET to DMT in the presence of potassium carbonate (K<sub>2</sub>CO<sub>3</sub>), an inexpensive and non-toxic salt at ambient temperature. PET was completely converted into DMT with a yield of 93.1% achieved within 24 hours at 25 °C, using methanol, dichloromethane, and K<sub>2</sub>CO<sub>3</sub> with molar ratios to PET repeating units of 50, 50, and 0.2, respectively. The initial molar ratio of moisture to PET monomers was optimized to be 0.4:1 in this experiment [27]. While this process proves to be energy efficient in comparison with conventional methanolysis processes, the overall reaction rate of the developed system is slow and the harmful solvent dichloromthane is used [28],

In another investigation, the methanolytic depolymerization of PET was studied using polyionic liquids (PILs) which was formed by utilizing 1-vinyl-3-ethylimidazolium acetates ([VEIm]Ac) as precursors. Under optimized conditions, 2 weights% of the catalyst PIL-Zn<sub>2</sub>+ completely conversion of PET with a dimethyl terephthalate (DMT) yield of 90.3% at a temperature of 170 °C within 1 hour and a methanol to PET ratio of 4:1. The catalyst, PIL-Zn<sub>2</sub>+, was recyclable by filtration after the reaction and was usable for six cycles without a considerable decrease in PET conversion and yield of DMT. After the reaction, the mixture was cooled down to room temperature, dissolved completely in acetonitrile, filtered, and separated to recover the unreacted products and the catalyst [30].

Another recent study focused on PET depolymerization via methanolysis using dimethyl carbonate (DMC) as the primary trapping agent<sup>5</sup>. Post-consumer PET bottles were initially

<sup>&</sup>lt;sup>5</sup> DMC is used in methanolytic depolymerization to trap EG to produce ethylene carbonate (EC) that is thermodynamically more stable while also trapping methanol, resulting in shifting the depolymerization equilibrium toward DMT production [88].

pulverized into a powder form and then exposed to depolymerization at 65 °C for 5 hours in the presence of an alkali metal alkoxide catalyst, Lithium methoxide (LiOMe). In the presence of 10 mol% of LiOMe, 0.5 ml (2.4 mol) of methanol, and 1.5 ml (3.4 mol) of DMC, the methanolysis reaction yielded over 90% of DMT. DMC and methanol were removed from the filtrate via distillation under reduced pressure at atmospheric temperature. Then, the remaining mixture was washed with water, resulting in the isolation of analytically pure DMT and ethylene carbonate which was the major component of the aqueous washing [31].

A biocatalytic methanolysis of PET was performed using bamboo leaf ash (BLA) as a greener catalyst with a methanol to PET mola ratio of 45.5:1, 100 mg of catalyst. The reaction was maintained at 200 °C for 2 hours. Once the reaction was completed, the BLA catalyst was separated by filtration followed by washing with 40 mL of heated methanol. The filtrate was cooled to room temperature and refrigerated at 2 °C for 4 hours, yielding 78 weight% of crystallized DMT which was filtered and dried. Despite the green nature of the catalyst, the production process of the catalyst from bamboo leaves involved drying the washed leaves at 80 °C for 8 hours, followed by burning them to ash and calcination of the ash at 700 °C for 4 hours. The collected product was crushed into a powder, sieved, and stored at room temperature [32].

A very recent study reported on cosolvent-enhanced methanolysis of PET could achieve 100% conversion of PET within 1 hour at 170 °C yielding 90.1% DMT. Acetonitrile was identified as the most effective cosolvent for the reaction increasing the specific surface area of PET, leading to the facilitation of mass transfer of methanol, and increasing the rate of the polymerization. The catalyst was a deep eutectic solvent (DES) synthesized from choline chloride and zinc acetate (1:1). Once the reaction was completed, the mixture was cooled to room temperature and dissolved in acetonitrile and filtered to separate the unreacted PET bottle flakes and oligomers [33].

In another recent study, a greener and recyclable heterogeneous catalyst, orange peel ash@Fe<sub>3</sub>O<sub>4</sub> (OPA@Fe<sub>3</sub>O<sub>4</sub>) magnetic nano-catalyst, was synthesized using orange peel ash (OPA). The OPA extraction process involved burning orange peels in the open air after drying at 80 °C for 10-12 hours, followed by stirring the ash for 1 hour at 80 °C to extract OPA. Additionally, magnetite nanoparticles were synthesized using a mixture of FeSO<sub>4</sub>·7H<sub>2</sub>O, FeCl<sub>3</sub>, and deionized water at 90 °C with vigorous stirring. The nanoparticles were then mixed with OPA and 1 M ammonia solution to yield the nano-catalyst after evaporation of water. The methanolysis reaction was conducted in the presence of 4 wt% of OPA@Fe<sub>3</sub>O<sub>4</sub> catalyst and 49 molar equivalents of methanol at 200 °C for 1 hour to yield dimethyl terephthalate (DMT). DMT was crystallized with an 83% yield at 2 °C within 4 hours after washing with 40 mL of hot methanol [34].

A very recent organocatalyzed methanolytic process has been developed to depolymerize PET with easy isolation of the monomers. With a solvent/substrate ratio of 3:1, in an initial investigation, the reaction was conducted at 200 °C using easily recoverable triethylamine (NEt<sub>3</sub>) as a catalyst, resulting in an 82% yield of DMT within 2 h. Additionally, performing the reaction in a 1:1 mixture of methanol and toluene as a cosolvent, and 13 volumetric percent of NEt<sub>3</sub> yielded 88% DMT at 200 °C within 2 hours [35].

#### 2.1.3 Glycolysis

Amongst the chemical recycling pathways, glycolysis is known as the most common method for PET waste recycling with least expensive capital investment [18], [34]. Glycolysis depolymerization is the most extensively researched process that was initially patented in 1965, and commercial facilities scaled up in Europe, the USA, and Japan. The advantage of glycolysis lies in the simplicity of the process to generate high BHET yields which can be incorporated into fresh BHET following a purification process and PET repolymerization, without the need for an

esterification step [36]. Therefore, it stands out as the most cost-effective and economically viable process for chemically recycling PET bottles.

*Figure 2-3. Full glycolytic depolymerization of PET to the monomer, BHET.* 

The glycolytic depolymerization reaction of PET to the parent monomer, bis (2-hydrocyethyl) terephthalate (BHET) is derived from a publication [19] and shown in **Figure 2-3**. In the following paragraphs, some recent methods for glycolysis of PET are summarized.

In investigation, ionic liquid called 1-butyl-3-vinylimidazolium an an bis[(trifluoromethyl)sulfonyl]imide ([BVim]NTf<sub>2</sub>) was polymerized into a polyionic liquid, which was then utilized to immobilize metal ions for catalyzing the glycolysis of PET. The synthesis of the catalyst involved stirring 1-vinylimidazole and bromobutane for 24 hours at room temperature, followed by washing with ethyl acetate, drying, and then mixing with ethanol and azobisisobutyronitrile (AIBN) while stirring for 12 hours. Acetonitrile was used to precipitate the intermediate, followed by dissolution in water and the addition of LiNTf<sub>2</sub> while stirring for 24 hours at 25 °C. The dried polymer [BVim]NTf<sub>2</sub> was ground and dissolved in methanol and stirred for 24 hours after the addition of a metal salt. For precipitation of the polymer [BVim]NTf<sub>2</sub>-metal ion complex, ethylene glycol was used, and the catalyst system was washed with deionized water

and dried in an oven at 60 °C. A 20 weight% of this catalyst was used to depolymerize PET with a PET:EG ratio of 13:1 at 195 °C within 120 minutes [37].

Another glycolytic process was reported utilizing ultrathin exfoliated MnO<sub>2</sub> nanosheets (e-MON) as a catalyst. The production of the catalyst involved mixing manganese carbonate (MnCO<sub>3</sub>) and potassium carbonate (K<sub>2</sub>CO<sub>3</sub>) in isopropyl alcohol (IPA) and calcination in a furnace at 800 °C for 24 hours in the air. This was followed by an exfoliation step lasting 1 hour while mixing that improved the filled interlayer voids of MnO<sub>2</sub> with potassium ions. It was followed by centrifugation for 150 minutes, de-exfoliation, and freeze-drying for 24 hours. The e-MON catalyst could depolymerize PET to 100% BHET within 30 minutes at 200 °C. Importantly, the high yield with five times recycling depicted the reusability of the e-MON catalyst [38].

Glycolytic depolymerization was studied using niobia-based catalysts. A 20 weight% sulfated niobia catalyst treated at 300 °C could lead to full conversion of PET yielding 85% BHET in the presence of 6.2:1 EG to PET mola ratio at 195 °C in 220 minutes. The catalyst, SO<sub>4</sub><sup>2-</sup>/Nb<sub>2</sub>O<sub>5</sub>·nH<sub>2</sub>O, was synthetized by adding (NH<sub>4</sub>)<sub>2</sub>SO<sub>4</sub> solution to niobium oxide at 80 °C while stirring for 3 hours under reflux, followed by filtering, and drying at 110°C for 16 hours. The resulting powder was pulverized and calcined at 300 °C for 2 hours [39].

In a novel investigation, 1,3-dimethylimidazolium-2-carboxylate was used as an organocatalyst to the glycolytic conversion of waste PET resulted in full conversion in less than 1 hour when 15 mol% of catalyst and a 10:1 molar ratio of ethylene glycol (EG) to PET were used at 185 °C, yielding 65% of BHET. The catalyst was synthesized by the reaction of dimethylcarbonate and methylimidazole in a pressure tube at 140 °C, followed by filtration and washing with diethyl ether, acetone, and acetonitrile to obtain a crystalline solid [40].

In another research study, a dual-catalytic method was reported to glycolyze PET with a

combination of inexpensive and commercially available Lewis acid–base pairs that resulted in the cooperative activity of catalysts. By combining zinc acetate (Zn(OAc)<sub>2</sub>) with 4-dimethylaminopyridine (DMAP) showed 96% conversion within 3 hours. For the preparation of the catalytic system, DMAP was dissolved in methanol and mixed with Zn(OAc)<sub>2</sub> while stirring overnight, followed by the separation of the solvent under vacuum. Depolymerization occurred using 1.5 mol% of catalyst and an EG to PET molar ratio of 20:1 at 180 °C. The produced BHET was crystallized in water and dried for 24 hours [41].

The deployment of an aromatic compound containing the alkoxy group, such as anisole facilitated the glycolytic depolymerization of PET to BHET at 153 °C. Anisole, known for its low cost, non-toxicity, and biodegradability, was used as a green co-solvent with a PET:EG:anisole molar ratio of 1:12:4 to lower the energy demand of the reaction. Optimal reaction conditions were achieved by using alkali metal acetates (such as Na or K), during which PET was completely decomposed within 2 hours yielding 86% BHET. In the same solvent system, when a guanine-based organocatalyst, Triazabicyclodecene (TBD), was used, PET was fully depolymerized while yielding 81.8% of BHET. However, a considerable fraction of irreversible byproduct (up to 2.2% 2-Hydroxyethyl terephthalic acid (MHET)) was produced, suggesting that TBD is not an effective catalyst for products generated in the co-solvolysis of PET [42].

A group of scientists at International Business Machines Corporation (IBM) researched a variety of volatile organocatalysts from 2008 to 2013. Their initial study introduced the most effective catalyst, TBD that could depolymerize PET at 190 °C within 325 min and 10 min at catalyst concentrations of 0.5 mol% and 10 mol%, respectively [43]. In a later investigation, 1,8-diaza-bicyclo[5.4.0]undec-7-ene (DBU) was introduced to depolymerize PET at 190 °C within 220 min and 7 min with 0.5 mol% and 10 mol% of catalyst, respectively [44]. Following their

outstanding findings, researchers aimed to enhance the performance of these two catalysts in various ways.

In one of these investigations, a combination of a metal catalyst, zinc acetate (Zn(OAc)<sub>2</sub>), and an organocatalyst, 1,8-diazabicyclo[5.4.0]undec-7-ene (DBU), with a molar ratio of Zn(OAc)<sub>2</sub> to DBU of 1:2, was employed to depolymerize waste PET into BHET. PET was fully depolymerized at 180 °C within 77 minutes, when an EG to PET molar ratio of 10:1 was used, yielding 78.2% of crystallized BHET [45].

Another effort involved using a solvent-free system, to fully depolymerize PET in the presence of 5 mol% of 1,5,7-triazabicyclo[4.4.0]dec-5-ene (TBD) and methanesulfonic acid (MSA) (1:1 molar ratio), with an EG to PET molar ratio of 20:1, in less than 2 hours, yielding 91% BHET at 180 °C. The thermal stability of the TBD:MSA (1:1) salt enabled the recyclability of the catalyst for at least 5 cycles. The catalyst was recovered at 250–270 °C within 1 hour of stirring followed by vacuuming for 4 hours at the same temperature. Then, the dissolution of PET in chloroform and trifluoroacetic acid (8:1) mixture and precipitation in excess methanol was used to purify the product [46].

Another group of researchers synthesized a functionalized TBD<sup>6</sup>, called methyl 4-(2,3,4,6,7,8-hexahydro-1H-pyrimido[1,2-a]pyrimidine-1-carbonyl), by reacting dimethyl terephthalate (DMT) with TBD in refluxing benzene, to be used as a catalyst. PET waste was then reacted with 15 molar equivalents of EG in the presence of 10 mol% of catalyst at 190 °C to yield 91% BHET within 45 minutes [47].

Recently, Scientists utilized carboxylate anions (OAc-) and HTBD+ cations to construct a novel TBD-based protic ionic salt for the glycolytic catalysis of PET. The HTBD-OAc catalyst

.

<sup>&</sup>lt;sup>6</sup> 1,5,7-triazabicyclo[4.4.0]dec-5-ene

was synthesized by reacting TBD and acetic acid. PET was depolymerized using 3 mol% of catalyst and an EG to PET molar ratio of 13:1 at 190 °C within 90 minutes yielding 85.9% of BHET[48].

In another effort to enhance TBD's performance and recyclability, a team of scientists substituted TBD with modified silica gel, treated with TBD (Si-TBD) owing to its superior thermal stability and favorable catalytic activity compared to TBD. Under optimized reaction parameters, utilizing a 12.5:1 molar ratio of ethylene glycol to PET and the addition of 15.5 mol% Si-TBD, PET was completely glycolyzed at 190 °C within 1.7 hours, yielding an 88% BHET monomer [49].

Another study was very recently published on dual solvolysis of PET in the presence of a 10:3:1 molar ratio of 1-methylimidazole, ethylene glycol, and PET. Various catalysts, including DMAP, TBD, 7-methyl-TBD (Me-TBD), and DBU, were tested at 100 °C for 30 minutes. The results indicated that using 20% and 50% TBD as a catalyst can completely depolymerize PET in 15 minutes, yielding BHET with yields of 82% and 88%, respectively. Additionally, the addition of an extra 20% of potassium tert-butoxide (tBuOK) and reducing the TBD to 10% resulted in a BHET yield of 92% at 100 °C within 15 minutes [50].

**Table 2-1.** Summary of some recent investigations on chemical recycling of PET.

Co- solvent	Solvent: cosolvent: PET molar ratio	Catalyst	Catalyst content	Yield (Mol%)	Temp. (°C)	Pres. (MPa)	Time (min)	Ref.
Hydrolysis	s <sup>7</sup>							
-	-	TBHDPB <sup>8</sup>	20 wt.%	93.5	100	-	240	[8]

<sup>&</sup>lt;sup>7</sup> The final product of all listed hydrolysis processes is terephthalic acid.

<sup>&</sup>lt;sup>8</sup> Tributylhexadecylphosphonium bromide

**Table 2- 1.** (cont'd)

-		9 10	40 : 07	05.7	105	2	100	FO3	
-	-	NaHCO <sub>3</sub> <sup>9</sup> - KHCO <sub>3</sub> <sup>10</sup> (1:1)	40 wt.%	95.7	195	3	120	[9]	
-	10:0:1	None	-	93.5	300	3	1	[11]	
-	-	Hydrolase enzyme	-	98	68	1	1440	[3]	
Methanoly	sis <sup>11</sup>								
DCM <sup>12</sup>	50:50:1	K <sub>2</sub> CO <sub>3</sub> <sup>13</sup>	20 wt%	93.1	25	1	1440	[27]	
-	4:0:1	PIL-Zn <sub>2</sub> + <sup>14</sup>	2 wt%	90.3	170	-	60	[30]	
DMC <sup>15</sup>	2.4:3.4:1	LiOMe <sup>16</sup>	10 mol%	90	65	-	300	[31]	
ACN <sup>17</sup>	2.5:2.5:1	(ChCl/Zn(OAc)2 <sup>18</sup>	5 wt.%	90.1	170	-	60	[33]	
-	50:0:1	BLA <sup>19</sup>	21 wt.%	78	200		120	[32]	
-	49:0:1	OPA@Fe <sub>3</sub> O <sub>4</sub> <sup>20</sup>	4 wt%	83	200	-	60	[34]	
-	3:0:1	NEt <sub>3</sub>	17 v%	82	200	-	120	[35]	
Toluene	3:3:1	NEt <sub>3</sub>	17 v%	88	200	-	120	[35]	
Glycolysis <sup>21</sup>									
-	13:0:1	[BVim]NTf <sub>2</sub> -Zn <sup>2+22</sup>	20 wt.%	77.8	195	-	120	[51]	
-	59:0:1	e-MON <sup>23</sup>	0.01 wt.%	100	200	-	30	[38]	

Sodium bicarbonate
 Potassium bicarbonate
 The final product of all methanolysis processes is dimethyl terephthalate.

<sup>&</sup>lt;sup>12</sup> Dichloromethane

<sup>&</sup>lt;sup>13</sup> Potassium carbonate

<sup>&</sup>lt;sup>14</sup> Polyionic liquid (PIL)-zinc+

Dimethyl carbonateLithium methoxide

<sup>&</sup>lt;sup>17</sup> Acetonitrile

<sup>18</sup> Deep Eutectic solvent of Choline chloride-zinc acetate (1:1)
19 Bamboo leaf ash

Daniboo lear asin
 Orange peel ash-Fe<sub>3</sub>O<sub>4</sub>
 The product of PET glycolysis is bis(2-hydroxyethyl) terephthalate
 1-butyl-3-vinylimidazolium bis[(trifluoromethyl)sulfonyl] imide-zinc

<sup>&</sup>lt;sup>23</sup> Ultrathin exfoliated MnO<sub>2</sub> nanosheets

**Table 2- 1.** (cont'd)

-	6.2:0:1	SO <sub>4</sub> <sup>2-</sup> /HY-340 <sup>24</sup>	20 wt.%	85	195	-	220	[52]
-	10:0:1	DMIAC <sup>25</sup>	15 mol%	65	185	-	60	[53]
-	20:0:1	Zn(OAc) <sub>2</sub> - DMAP <sup>26</sup>	1.5 mol%	96 <sup>27</sup>	180	-	180	[41]
Anisole	12:4:1	Alkali metal <sup>28</sup>	4 mol%	86	153	-	120	[42]
Anisole	10:3:1	TBD	2 mol%	81.8	153	-	120	[42]
-	10:0:1	Zn(OAc) <sub>2</sub> -DBU <sup>29</sup>	0.4 wt.%	78.2	180	-	77	[45]
-	20:0:1	TBD:MSA <sup>30</sup>	5 mol%	91	180	-	120	[46]
-	15:0:1	Functionalized TBD <sup>31</sup>	10 mol%	91	190	-	45	[47]
-	13:0:1	HTBD-OAc <sup>32</sup>	3 mol%	85.9	190	-	90	[54]
-	12.5:0:1	Si-TBD <sup>33</sup>	15.5 mol%	88	190	-	102	[49]
MIA <sup>34</sup>	3:10:1	TBD	20 mol%	82	100	-	15	[50]
MIA	3:10:1	TBD	50 mol%	88	100	-	15	[50]
MIA- tBuOK <sup>35</sup>	3:0.2:10:1	TBD	10 mol%	92	100	-	15	[50]

Despite extensive research in the chemical depolymerization of PET, there is a persisting disparity between academic investigations and the practical needs of industries and current

<sup>24</sup> Nb<sub>2</sub>O<sub>5</sub>·nH<sub>2</sub>O

<sup>&</sup>lt;sup>25</sup> 1,3-dimethylimidazolium-2-carboxylate

<sup>&</sup>lt;sup>26</sup> Zinc acetate-4-dimethylaminopyridine

<sup>&</sup>lt;sup>27</sup> This number is the conversion; the yield was not reported.

<sup>&</sup>lt;sup>28</sup> Zinc acetate, sodium acetate, potassium acetate
<sup>29</sup> Zinc acetate-1,8-diazabicyclo[5.4.0]undec-7-enec (1:2)
<sup>30</sup> 1,5,7-Triazabicyclo[4.4.0]dec-5-ene:methanesulfonic acid
<sup>31</sup> Methyl 4-(2,3,4,6,7,8-hexahydro-1H-pyrimido[1,2-a]pyrimidine-1-carbonyl)

<sup>&</sup>lt;sup>32</sup> 1,5,7-Triazabicyclo[4.4.0]dec-5-ene-based protic ionic salt synthetized from acetate anion and HTBD<sup>+</sup> cation

<sup>&</sup>lt;sup>33</sup> Silica gel treated with 1,5,7-Triazabicyclo[4.4.0]dec-5-ene

<sup>&</sup>lt;sup>34</sup> 1-methylimidazole

<sup>&</sup>lt;sup>35</sup> 1-methylimidazole-potassium tert-butoxide

recycling infrastructure. One major obstacle is the utilization of non-commercialized catalysts, the commercialization of which requires a long time and effort and therefore cannot be deployed soon. Additionally, the large amount of the catalyst required further aggravates this challenge by considerably elevating the costs, with recovery that introduces another challenge. Even with affordable metallic salts, such as zinc acetate that are currently utilized on an industrial scale, separating the catalyst is nearly impossible. Lengthy processes further contribute to the issue, whether using non-commercialized or costly catalysts. Moreover, existing recycling companies have heavily invested in mechanical recycling and extrusion processes, hence it is crucial to reduce the additional capital expenditure by utilizing the existing resources effectively which encourages the adoption of chemical depolymerization techniques.

## 2.2 Paper Coating

Paper is a promising material for a wide variety of applications, including packaging, thanks to its low cost, abundant availability, flexibility, biodegradability, and high recyclability. Paper consists of long cellulosic fibers with slender structures that create its basic building blocks. The strength and flexibility of paper mainly stem from these fibers while they also contribute to the overall properties of paper such as tensile strength, and tear resistance [55].

Despite its advantages, paper has inherent limitations in its resistance to liquids and gases due to its hydrophilic nature and porous structure. Liquids such as water or oil can easily penetrate resulting in weakened properties when exposed to moisture or oil. To address these limitations, a variety of solutions such as treatments by coating, lamination, or functionalization can be applied to improve the mechanical and barrier properties of paper [56].

Substances such as paraffin wax, per- and polyfluoroalkyl compounds (PFAS) [57], and low-density polyethylene (LDPE) [58], are used as sizing agents in paper coatings or as

coatings/laminates themselves to improve water and oil permeability to paper. Unfortunately, PFAS is found to leach out from paper during the repulping processes, leading to environmental damage risks. Moreover, LDPE is non-biodegradable and cannot be recycled through the repulping processes [59].

Several eco-friendlier alternative materials for paper coatings are introduced using starch [60]–[62], polyvinyl alcohol (PVOH) [56], [63], soybean oil [64], and chitosan [59], [60], [65]–[68]. Additionally, polyhydroxyalkanoate (PHA) is recognized as biodegradable polymers that have been used as coating materials in the packaging industry. The disadvantage of biodegradability has been revealed to lack sufficient oxygen and water barrier properties that are necessary for packaging applications in commercial settings [69].

## 2.2.1 Polybutylene adipate-co-terephthalate (PBAT) for paper coating applications

PBAT is a hydrophilic polymer that has been commercialized for several decades as a substitute alternative for non-degradable material with wide applications in packaging. Its full biodegradability, thermoplasticity, high flexibility, and easy processability are underlying reasons for its potential applicability as a coating material. However, the poor mechanical and thermomechanical properties of PBAT can limit its mass application [70], [71].

Various methodologies are developed such as blending PBAT with thermoplastic starch, and bio-fillers such as cellulose, lignin, and chitin to enhance its properties while preserving its biodegradability [72]–[74]. Moreover, PLA/PBAT blends hold promise due to the combination of PLA's mechanical strength and PBAT's flexibility [75].

Studies show that lignin has several limitations including thermal and oxidative degradability, the tendency to agglomerate within host matrices, and variability in chemical structure depending on the feedstock source [76]. Additionally, low interfacial adhesion and

macro-phase separation between compounded PBAT with polylactic acid (PLA) potentially lead to immiscibility despite the similarity in carbonyl groups between PLA and PBAT [77]. There have been attempts to address this issue, such as the addition of corn stover as biomass filler [78], the addition of potato fruit juice in glycerol followed by extrusion-coating with a blend of PLA and PBAT in a multilayer coating [79], or compounding with Polyhedral oligomeric silsesquioxanes (POSS<sub>(epoxy)8</sub>) as an additive [80].

## 2.2.2 Economic feasibility of paper coating materials

Currently, the substitution of petrochemical-derived plastics for paper coating applications with biodegradable plastics elevates the packaging cost 6 to 10 times [81], [82]. So far, some investigations, only considering the cost of raw materials, have mentioned that bio-derived compounds, such as polysaccharides, are more readily available and tend to be less costly compared to synthetic compounds making them potential alternatives for food paper packaging applications [82]–[84].

Several publications have reported on the reduced cost of shipping due to the light weight of paper-based packages [85], the high cost of the lamination technique [81], the cost-inefficiency of using organic solvents in paper coating material synthesis [86], the low cost of the dip-casting coating process [85], the expensive production cost of nanoparticles for paper coating applications [85], and energy-intensive and costly process of treating of PBAT with isocyanate [85].

In summary, despite valuable investigations on analyzing the cost of large-scale production through natural synthesis, the cost-ineffectiveness and failure to manage the market needs through natural synthesis, have limited applications of biopolymer blends [87]. Hence modifying commercially available biodegradable and recyclable for paper coating applications is necessary.

#### REFERENCES

- [1] R. D. Allen and M. I. James, "Chemical Recycling of PET," *ACS Symp. Ser.*, vol. 1391, pp. 61–80, 2021.
- [2] J. Chen *et al.*, "Mechanical recycling of PET containing mixtures of phosphorus flame retardants," *J. Mater. Sci. Technol.*, vol. 194, pp. 167–179, 2024.
- [3] G. Arnal *et al.*, "Assessment of Four Engineered PET Degrading Enzymes Considering Large-Scale Industrial Applications," *ACS Catal.*, vol. 13, no. 20, pp. 13156–13166, 2023.
- [4] J. Zhou, T. G. Hsu, and J. Wang, "Mechanochemical Degradation and Recycling of Synthetic Polymers," *Angew. Chemie Int. Ed.*, vol. 62, no. 27, 2023.
- [5] Z. Laldinpuii, S. Lalhmangaihzuala, Z. Pachuau, and K. Vanlaldinpuia, "Depolymerization of poly(ethylene terephthalate) waste with biomass-waste derived recyclable heterogeneous catalyst," *Waste Manag.*, vol. 126, pp. 1–10, May 2021.
- [6] J. J. Rubio Arias and W. Thielemans, "Instantaneous hydrolysis of PET bottles: An efficient pathway for the chemical recycling of condensation polymers," *Green Chem.*, vol. 23, no. 24, pp. 9945–9956, 2021.
- [7] S. Zhang, Y. Xue, Y. Wu, Y. X. Zhang, T. Tan, and Z. Niu, "PET recycling under mild conditions via substituent-modulated intramolecular hydrolysis," *Chem. Sci.*, vol. 14, no. 24, pp. 6558–6563, 2023.
- [8] A. Barredo *et al.*, "Chemical recycling of monolayer PET tray waste by alkaline hydrolysis," *J. Environ. Chem. Eng.*, vol. 11, no. 3, 2023.
- [9] D. Stanica-Ezeanu and D. Matei, "Natural depolymerization of waste poly(ethylene terephthalate) by neutral hydrolysis in marine water," *Sci. Rep.*, vol. 11, no. 1, pp. 1–7, 2021.
- [10] F. Quartinello *et al.*, "Synergistic chemo-enzymatic hydrolysis of poly(ethylene terephthalate) from textile waste," *Microb. Biotechnol.*, vol. 10, no. 6, pp. 1376–1383, 2017.
- [11] A. Cəta, M. Micləu, I. Ienaşcu, D. Ursu, C. Tənasie, and M. N. Ştefənuţa, "Chemical recycling of Polyethylene Terephthalate (PET) waste using Sub- and supercritical water," *Rev. Roum. Chim.*, vol. 60, no. 5–6, pp. 579–585, 2015.
- [12] L. Shi and L. Zhu, "Recent Advances and Challenges in Enzymatic Depolymerization and Recycling of PET Wastes," *ChemBioChem*, vol. 25, no. 2, 2024.
- [13] B. Guo *et al.*, "Conformational Selection in Biocatalytic Plastic Degradation by PETase," *ACS Catal.*, vol. 12, no. 6, pp. 3397–3409, 2022.
- [14] B. Shojaei, M. Abtahi, and M. Najafi, "Chemical recycling of PET: A stepping-stone toward sustainability," *Polym. Adv. Technol.*, vol. 31, no. 12, pp. 2912–2938, 2020.

- [15] R. Brackmann, C. de Oliveira Veloso, A. M. de Castro, and M. A. P. Langone, "Enzymatic post-consumer poly(ethylene terephthalate) (PET) depolymerization using commercial enzymes," *3 Biotech*, vol. 13, no. 5, pp. 1–9, 2023.
- [16] I. Taniguchi, S. Yoshida, K. Hiraga, K. Miyamoto, Y. Kimura, and K. Oda, "Biodegradation of PET: Current Status and Application Aspects," ACS Catal., vol. 9, no. 5, pp. 4089–4105, 2019.
- [17] A. Khan, M. Naveed, Z. Aayanifard, and M. Rabnawaz, "Efficient chemical recycling of waste polyethylene terephthalate," *Resour. Conserv. Recycl.*, vol. 187, p. 106639, Dec. 2022.
- [18] M. Han, Depolymerization of PET Bottle via Methanolysis and Hydrolysis. Elsevier Inc., 2019.
- [19] A. M. Al-sabagh, F. Z. Yehia, G. Eshaq, A. M. Rabie, and A. E. Elmetwally, "Greener routes for recycling of polyethylene terephthalate," no. November, 2015.
- [20] W. K. Andrius A. Naujokas and M. Ryan, "RECOVERY PROCESS FORETHYLENE GLYCOL AND DIMETHYLTEREPHTHALATE," vol. 26, no. 19, 1991.
- [21] J. Scheirs, Polymer recycling: science, technology, and applications. 1998.
- [22] M. Goto, H. Koyamoto, A. Kodama, T. Hirose, and S. Nagaoka, "Depolymerization of polyethylene terephthalate in supercritical methanol," *J. Phys. Condens. Matter*, vol. 14, no. 44 SPEC ISS., pp. 11427–11430, 2002.
- [23] B. K. Kim, G. C. Hwang, S. Y. Bae, S. C. Yi, and H. Kumazawa, "Depolymerization of polyethyleneterephthalate in supercritical methanol," *J. Appl. Polym. Sci.*, vol. 81, no. 9, pp. 2102–2108, 2001.
- [24] Y. Yang, Y. Lu, H. Xiang, Y. Xu, and Y. Li, "Study on methanolytic depolymerization of PET with supercritical methanol for chemical recycling," *Polym. Degrad. Stab.*, vol. 75, no. 1, pp. 185–191, 2002.
- [25] M. Goto, "Chemical recycling of plastics using sub- and supercritical fluids," *J. Supercrit. Fluids*, vol. 47, no. 3, pp. 500–507, 2009.
- [26] M. Genta, M. Goto, and M. Sasaki, "Heterogeneous continuous kinetics modeling of PET depolymerization in supercritical methanol," *J. Supercrit. Fluids*, vol. 52, no. 3, pp. 266–275, 2010.
- [27] D. D. Pham and J. Cho, "Low-energy catalytic methanolysis of poly(ethyleneterephthalate)," *Green Chem.*, vol. 23, no. 1, pp. 511–525, 2021.
- [28] M. Shestakova and M. Sillanpää, "Chemosphere Removal of dichloromethane from ground and wastewater: A review," *Chemosphere*, vol. 93, no. 7, pp. 1258–1267, 2013.

- [29] N. Cayot, C. Lafarge, E. Bou-maroun, and P. Cayot, "Substitution of carcinogenic solvent dichloromethane for the extraction of volatile compounds in a fat-free model food system," *J. Chromatogr. A*, vol. 1456, pp. 77–88, 2016.
- [30] Z. Jiang *et al.*, "Poly(ionic liquid)s as efficient and recyclable catalysts for methanolysis of PET," *Polym. Degrad. Stab.*, vol. 199, p. 109905, 2022.
- [31] S. Tanaka, J. Sato, and Y. Nakajima, "Capturing ethylene glycol with dimethyl carbonate towards depolymerisation of polyethylene terephthalate at ambient temperature," *Green Chem.*, vol. 23, no. 23, pp. 9412–9416, 2021.
- [32] Z. T. Laldinpuii *et al.*, "Methanolysis of PET Waste Using Heterogeneous Catalyst of Biowaste Origin," *J. Polym. Environ.*, vol. 30, no. 4, pp. 1600–1614, 2022.
- [33] J. Tang *et al.*, "Mechanistic Insights of Cosolvent Efficient Enhancement of PET Methanol Alcohololysis," *Ind. Eng. Chem. Res.*, vol. 62, no. 12, pp. 4917–4927, 2023.
- [34] S. Lalhmangaihzuala, Z. T. Laldinpuii, V. Khiangte, G. Lallawmzuali, Thanhmingliana, and K. Vanlaldinpuia, "Orange peel ash coated Fe3O4 nanoparticles as a magnetically retrievable catalyst for glycolysis and methanolysis of PET waste," *Adv. Powder Technol.*, vol. 34, no. 7, p. 104076, 2023.
- [35] S. Muangmeesri, K. R. Baddigam, K. Navare, V. Apostolopoulou-kalkavoura, A. P. Mathew, and K. Van Acker, "Recycling of Polyesters by Organocatalyzed Methanolysis Depolymerization: Environmental Sustainability Evaluated by Life Cycle Assessment," pp. 3–9, 2024.
- [36] H. Abedsoltan, "A focused review on recycling and hydrolysis techniques of polyethylene terephthalate," *Polym. Eng. Sci.*, vol. 63, no. 9, pp. 2651–2674, 2023.
- [37] T. Wang, C. Shen, G. Yu, and X. Chen, "Metal ions immobilized on polymer ionic liquid as novel efficient and facile recycled catalyst for glycolysis of PET," *Polym. Degrad. Stab.*, vol. 194, Dec. 2021.
- [38] S. G. Son *et al.*, "Exfoliated manganese oxide nanosheets as highly active catalysts for glycolysis of polyethylene terephthalate," *FlatChem*, vol. 36, Nov. 2022.
- [39] S. Shirazimoghaddam, I. Amin, J. A. Faria Albanese, and N. R. Shiju, "Chemical Recycling of Used PET by Glycolysis Using Niobia-Based Catalysts," *ACS Eng. Au*, vol. 3, no. 1, pp. 37–44, Feb. 2023.
- [40] L. Wang, G. A. Nelson, J. Toland, and J. D. Holbrey, "Glycolysis of PET Using 1,3-Dimethylimidazolium-2-Carboxylate as an Organocatalyst," *ACS Sustain. Chem. Eng.*, vol. 8, no. 35, pp. 13362–13368, Sep. 2020.
- [41] K. R. D. Chiaie, A. P. Dove, F. R. Mcmahon, E. J. Williams, and M. J. Price, "Polymer Chemistry Dual-catalytic depolymerization of polyethylene," pp. 1450–1453, 2020.

- [42] N. H. Le, T. T. N. Van, B. Shong, and J. Cho, "Low-Temperature Glycolysis of Polyethylene Terephthalate," 2022.
- [43] S. Matsumura *et al.*, "Stability and Utility of Pyridyl Disulfide Functionality in RAFT and Conventional Radical Polymerizations," *J. Polym. Sci. Part A Polym. Chem.*, vol. 46, no. April, pp. 7207–7224, 2008.
- [44] K. Fukushima *et al.*, "Unexpected efficiency of cyclic amidine catalysts in depolymerizing poly(ethylene terephthalate)," *Journal of Polymer Science, Part A: Polymer Chemistry*, vol. 51, no. 7. pp. 1606–1611, 2013.
- [45] W. Chen, M. Li, X. Gu, L. Jin, W. Chen, and S. Chen, "Efficient glycolysis of recycling poly(ethylene terephthalate) via combination of organocatalyst and metal salt," *Polym. Degrad. Stab.*, vol. 206, Dec. 2022.
- [46] C. Jehanno, I. Flores, A. P. Dove, A. J. Müller, F. Ruipérez, and H. Sardon, "Organocatalysed depolymerisation of PET in a fully sustainable cycle using thermally stable protic ionic salt," *Green Chem.*, vol. 20, no. 6, pp. 1205–1212, 2018.
- [47] S. Nica *et al.*, "Functionalized 1,5,7-triazabicyclo [4.4.0] dec-5-ene (TBD) as Novel Organocatalyst for Efficient Depolymerization of Polyethylene Terephthalate (PET) Wastes," 2018.
- [48] C. Zhu, L. Yang, C. Chen, G. Zeng, and W. Jiang, "Metal-free recycling of waste polyethylene terephthalate mediated by TBD protic ionic salt: the crucial role of anionic ligand," *Phys. Chem. Chem. Phys.*, 2023.
- [49] Z. Fehér *et al.*, "Optimisation of PET glycolysis by applying recyclable heterogeneous organocatalysts," *Green Chem.*, vol. 24, no. 21, pp. 8447–8459, 2022.
- [50] I. Olazabal, E. J. L. Barrios, S. De Meester, C. Jehanno, and H. Sardon, "Overcoming the Limitations of Organocatalyzed Glycolysis of Poly(ethylene terephthalate) to Facilitate the Recycling of Complex Waste Under Mild Conditions," 2024.
- [51] T. Wang, C. Shen, G. Yu, and X. Chen, "Metal ions immobilized on polymer ionic liquid as novel efficient and facile recycled catalyst for glycolysis of PET," *Polym. Degrad. Stab.*, vol. 194, p. 109751, 2021.
- [52] S. Shirazimoghaddam, I. Amin, J. A. F. Albanese, and N. R. Shiju, "Chemical Recycling of Used PET by Glycolysis Using Niobia-Based Catalysts," 2023.
- [53] L. Wang, G. A. Nelson, J. Toland, and J. D. Holbrey, "Glycolysis of PET Using 1,3-Dimethylimidazolium-2-Carboxylate as an Organocatalyst," 2020.
- [54] C. Zhu, L. Yang, C. Chen, and G. Zeng, "Metal-free recycling of waste polyethylene terephthalate mediated by TBD protic ionic salts: the crucial role of anionic ligands †," pp. 27936–27941, 2023.

- [55] R. Aguado, D. Murtinho, and A. J. M. Valente, "A broad overview on innovative functionalized paper solutions," *Nord. Pulp Pap. Res. J.*, vol. 34, no. 4, pp. 395–416, 2019.
- [56] S. S. Hamdani, Z. Li, N. Sirinakbumrung, and M. Rabnawaz, "Zein and PVOH-Based Bilayer Approach for Plastic-Free, Repulpable and Biodegradable Oil- And Water-Resistant Paper as a Replacement for Single-Use Plastics," *Ind. Eng. Chem. Res.*, vol. 59, no. 40, pp. 17856–17866, 2020.
- [57] X. Trier, C. Taxvig, A. K. Rosenmai, and G. A. Pedersen, *Pfas in Paper and Board for food contact*. 2018.
- [58] R. H. Moynihan, D. G. Baird, and R. Ramanathan, "Additional observations on the surface melt fracture behavior of linear low-density polyethylene," *J. Nonnewton. Fluid Mech.*, vol. 36, no. C, pp. 255–263, 1990.
- [59] D. Kansal, S. S. Hamdani, R. Ping, N. Sirinakbumrung, and M. Rabnawaz, "Food-Safe Chitosan-Zein Dual-Layer Coating for Water- And Oil-Repellent Paper Substrates," ACS Sustain. Chem. Eng., vol. 8, no. 17, pp. 6887–6897, 2020.
- [60] A. Nair, D. Kansal, A. Khan, and M. Rabnawaz, "New alternatives to single-use plastics: Starch and chitosan- graft -polydimethylsiloxane-coated paper for water- and oil-resistant applications," *Nano Sel.*, vol. 3, no. 2, pp. 459–470, 2022.
- [61] S. S. Hamdani, Z. Li, E. Rolland, M. Mohiuddin, and M. Rabnawaz, "Barrier and mechanical properties of biodegradable paper bilayer-coated with plasticized starch and zein," *J. Appl. Polym. Sci.*, vol. 140, no. 8, pp. 1–15, 2023.
- [62] D. Kansal, S. S. Hamdani, R. Ping, and M. Rabnawaz, "Starch and Zein Biopolymers as a Sustainable Replacement for PFAS, Silicone Oil, and Plastic-Coated Paper," *Ind. Eng. Chem. Res.*, vol. 59, no. 26, pp. 12075–12084, 2020.
- [63] S. S. Hamdani, Z. Li, P. Ruoqi, E. Rollend, and M. Rabnawaz, "Oxygen and water vapor barrier properties of polyvinyl alcohol and zein bilayer-coated paper," *J. Appl. Polym. Sci.*, vol. 139, no. 7, 2022.
- [64] V. Kumar, A. Khan, and M. Rabnawaz, "A plant oil-based eco-friendly approach for paper coatings and their packaging applications," *Prog. Org. Coatings*, vol. 176, no. November 2022, p. 107386, 2023.
- [65] Z. Li and M. Rabnawaz, "Oil- And Water-Resistant Coatings for Porous Cellulosic Substrates," ACS Appl. Polym. Mater., vol. 1, no. 1, pp. 103–111, 2019.
- [66] A. Nair, D. Kansal, A. Khan, and M. Rabnawaz, "Oil- and water-resistant paper substrate using blends of chitosan-graft-polydimethylsiloxane and poly(vinyl alcohol)," *J. Appl. Polym. Sci.*, vol. 138, no. 21, pp. 1–12, 2021.
- [67] Z. Li, M. Rabnawaz, and B. Khan, "Response Surface Methodology Design for Biobased and Sustainable Coatings for Water- And Oil-Resistant Paper," ACS Appl. Polym. Mater.,

- vol. 2, no. 3, pp. 1378–1387, 2020.
- [68] D. Kansal and M. Rabnawaz, "Fabrication of oil- and water-resistant paper without creating microplastics on disposal," *J. Appl. Polym. Sci.*, vol. 138, no. 3, 2021.
- [69] L. Chen, P. Li, J. Guan, C. Xu, C. A. Xu, and Z. Yang, "Castor oil-based paper packaging coating with water resistance and degradability obtained by thiol-ene click reaction," *J. Appl. Polym. Sci.*, no. January, pp. 1–13, 2024.
- [70] S. Shankar and J. W. Rhim, "Effects of poly(butylene adipate-co-terephthalate) coating on the water resistant, mechanical, and antibacterial properties of Kraft paper," *Prog. Org. Coatings*, vol. 123, no. April, pp. 153–159, 2018.
- [71] D. K. Debeli, L. Wu, and F. Huang, "PBAT-based biodegradable nanocomposite coating films with ultra-high oxygen barrier and balanced mechanical properties," *Polym. Degrad. Stab.*, vol. 216, no. July, p. 110489, 2023.
- [72] S. J. Xiong *et al.*, "A strong, tough and cost-effective biodegradable PBAT/lignin composite film via intrinsic multiple noncovalent interactions," *Green Chem.*, vol. 25, no. 8, pp. 3175–3186, Mar. 2023.
- [73] S. J. Xiong *et al.*, "Economically Competitive Biodegradable PBAT/Lignin Composites: Effect of Lignin Methylation and Compatibilizer," *ACS Sustain. Chem. Eng.*, vol. 8, no. 13, pp. 5338–5346, 2020.
- [74] S. J. Xiong *et al.*, "Economically Competitive Biodegradable PBAT/Lignin Composites: Effect of Lignin Methylation and Compatibilizer," *ACS Sustain. Chem. Eng.*, vol. 8, no. 13, pp. 5338–5346, Apr. 2020.
- [75] M. Mohammadi, M. C. Heuzey, P. J. Carreau, and A. Taguet, "Morphological and rheological properties of PLA, PBAT, and PLA/PBAT blend nanocomposites containing CNCs," *Nanomaterials*, vol. 11, no. 4, 2021.
- [76] R. Shorey and T. H. Mekonnen, "Sustainable paper coating with enhanced barrier properties based on esterified lignin and PBAT blend," *Int. J. Biol. Macromol.*, vol. 209, no. PA, pp. 472–484, 2022.
- [77] Y. Ding, B. Lu, P. Wang, G. Wang, and J. Ji, "PLA-PBAT-PLA tri-block copolymers: Effective compatibilizers for promotion of the mechanical and rheological properties of PLA/PBAT blends," *Polym. Degrad. Stab.*, vol. 147, pp. 41–48, Jan. 2018.
- [78] R. Li, X. Zhu, F. Peng, and F. Lu, "Biodegradable, Colorless, and Odorless PLA/PBAT Bioplastics Incorporated with Corn Stover," *ACS Sustain. Chem. Eng.*, Jun. 2023.
- [79] S. Poulose, J. Toriseva, J. Lahti, I. Jönkkäri, M. S. Hedenqvist, and J. Kuusipalo, "A Green High Barrier Solution for Paperboard Packaging based on Potato Fruit Juice, Poly(lactic acid), and Poly(butylene adipate terephthalate)," *ACS Appl. Polym. Mater.*, vol. 4, no. 6, pp. 4179–4188, 2022.

- [80] S. Qiu, Y. Zhou, I. N. Waterhouse, R. Gong, J. Xie, and K. Zhang, "Optimizing interfacial adhesion in PBAT / PLA nanocomposite for biodegradable packaging fi lms," vol. 334, no. June 2020, 2021.
- [81] A. Ojha, A. Sharma, M. Sihag, and S. Ojha, "Food packaging materials and sustainability-A review," *Agric. Rev.*, vol. 36, no. 3, p. 241, 2015.
- [82] M. Stoica, V. Marian Antohi, M. Laura Zlati, and D. Stoica, "The financial impact of replacing plastic packaging by biodegradable biopolymers A smart solution for the food industry," *J. Clean. Prod.*, vol. 277, p. 124013, 2020.
- [83] A. P. Ananda *et al.*, "A Relook at Food Packaging for Cost Effective by Incorporation of Novel Technologies," *J. Packag. Technol. Res.*, vol. 1, no. 2, pp. 67–85, 2017.
- [84] K. V. Aleksanyan, "Polysaccharides for Biodegradable Packaging Materials: Past, Present, and Future (Brief Review)," *Polymers (Basel)*., vol. 15, no. 2, 2023.
- [85] K. Zeng, J. Gu, and C. Cao, "Facile Approach for Ecofriendly, Low-Cost, and Water-Resistant Paper Coatings via Palm Kernel Oil," *ACS Appl. Mater. Interfaces*, vol. 12, no. 16, pp. 18987–18996, 2020.
- [86] Z. Li *et al.*, "A closed-loop and sustainable approach for the fabrication of plastic-free oil-And water-resistant paper products," *Green Chem.*, vol. 21, no. 20, pp. 5691–5700, 2019.
- [87] V. T. Weligama Thuppahige and M. A. Karim, "A comprehensive review on the properties and functionalities of biodegradable and semibiodegradable food packaging materials," *Compr. Rev. Food Sci. Food Saf.*, vol. 21, no. 1, pp. 689–718, 2022.
- [88] S. Tanaka *et al.*, "Depolymerization of Polyester Fibers with Dimethyl Carbonate-Aided Methanolysis," *ACS Mater. Au*, 2023.

## **Chapter 3. MATERIALS AND METHODS**

Part of this chapter is published as:

Khan, A., Naveed, M., Aayanifard, z., and Rabnawaz, M., "Efficient chemical recycling of waste polyethylene terephthalate," *Resources, Conservation and Recycling*, 2022.

Aayanifard, Z., Khan, A., Naveed, N., Schager, J., Rabnawaz, M., "Rapid depolymerization of PET by employing an integrated melt-treatment and diols," *Polymer*, 2023.

Aayanifard, Z., Saffron, C. M., Hamdani, S. S., Elkholy, H. M., Rabnawaz, M., "Technoeconomic Analysis for Biodegradable and Recyclable Paper Coated with Synthetic Ionic PBAT For Packaging Application," *ACS Sustainable Chemistry and Engineering*, 2024.

Part of it is submitted as:

Aayanifard, Z., Khan, A., Naveed, N., Saffron, C. M., Rabnawaz, M., "Enhanced Glycolysis of Post-Consumer Polyethylene Terephthalate: Synergizing Melt-Pretreatment with Organic Catalysis," 2024.

This chapter gives detailed information related to the materials and methods used for the chemical depolymerization of polyethylene terephthalate (PET). Additionally, it gives insights into the methods of technoeconomic analysis (TEA) of ionic polybutylene adipate-co-terephthalate (CPBAT) paper coating.

#### 3.1 Materials

Polyethylene terephthalate (PET) coke bottles (SP code #1) were purchased from a local Meijer store in Michigan, USA. Zinc acetate (Sigma Aldrich), zinc 2-ethyl hexanoate (AlfaAesar), bis (2-hydroxyethyl) terephthalate (BHET, Sigma Aldrich), 1,4-cyclohexanedimethanol (CHDM, Sigma Aldrich), 4,8-bis(hydroxymethyl)tricyclo[5.2.1.0<sup>2.6</sup>]decane (BHTD, Sigma Aldrich), ethylene glycol anhydrous (EG, 99.8 Sigma Aldrich), methanol (MeOH, 99.8%, Sigma Aldrich), dimethyl terephthalate (DMT, Sigma Aldrich), phenol crystal (unstabilized, reagent plus, >99%, Sigma Aldrich), 1,1,2,2-tetrachloroethane (98.5+%, Thermo Scientific), 1,5,7-triazabicyclo[4.4.0]dec-5-ene (TBD, 98%, Sigma Aldrich), 1,8-diazabicyclo[5.4.0]undec-7-ene (DBU, 96%, Sigma Aldrich) were used as received.

#### 3.2 Pretreatment Process

The melt pretreatment was performed using a DSM Xplore 15 cc Micro Extruder equipped with a co-rotating conical twin-screw. Before extrusion, the PET waste bottles were shredded, cleaned, and vacuum-dried at 60-70 °C. Afterward, the clean PET was ground using a Wiley® Mini Cutting Mill from a ~3 cm² surface area to a size of ~1 mm². For samples containing catalysts, ground PET was mixed with the catalyst and diols, and fed into Micro Extruder through a hopper for compounding for 4 minutes at 280 °C. The melted polymer samples were injection molded using a 3.5 cc injection mold and fed into a cooled MeOH bath. The pretreated PET samples were dried at room temperature and kept in an air-tight bag.

When metallic catalysts at higher concentrations than 1% were used, the catalyst was directly added at the time of extrusion, otherwise, the catalyst was initially dissolved in a solution, mixed with PET, and vacuum-dried for homogeneous dispersion of catalyst and ground PET. Then the mixture of PET and catalyst was extruded with/without the addition of selected diols. Schematic of the melt-pretreatment process is depicted in *Figure 3-1*.



**Figure 3-1.** Melt-pretreatment procedure starting from a) removing the cap and label of the PET bottle, b) washing with water and detergent, c) shredding, d) grinding, e) Addition of catalyst with/without diols, f) extrusion, and g) quenching in cold methanol.

## 3.3 Depolymerization Process

In all scenarios, the depolymerization reaction was carried out inside a 15 mL high-pressure reaction flask using approximately 300 mg of unpretreated/pretreated PET. Depending on the experiment, a certain amount of catalyst was added during the depolymerization. Once a clear solution was obtained, the reaction was considered to be finished.

## 3.3.1 Methanolysis

The methanolytic depolymerization of some of the samples occurred in the presence of 1.35 mol% zinc acetate, referred to as the external catalyst in the published manuscript. When the methanolysis reaction was finished, the reaction flask was cooled to room temperature, and the unreacted compounds were filtrated, followed by washing with chloroform to dissolve the monomers. The filtered residue with the filter was vacuum-dried at 60-70 °C for 2 hours. After evaporation of the solvent, the filter paper was weighed to reveal the mass of PET that was not depolymerized. To calculate the % depolymerization the following equation was used:

 $\% \ depolymerization \\ = \frac{\textit{Initial weight of PET} - \textit{Solid residues left after depolymerization}}{\textit{Initial weight of PET}} \times 100$ 

#### 3.3.2 Glycolysis

In the case of PET glycolysis, the addition of the so-called external catalyst was eliminated, and the catalyst was added only during the melt-pretreatment process. After the glycolytic reaction was finished and the reaction was slightly cooled down, boiling water was added, and the water-insoluble residue was filtered. The filter paper with residual PET and other compounds was vacuum-dried at 60 °C for analysis. The filtrate was cooled down overnight at 4 °C to form BHET crystals. The needle-like crystals were vacuum-dried at 60 °C. The weighed crystal was used to calculate the yield of the reaction.

#### 3.4 Characterization

## 3.4.1 Analysis of pretreated samples

Pretreated samples were characterized by their degree of crystallinity and molecular weights. The characterization methods are explained in detail in the following sections.

## 3.4.1.1 Differential Scanning Calorimetry (DSC)

For analyzing the thermal properties of polymers, Differential Scanning Calorimetry

(DSC) is the most widely used technique used to measure the heat flow rate between a substance and a reference when the sample is exposed to a controlled temperature program. Using this technique, the temperature is ramped linearly while the calorimetric data is quantitatively recorded [1]. This method allows the determination of melting  $(T_m)$ , crystallization  $(T_c)$ , and glass transition temperatures  $(T_g)$ , as well as revealing data about the enthalpy and entropy changes. Characterization of glass transition and the alterations in heat capacity and latent heat [2].

The glassy state is a thermodynamic phenomenon that is not only observed in polymers but also inorganic melts, metallic elements, nonmetallic, etc. The definition and nature of glass transition and glass transition temperature is a controversial topic in condensed matter physics. So far, it has been revealed that the glass transition temperature is related to the number-averaged molecular weight and cohesive energy of the polymer. There also exists a correlation between glass transition temperature and the melting point [3].

Crystallization of polymers during processing is a complex phenomenon that is impacted by mechanical (such as flow and pressure) and thermal (such as cooling rate and temperature gradient) conditions as well as the surface of the processing tools [4]. When the PET sample is heated during the DSC analysis, cold crystallization occurs at temperatures above the  $T_g$  and well below the melting temperature, triggered by the nuclei that were grown during the previous cooling step or by exposure to temperatures below the  $T_g$  [5].

To calculate the degree of crystallinity of the PET samples, it is necessary to determine the heat of fusion of the sample [2]. The crystalline melting temperature in the DSC plot is an endothermal peak. By integrating the area of endothermal peak, heat of fusion can be calculated within the melting temperature range. Using the data from the second heating cycle, the degree of crystallinity can be obtained from the equation below, with the assumption that the relationship between endothermal peak area and crystallinity is linear [5], which strongly depends on the

estimation of the baseline position [2]. The absolute mass degree of crystallinity is the ratio of the enthalpy of fusion, the difference of the enthalpy of melting ( $\Delta H_{\rm m}$ ) and the enthalpy of cold crystallization ( $\Delta H_{\rm c}$ ), of the semi-crystalline PET sample and the enthalpy of fusion fully crystalline PET ( $\Delta m^{\circ} = 140.1 \text{ J/g}$ ) [6]–[9].

% Crystallinity = 
$$\frac{\Delta H_m - \Delta H_c}{\Delta m^0} \times 100$$

Differential Scanning Calorimetry (DSC) analysis of various PET samples was performed using Q-100 (TA Instruments, New Castle, DE) instrument. 5 to 10 mg of the samples were weighed and, in the first cycles, heated in the range of -80 °C to 300 °C with an equilibration rate of 10 °C/min to remove processing history of the polymer (e.g., previous shear stress, thermal, mechanical, and crystallization) [7]. In the second cycle, the samples were cooled down to 0 °C and heated to 300 °C at the same ramping heat. The  $T_g$ ,  $T_c$ , and  $T_m$  were determined using Universal Analysis 2000 software, V4.5 (TA Instruments, Delaware).

#### 3.4.1.2 Inherent viscosity

Viscosity is dependent on molecular weight distribution for polymers and increases with an increase in the Mw. Determining the viscosity of a diluted solution can reveal information about some of the molecular characteristics of PET, such as molecular weight and chain length [10]. In most cases, the viscosity of the polymer is reduced during the extrusion process [11]. Since the viscosity of a polymer dissolved in a solution depends on the solvent and temperature, the condition for all samples were kept constant [10].

Herein, the inherent viscosity was used to indirectly measure the molecular weight of some of the PET samples, where higher inherent viscosity shows higher molecular weight and viceversa. In this analysis, ~0.25 g of PET sample was dissolved in 60/40 phenol/1,1,2,2-tetrachloroethane solution following ASTM D6303-18 (Standard Test Method for Determining

Inherent Viscosity of Poly(Ethylene Terephthalate)-PET) [12]. For determining the solution viscosity using this method a single concentration was required to measure the flow time of the solution and no successive dilution was needed [10].

After the dissolution of PET samples in the solvent, the solution was cooled down to room temperature and poured into an Ubbelohde viscometer. The time of solution containing the sample traveling a specific distance in the Ubbelohde viscometer compared to the time for the solution alone was used for calculating the inherent viscosity using the following formula:

$$\eta_{inh} = \ln \frac{\frac{t}{t_0}}{c}$$

In this formula, t is the flow time of polymer solution (s),  $t_0$  is the flow time of pure solvent mixture (s), and c is the polymer solution concentration (g/dl).

## 3.4.1.3 Dispersive X-ray Spectroscopy (EDX)

EDX is a non-destructive analysis of pure or mixtures of multiple compounds revealing qualitative and quantitative data about the crystal size and structure, degree of crystallinity, microstructure, and unknown crystalline materials and solids. This analytical technique is widely used in catalysis and nanomaterials by generating patterns of components in multi-component mixtures [11]. To identify the presence of zinc atoms after the melt-extrusion process, EDX was used. The instrument was a Tescan MIRA to perform the scanning electron microscopy (SEM) analysis with an EDAX Pegasus II EDS detector using Team software.

#### 3.4.2 Analysis of depolymerization reaction

## 3.4.2.1 Attenuated Total Reflection-Fourier Transform Infrared (ATR-FTIR)

To monitor the progress of the depolymerization and the formation of monomers, ATR-FTIR analysis was used to identify the characteristic peaks of both the polymer and monomer. The ATR-FTIR analysis was performed using a Shimadzu FTIR spectrometer IR-Prestige21

(Shimadzu Co., Columbia, MD), that was equipped with an attenuated-total-reflection (ATR) accessory (PIKE Technologies, Madison, WI). Samples were taken from the clear upper layer of the reaction mixture, and ATR-FTIR spectra were recorded at 22 °C, averaging 64 scans over a wavenumber range of 4000-400 cm-1 with a resolution of 4 cm<sup>-1</sup>.

#### 3.4.3 Analysis of products

## 3.4.3.1 Gas Chromatography-Mass Spectrometry (GC-MS)

Gas chromatography (GC) is an analytical technique to separate volatile and semi-volatile compounds while mass spectrometry (MS) is utilized to identify the compounds using the obtained structural information [13].

100 μL of NMZA samples at a concentration of 500 ng/μL were evaporated to dryness, followed by the addition of 100 μL of N-methyl-N-tertbutyldimethylsilyltrifluoroacetamide (MTBSTFA, Sigma Aldrich, St. Louis, MO) with 1% tert-butyldimethylsilyl chloride (TBDMSCl, Sigma Aldrich, St. Louis, MO), derivatized at 60 °C for 16 hours. For conducting the GC-MS analysis, 1 μL of the derivatized sample was injected in split mode (1:10) with an injector temperature of 275 °C. Helium was used as the carrier with flow rate of 1.0 mL/min. Separation was achieved with the following temperature program: 40 °C for 1 minute; ramped at 20 °C/min to 320 °C; held at 320 °C for 5 minutes.

GC-MS analysis was carried out using an Agilent 7890A GC that uses capillary flow technology (CFT) that is also capable of two-dimension gas chromatography (GCxGC) [14], [15]. The GC column was coupled a quadrupole spectrometer, 5975C inert XL MSD (Agilent, Santa Clara, CA), which is a Mass Selective Detector (MSD) with the Triple-Axis High Energy Diode (HED) Electron Multiplier (EM) detector [16]. For separation, Agilent J&W VF-5ms column (30 m x 0.25 mm x 0.25 μm) was utilized with an inert 5% phenylmethyl polysiloxane column that

has excellent selectivity and inertness to a wide range of semipolar and even polar compounds [17].

The carrier gas with the analytes was sprayed from a small nozzle into a partially vacuumed chamber. Helium was sprayed at a wider angle due to higher diffusion coefficient while the heavier compounds were sprayed at a narrower angle. This resulted in the organic compound becoming separated from helium by passing the vacuum region straightly and entering the ion source [13]. Ionization was performed using 70 eV electron ionization during which energetic electrons bombarded the molecules leading to fragmentation of some of the molecules. The accelerated ions were rapidly sorted based on their mass (m) to charge (z) ratio (m/z) in a mass analyzer by use of a magnetic or electric field [18].

The mass spectrometer was operated in scanning mode with a scan range of m/z 45 to 500. The mass spectrometer (MS) was served as the detector, producing a chromatogram that shows the amount of each compound based to its retention time with the essential data dimension referring to as a mass spectrum that presents a histogram exhibiting the quantity of each ion against its m/z [18]. MS worked as a unique identifier that enabled the identification of the ethylene glycol and the 2TBDMS peak with retention time of 8.9 min on the chromatogram by comparing the background-subtracted mass spectrum to the National Institute of Standards and Technology (NIST) library.

# 3.4.3.2 Liquid Chromatography-Mass Spectrometry (LC-MS)

Another analytical technique for identifying the compounds present in a multi-compound sample is LC-MS. Using this technique combined with photodiode array (PDA), the depolymerization products were identified and quantified after the reaction was finished. Several mg of the sample was weighed out in a microfuge tube, then dissolved in 1 mL methanol, followed by dilution in 75% methanol (1:100 and 1:1000). Analysis was performed using Liquid

chromatography-photodiode-array-mass spectrometry (LC-PDA-MS).

Water ACQUITY UPLC BEH C18 Column, (130Å (pore size), 1.7 µm (particle size), 2.1 mm (inner diameter) X 100 mm (length)) was used for the ultra-performance liquid chromatography (UPLC) separations. BEH C18 (ethylene bridged hybrid- cyclo[18]carbon) is a nonpolar stationary phase with trifunctionally bonded amide particles to retain polar compounds in what is called hydrophilic interaction chromatography [19]. Water + 0.1% formic acid was used as the mobile phase.

Data obtained from MS (e.g., accurate mass, retention time, structure of the unknown compounds through the fragmentation patterns, etc.) was used to identify compounds, while photodiode array (PDA) gave data for quantification of the compounds. A standard curve was made from standard BHET (monomer, dimer, trimer).

## 3.4.3.2 Nuclear Magnetic Resonance (NMR)

To record the  $^{1}$ H and  $^{13}$ C NMR spectra for the selected PET samples, a 500/54 Premium Shielded Spectrometer of Agilent Technologies was used. The chemical shifts  $\delta$  of these spectra were recorded in ppm. Deuterated chloroform was used to dissolve the methanolytic products while glycolytic products were dissolved in Deuterated Dimethyl sulfoxide-d6 (DMSO).

#### 3.5 Energy Requirement Calculation

For comparing the energy requirement of the two-step recycling of PET with a base case scenario where PET is directly exposed to depolymerization without melt-pretreatment, the energy demand for both processes was calculated and compared. In this analysis, the mass balance was reported in grams while energy balance values were based on kilojoules (kJ). The reference conditions of 25 °C and 1 bar of pressure were assumed. When determining thermophysical

properties such as specific heat and latent heat of vaporization, the NIST<sup>36</sup> database through Aspen software or estimation based on Group Contribution was adopted. Data from bench-top experiments were used for calculating the energy requirement and the instrument was utilized in the laboratories at School of Packaging at Michigan State University.

# 3.6 Technoeconomic analysis (TEA) of ionic polybutylene adipate-co-terephthalate

## (CPBAT) for paper coating applications

Technoeconomic analysis (TEA) demonstrates technical requirement, feasibility, and economic viability of a process, method, product and so on. TEA usually concentrates on the production phase, but it can also include upstream and downstream processes. The outcomes of a TEA are valuable for optimizing the process design, evaluation the total capital investment and determining the minimum selling price of the final product, like the cost per kilogram of a biofuel. In a comprehensive TEA, mass and energy balances are calculated for each unit operation, along with estimates of capital and operating costs. TEA aids decision-making, including R&D support or investment decisions, from both technological and economic viewpoints [20].

A spreadsheet was created to outline the processes starting from drying commercial PBAT to the sale of ionized/COOH-PBAT (CPBAT) and CPBAT coated on Kraft paper (CPBAT-K) as well as on starch-coated paper (CPBAT-S). The process flow diagram (PFD) was designed using *Visio* software illustrating the production journey, from the drying of PBAT in a rotary dryer, followed by treating the high molecular weight underwent to produce low molecular PBAT-diols. The PBAT-diols were, then, subjected to ring opening addition reactions yielding CPBAT polymers, the ionization of which occurred by mixing with ammonium hydroxide aqueous solution. The emulsified CPBAT was coated on both Kraft paper (CPBAT-K) and starch-coated

\_

<sup>&</sup>lt;sup>36</sup> National Institute of Standards and Technology

paper (CPBAT-S) and dried as final products.

The equipment were designed either using Aspen *HYSYS* software or available published resources [21], [22]. Equipment costs were determined through quotations from suppliers and insights from other publications [21]–[24]. To determine the total capital investment, various components of direct costs (e.g., purchased equipment, instrumentation, piping, etc.), as well as indirect costs (e.g., engineering, construction, legal fees, etc.), were considered. Finally, cost, and minimum selling price (MSP) of CPBAT (\$/kg), CPBAT-K (\$/m²), and CPBAT-S (\$/m²) were determined.

#### REFERENCES

- [1] R. B. P. Joseph D. Menczel, *Thermal Analysis of Polymers Fundamentals and Applications*. 2009.
- [2] P. Gray, "POLYMER DETERMINATIONS BY DSC," vol. 1, pp. 563–579, 1970.
- [3] J. Wu, "The Glassy State, Ideal Glass Transition, and Second-Order Phase Transition," no. June 1998, pp. 143–150, 1999.
- [4] J. Haudin and S. A. E. Boyer, "Crystallization of Polymers in Processing Conditions: An Overview," *Int. Polym. Process.*, vol. 32, pp. 545–554, 2017.
- [5] M. C. Righetti, "Crystallization of polymers investigated by temperature-modulated DSC," *Materials (Basel).*, vol. 10, p. 442, 2017.
- [6] P. G. Karagiannidis, A. C. Stergiou, and G. P. Karayannidis, "Study of crystallinity and thermomechanical analysis of annealed poly(ethylene terephthalate) films," *Eur. Polym. J.*, vol. 44, no. 5, pp. 1475–1486, 2008.
- [7] R. Sharma, S. N. Maiti, R. Sharma, and S. N. Maiti, "Effects of Crystallinity of PP and Flexibility of SEBS- g-MA Copolymer on the Mechanical Properties of PP / SEBS-g-MA Blends Effects of Crystallinity of PP and Flexibility of SEBS-g-MA Copolymer on the Mechanical Properties of PP / SEBS-g-MA Blends," vol. 2559, 2014.
- [8] Y. Kong and J. N. Hay, "The enthalpy of fusion and degree of crystallinity of polymers as measured by DSC," *Eur. Polym. J.*, vol. 39, no. 8, pp. 1721–1727, 2003.
- [9] Z. Yang, H. Peng, W. Wang, and T. Liu, "Crystallization behavior of poly(ε-caprolactone)/layered double hydroxide nanocomposites," *J. Appl. Polym. Sci.*, vol. 116, no. 5, pp. 2658–2667, 2010.
- [10] N. B. Sanches, M. L. Dias, and E. B. A. V Pacheco, "Comparative techniques for molecular weight evaluation of poly (ethylene terephthalate) (PET)," vol. 24, pp. 688–693, 2005.
- [11] G. S. P. Hayat Khan, Aditya S. Yerramilli, Adrien D'Oliveira, Terry L. Alford, Daria C. Boffito, "Khan Experimental methods in chemical engineering X-ray diffraction spectroscopy XRD." Canadian Journal Chemical Engineering, 2020.
- [12] ASTM International, "Determining Inherent Viscosity of Poly (Ethylene iTeh Standards iTeh Standards," pp. 5–6.
- [13] R. A. Hites, "Gas Chromatography Mass Spectrometry," *Environmetal Sci. Technol.*, pp. 609–626, 2015.
- [14] "Agilent 7890B GC System." [Online]. Available: https://www.agilent.com/en/product/gas-chromatography/gc-systems/7890b-gc-system.

- [15] W. M. Geiger and B. A. Mcelmurry, *Sample Introduction Systems in ICPMS and ICPOES*. Elsevier B.V., 2020.
- [16] M. S. D. Overview, "Agilent 5975C TAD Series GC / MSD System Data Sheet GC / MSD Overview Agilent 5975C TAD Series MSD System."
- [17] "Agilent J&W VF-5ms," 2024. [Online]. Available: https://www.agilent.com/en/product/gc-columns/low-bleed-gc-ms-columns/vf-5ms-columns.
- [18] T. M. Lovestead and K. N. Urness, "Gas Chromatography Mass Spectrometry (GC MS)\*," vol. 10, pp. 1–16.
- [19] "ACQUITY UPLC BEH C18 Column, 130Å, 1.7 μm, 2.1 mm X 100 mm," 2024. [Online]. Available: https://www.waters.com/nextgen/us/en/shop/columns/186002352-acquity-uplc-beh-c18-column-130a-17--m-21-mm-x-100-mm-1-pk.html.
- [20] R. Mahmud, S. Moniruzzaman, K. High, and M. Carbajales-dale, "Integration of technoeconomic analysis and life cycle assessment for sustainable process design A review," *J. Clean. Prod.*, vol. 317, no. July, p. 128247, 2021.
- [21] M. S. Peters and K. D. Timmerhaus, *Plant design and economics for chemical engineers*. Journal of Chemical Education, 1958.
- [22] A. Singh *et al.*, "Socioeconomic Impact Analysis of Enzymatic Recycling of Poly (Ethylene Terephthalate)," *Joule*, vol. 5, pp. 1–25, 2021.
- [23] P. Huang *et al.*, "Peng Huang, Ashiq Ahamed, Ruitao Sun, Guilhem X. De Hoe, Joe Pitcher, Alan Mushing, Fernando Lourenc, o, and Michael P. Shaver \*," 2023.
- [24] T. Uekert *et al.*, "Technical, Economic, and Environmental Comparison of Closed-Loop Recycling Technologies for Common Plastics," *ACS Sustain. Chem. Sci. Eng.*, vol. 11, no. 3, pp. 965–978, 2023.

# Chapter 4. EFFICIENT CHEMICAL RECYCLING OF POLYETHYLENE TEREPHTHALATE (METHANOLYSIS)

A version of this chapter is published as:

Khan, A., Naveed, M., Aayanifard, Z., Rabnawaz, M., "Efficient chemical recycling of waste polyethylene terephthalate," *Resources, Conservation and Recycling*, 2022.

## 4.1 Summary

In this chapter, the details of an energy-efficient depolymerization methodology for recycling post-consumer poly (ethylene terephthalate) (PET) into its parent monomers are presented. The process started with a melt pretreatment in the presence of various catalysts with or without diols, followed by quenching in cold methanol. Subsequently, the pretreated PET samples underwent a methanolysis reaction with a secondary catalyst at different temperatures, methanol:PET molar ratios, catalyst concentrations, and reaction periods. In this research, the lowcost and environmentally benign zinc 2-ethylhexanoate catalyst was utilized for the first time in the chemical recycling of PET. The findings revealed that integrating the melt-pretreatment process can drastically reduce depolymerization time by lowering the crystallinity of the PET samples and creating active sites within the PET structure. Differential Scanning Calorimetry (DSC) was employed to gain insights into the impact of melt-pretreated PET samples. Additionally, analysis of the products using Nuclear Magnetic Resonance Spectroscopy (NMR) and Gas Chromatography-Mass Spectrometry (GC-MS) demonstrated a high yield of dimethyl terephthalate (DMT). Exploring the energy efficiency of the process revealed at least an 8-fold reduction in the energy demand for depolymerizing melt-treated PET compared to untreated PET.

## 4.2 Materials and Methods

#### 4.2.1 Materials

PET Coke bottles (SP code #1) were purchased from a local Meijer store in Michigan, USA. Zinc acetate (Zn(OAc)<sub>2</sub>), Bis (2-hydroxyethyl) terephthalate (BHET), 1,4-Cyclohexanedimethanol (CHDM), 4,8-Bis(hydroxymethyl)tricyclo[5.2.1.0<sup>2,6</sup>]decane (BHTD), Methanol (MeOH, 99.8%), and Dimethyl terephthalate (DMT) were purchased from Sigma Aldrich. Zinc 2-ethylhexanoate (Zn-EH) was purchased from AlfaAesar. DI water was used in all

experiments. All chemicals were used as received.

# 4.2.2 Experimental

*Melt pretreatment*: PET bottles were washed with water and detergent after removing caps and labels. They were shredded using scissors into ~3 cm<sup>2</sup> pieces followed by washing with acetone, drying, and grinding into a size of ~1 mm<sup>2</sup>. For initial screening, 10 grams of the ground PET was mixed with 0.25 g (1.35 mmol) of zinc acetate or 0.475 g of zinc 2-ethylhexanoate (1.35 mmol) and 0.7 g (17.5 weight%) of diol according to *Table 4- 1* and fed into the extruder at 280 °C for 4 minutes.

**Table 4-1**. Summary of sample specifications.

Sample	Formulation							
Code	PET	Extruded	<sup>1</sup> Zn(OAc) <sub>2</sub>	<sup>2</sup> Zn-EH	Additives (g)			
			(mmol)	(mmol)				
$S_0$	10.0 g	NO	-	-	-			
$S_1$	10.0 g	YES	-	-	-			
$S_2$	10.0 g	YES	1.35	-	-			
$S_3$	10.0 g	YES	-	1.35	-			
$S_4$	10.0 g	YES	1.35	-	<sup>3</sup> BHET (0.7 g)			
$S_5$	10.0 g	YES	-	1.35	BHET (0.7 g)			
$S_6$	10.0 g	YES	1.35	-	<sup>4</sup> CHDM (0.7 g)			
$S_7$	10.0 g	YES	-	1.35	CHDM (0.7 g)			
$S_8$	10.0 g	YES	1.35	-	<sup>5</sup> BHTD (0.9 g)			
$S_9$	10.0 g	YES	-	1.35	BHTD (0.9 g)			

<sup>&</sup>lt;sup>1</sup> Zinc acetate (used during the melt pretreatment, so-called "internal catalyst")

<sup>&</sup>lt;sup>2</sup> Zinc 2-ethylhexanoate (used during the melt pretreatment, so-called "internal catalyst");

<sup>&</sup>lt;sup>3</sup> Bis(2-hydroxyethyl) terephthalate (used during the melt pretreatment, so-called "internal additive")

<sup>&</sup>lt;sup>4</sup> 1,4-Cyclohexanedimethanol (used during the melt pretreatment, so-called "internal additive")

<sup>&</sup>lt;sup>5</sup> 4,8-Bis(hydroxymethyl)tricyclo[5.2.1.0<sup>2,6</sup>]decane (used during the melt pretreatment, so-called "internal additive")

## 4.2.2.1 Depolymerization reaction

Melt pretreatment in the absence of catalyst and diols: In the initial study, two samples, named S<sub>0</sub> and S<sub>1</sub>, were examined to investigate the impact of the hindrance by the crystalline region on the methanolysis of PET. The S<sub>0</sub> sample was not pretreated, while the S<sub>1</sub> sample was melted in an extruder followed by quenching in methanol to prevent any crystal growth which could enhance depolymerization. ~300 mg of each sample was separately depolymerized in methanol in the presence of 2 weight% (1 mmol) of zinc acetate as a catalyst (a so-called external catalyst that was directly added during the depolymerization process) at 160 °C. The reaction flask was cooled down to room temperature after 3 hours and the products from depolymerization were filtered and washed with chloroform followed by drying.

Melt pretreatment in the presence of only catalysts: In the second study, the impact of different catalysts, zinc acetate and zinc 2-ethylhexanoate, during the melt-extrusion process was tested. Zinc 2-ethylhexanoate was used in this study for the first time for depolymerization of PET, being 10 times less expensive than zinc acetate and a much safer and environmentally friendlier alternative, with LD50 oral of 3700 mg/kg (based on rats) compared to zinc acetate's 794 mg/kg (based on rats). The toxicity values are sourced from the SDS of Thermo Fisher Scientific. Additionally, zinc 2-ethylhexanoate is chemically more stable without any reported ecological damage.

Melt pretreatment in the presence of both catalysts and diols: To further expedite the depolymerization process, catalysts, and diols were added simultaneously during the extrusion process, according to *Table 4-1*. The hypothesis was that this would create active sites within the bulk of PET, carrying catalysts and diols, which in turn would facilitate rapid depolymerization. These sites, carrying catalysts and diols, could impact the depolymerization reaction in multiple

ways. Primarily, the simultaneous addition of diols and catalysts enabled depolymerization not only from the surface but also from within the PET chains. Additionally, the presence of diols during melt pretreatment enhances chain scission leading to reduced polymer chain length and expanding the molecular weight distribution, thereby accelerating depolymerization. Lastly, the reaction of diols with the PET forms a random copolymer that induces irregularity after melt treatment.

## 4.2.2.2 Reaction optimization

Amount of solvent: To determine the impact of solvent quantity on the depolymerization time, ~300 mg of the S<sub>3</sub> sample was depolymerized using 2 weight% zinc acetate and various methanol quantities (0.4 to 4.8 grams) at 170 °C.

Catalyst content used during depolymerization: By subjecting the S<sub>3</sub> sample to 2.5 mL of methanol and using various amounts of zinc acetate as an external catalyst (the catalyst that was used directly during the depolymerization process) (1-6 weight%) at 170 °C, the role of catalyst content was studied while the optimum amount was determined.

Reaction time: The impact of reaction time on the depolymerization rate was explored on the S<sub>3</sub> sample at 170 °C and in the presence of 2 weight% zinc acetate and 2.5 mL methanol. The depolymerized sample was filtered, washed, and dried at 30-minute intervals for 3 hours.

#### 4.2.2.3 Characterization

Glass transition, crystallization, and melting temperature of non-pretreated/pretreated samples: Samples were characterized using Differential Scanning Calorimetry (DSC) using Q-100 TA Instruments. For this purpose, 5 to 10 mg of the samples were put into a DSC pan. Two cycles of heating-cooling were run. During the first cycle, samples were initially cooled down to 0 °C followed by heating up to 280 °C, with an equilibration rate of 10 °C/min in both cycles. The

second cycle would eliminate the processing history of PET, including prior shear stress, mechanical or thermal treatment, as well as crystallization [1]. Using the Universal Analysis 2000 software, glass transition temperature (T<sub>g</sub>), crystallization temperature (T<sub>c</sub>), and melting point temperature (T<sub>m</sub>) were determined.

Degree of crystallinity of non-pretreated/pretreated samples: Using the data from the second cycle of the DSC analysis, the degree of crystallinity (% crystallinity) for selected PET samples (non-pretreated and pretreated) was determined. The absolute mass degree of crystallinity is the ratio of the enthalpy of fusion of the semi-crystalline PET sample and fully crystalline PET. The enthalpy of fusion was calculated from the difference of the enthalpy of melting ( $\Delta H_{\rm m}$ ) and the enthalpy of cold crystallization ( $\Delta H_{\rm c}$ ). % crystallinity was determined by integrating the area of the endothermic peak and a baseline drawn divided by the enthalpy of completely crystalline PET ( $\Delta m^{\circ} = 140.1 \text{ J/g}$ ) [1]–[4].

Gas Chromatography-Mass Spectrometry (GC-MS) of depolymerization products: GC-MS analysis started with drying 100 μL of the 500 ng/μL NMZA samples and addition of 100 μL of N-methyl-N-tertbutyldimethylsilyltrifluoroacetamide (MTBSTFA) and 1% tertbutyldimethylsilyl chloride (TBDMSCl). Samples were derivatized at 60 °C for 16 hours. Subsequently, 1 μL of the derivatized sample was injected into the chromatography column in a split mode ratio of 1 to 10 when the temperature of the injector was 275 °C and a carrier gas (helium) was flowed with the rate of 1.0 mL/min. the J&W VF-5ms column separated the compounds with the temperature profile of 40 °C for 1 min, a ramp of 20 °C min<sup>-1</sup> to 320 °C and remaining at 320 °C for 5 min. With electron ionization at 70 eV sample was fragmented and entered the mass spectrometer to be scanned in the range of m/z 45 to 500.

Nuclear Magnetic Resonance (NMR) of depolymerization reaction products: ~50 mg of

selected PET filtrates was dissolved in deuterated chloroform and examined to obtain the <sup>1</sup>H NMR and <sup>13</sup>C NMR spectra within chemical shifts of 0-14 and 0-220 ppm, respectively.

# 4.2.3 Energy requirement calculation

Calculating the energy requirement started from the grinding the clean PET (A) followed by extrusion (D) at 280 °C for 4 min, quenching in methanol (C), depolymerization in a pressure flask (D) and ended with filtering the unpolymerized residue with chloroform, as depicted in *Figure 4-1*. The table summary of the streams is included in **APPENDIX A: ENERGY REQUIREMENT ASSESSMENT FOR DEPOLYMERIZATION OF POLYETHYLENE TEREPHTHALATE (PET)**.

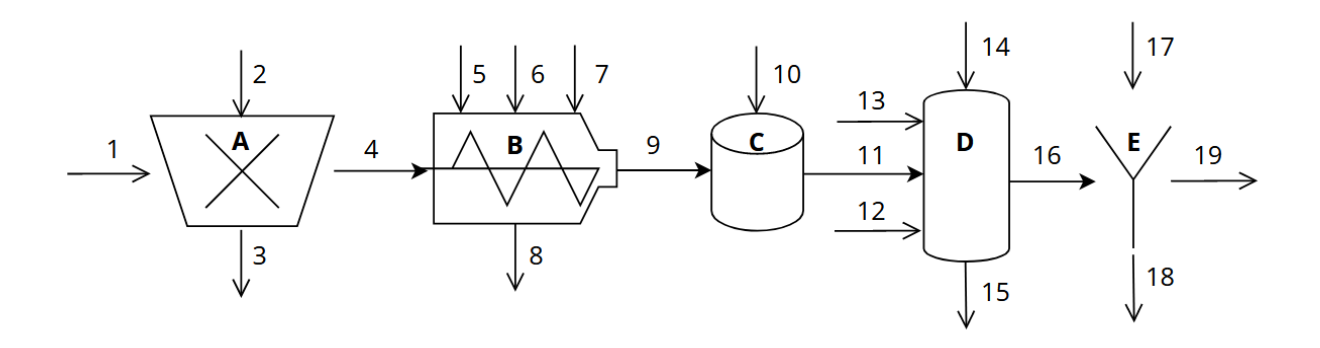


Figure 4-1. Process flow diagram for the two-step depolymerization process. PET flakes (1) were fed into the grinder (A), requiring energy (2) while losing part of it to the surroundings. The grinded PET (4) was extruded (B) in the presence of catalyst (5), short diol, with energy requiring for heating and mixing the sample (7), some of which were lost to the surroundings (8). Extruded PET (9) was quenched in methanol (10) yielding pretreated PET (11) which was subsequently fed into a pressure flux (D) along with an external catalyst (12) and reagent (13) for full depolymerization. The energy for depolymerization reaction (14) was sourced from the hot plate with an energy loss to the environment (5). Through a filtration step (E), the soluble products (16) were washed with chloroform for later isolation (17), and the unpolymerized PET (18) were filtered.

Grinding (A): Hand-shredded PET was fed to the grinder with the surface area of  $\sim 3$  cm<sup>2</sup> and exited the grinder with a size of  $\sim 1$  mm<sup>2</sup>. The energy requirement for this process was calculated using the maximum power written at the back of the instrument. Required energy (kJ)

was calculated by the multiplication of voltage (V) and current (A) and times (s), assuming that 10 grams of PET was ground within ~20 min and there was no material loss during the grinding process.

Extrusion (B): The energy requirement for the extrusion process was calculated similarly to the grinding process, based on the voltage and current or power of the extruder. The power has a nearly linear correlation with temperature below 600 K, based on multiple studies [5]–[7]. Therefore, extrusion at 280 °C requires 70% of the maximum power of the extruder that is at 400 °C. Preheating the instrument from room temperature to 280 °C and the heat loss from the extruder were not considered since in continuous processing they would be insignificant. After the extrusion of the PET samples, LDPE was extruded for 30 s to clean the instrument from potential residues from the extruder. Hence, the duration of the extrusion process is assumed to be ~4.5 minutes. The PET sample leaving the extruder was immediately immersed in a cold methanol beaker to avoid the growth of crystals.

Depolymerization (C): ~300 mg of the melt pretreated PET was added to a 15 mL pressure flask with 2.5 mL of methanol and 2 weight% of Zn(OAc)<sub>2</sub> and the pressure flask was dipped into an oil bath at 170 °C. The termination of the reaction was decided when the medium went clear. The energy from the oil bath to the reaction mixture to the pressure flask was calculated by the energy that hot plate requires, assuming that 30% of the energy input from the hot plate in transferred to the surrounding environment. Similar to the extrusion process, power was linearly correlated to the temperature [5]–[7]. Therefore, the energy requirement for the hotplate working at 85% (200 °C) of the maximum temperature of 200 °C was 85% of the maximum power.

## 4.3 Results and Discussion

The primary goal of this project was to devise an energy-efficient process for chemical recycling PET by alleviating the presence of crystalline regions and the formation of active sites that can enhance the depolymerization rate. For this purpose, a two-step process was developed involving a melt pretreatment in the presence of a catalyst and a short diol followed by subjecting the pretreated samples to methanol and a secondary catalyst. Zinc 2-ethylhexanoate was used for the first time for chemical recycling PET, added during the extrusion process. The melt extrusion was conducted in the presence of two different catalysts zinc 2-ethylhexanoate (Zn-EH) and zinc acetate (Zn(OAc)<sub>2</sub>)), and three short diols/additives, Bis (2-hydroxyethyl) terephthalate (BHET), 1,4-Cyclohexanedimethanol (CHDM), 4,8-Bis(hydroxymethyl)tricyclo[5.2.1.0<sup>2,6</sup>]decane (BHTD).

The system was optimized by various reaction parameters. Additionally, the pretreated samples as well as depolymerized products were characterized. Moreover, a comparison of the energy demand for depolymerization of the pretreated samples versus non-treated samples confirmed the energy efficiency of the process compared to that of depolymerizing unpretreated PET.



**Figure 4- 2.** A) Images of the non-pretreated sample  $(S_0)$  before (on the left) and after (on the right) the methanolysis at 160 °C for 3 hours. B) Images of the pretreated sample with no catalysts and additives/diols  $(S_1)$  before (on the left) and after (on the right) the depolymerization at 160 °C for 3 hours. C) Schematic of filtration of non-polymerized PET to calculate the monomer yield. D) Effect of temperature on rate of depolymerization for  $S_0$  and  $S_1$  samples.

To study the effect of melt-extrusion and quenching without the presence of any catalysts and additives/diols on the depolymerization process, two samples,  $S_0$  (neat PET) and  $S_1$  (extruded and quenched) were subjected to 2.5 mL methanol and 2 weight% zinc acetate at 160°C, as depicted in *Figure 4- 2A* and *4- 2B*. The procedure for isolation of the methanolysis monomer, dimethyl terephthalate (DMT), was through separation of non-polymerized products. The reaction was performed at various temperatures (from 140 to 200°C) to compare the dependence of depolymerization rate and conversion rate, revealing that at all temperatures, the rates were enhanced ~30-50% after pretreatment compared to neat PET, *Figure 4- 2D*.

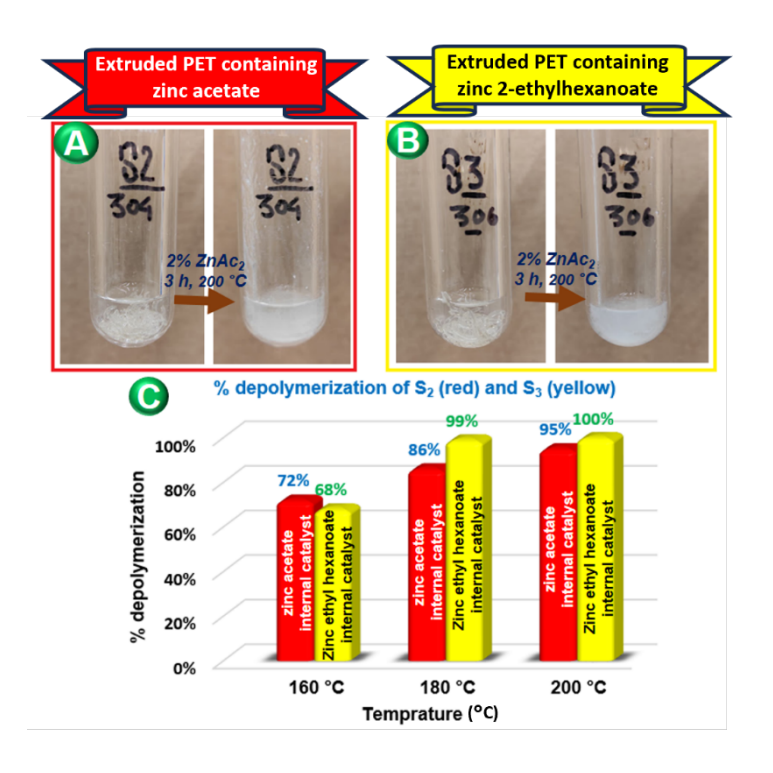


**Figure 4-3.** A) Images of sample  $S_2$  (containing zinc acetate added during melt-extrusion) before (on the left) and after (on the right) depolymerization within 3 hours at 180 °C. B) Images of sample  $S_3$  (containing zinc 2-ethylhexanoate added during melt-extrusion) before (on the left) and after (on the right) depolymerization within 3 hours at 180 °C. and C) Comparison of depolymerization rate of  $S_2$  and  $S_3$  at different temperatures.

Subsequently, the effect of the type of catalysts that were deployed during the pretreatment process was examined. S<sub>2</sub>, prepared by melt-extrusion in the presence of 2.5 mol% zinc acetate, and S<sub>3</sub>, prepared by addition of 2.5 mol% zinc 2-ethylhexanoate during pretreatment, were depolymerized in the presence of 2 weight% zinc acetate (as a so-called external catalyst) at various temperatures (160, 180, and 200 °C), *Figure 4- 3A* and *4- 3B*. Comparing the depolymerization rate of samples S<sub>2</sub> and S<sub>3</sub> revealed that the incorporation of zinc acetate during melt pretreatment triggered faster depolymerization compared to zinc 2-ethylhexanoate at a lower temperature (160 °C), while, at high temeratures, the performance of zinc 2-ethylehexanoate exceeds zinc acetate, as exhibited in *Figure 4- 3C*. When these samples were compared to S<sub>0</sub> and S<sub>1</sub>, the depolymerization rate was observed to be enhanced by nearly 200%, *Figure 4- 3D* and *Figure 4- 2C*. This confirmed that the addition of catalysts during melt processing enhances the

rate of PET depolymerization.

The presence of zinc-containing catalysts during the melt-extrusion of PET could potentially promote degradation through several mechanisms. If traces of water molecules are present in the extrusion process, zinc form complex with carbonyl oxygen in PET, facilitating the nucleophilic attack of water molecules on carbonyl carbon of the PET. This would lead to the cleavage of ester bonds and formation of carboxylic acid and alcohol end groups. This hydrolysis reaction leads to a reduction in M<sub>w</sub>.

The higher efficiency of zinc 2-ethylehexanoate (present in sample S3) compared to zinc acetate (present in sample S) is attributed to better miscibility and mixing of the former in PET, thus enhancing the catalytic activity of zinc 2-ethylhexanoate compared to zinc acetate in the degradation of PET. To expedite the depolymerization reaction, catalysts, and diols were simultaneously introduced during the melt pretreatment process. For this purpose, the two catalysts and three distinct short diols/additives were added in different combinations during the meltextrusion process to prepare samples S<sub>4</sub> to S<sub>9</sub>, compositions listed in *Table 4-1*. ~300 mg of each of these samples was depolymerized in the presence of 2 weight% zinc acetate and 2.5 mL of methanol at 170 °C and the time for full depolymerization were compared and depicted in Figure 4-4. A remarkable enhancement of depolymerization rate (~2-fold increase compared to samples subjected to mere melt-extrusion) with further acceleration (to 3- to 4-fold compared to S<sub>0</sub> (neat PET). Conducting the experiments at 200 °C showed that while non-pretreated PET (S<sub>0</sub>) was completely depolymerized within 166 minutes, depolymerization of melt pretreated PET with Zn-EH and CHDM (S<sub>7</sub>) only took 7 minutes. It was hypothesized that the presence of a catalyst and a diol accelerated the depolymerization reaction through induction of chain scission, the creation of active sites, that enabled the depolymerization from within the polymer bulk, and the introduction

of irregularity by the formation of random copolymers that led to permanent decrystallization.

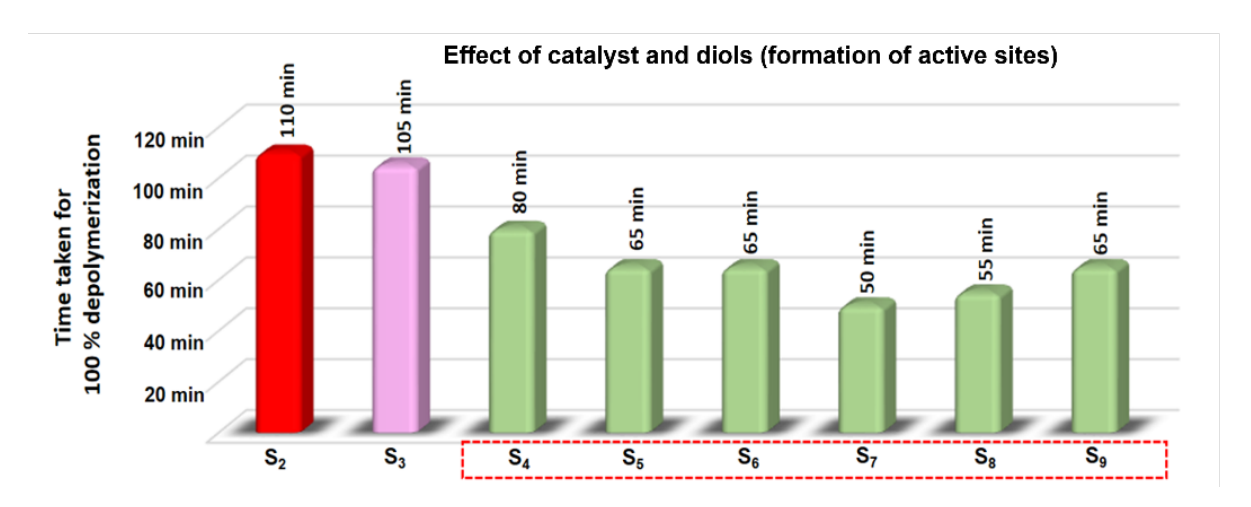


**Figure 4- 4.** Time for full depolymerization of samples containing only catalyst ( $S_2$  and  $S_3$ ) and samples carrying both catalyst and diol/additives ( $S_4$  -  $S_9$ ) in 2.5 mL methanol at 170°C.

When diols were present along with the zinc acetate or zinc 2-ethylhexanoate, the zinc catalyst could coordinate with the carbonyl oxygen of the ester bond in PET, making it more susceptible to nucleophilic attack of the diols. The coordination of zinc cation as a Lewis acid can enhance the electrophilic character of the ester carbon, thus attracting nucleophiles like the hydroxyl groups of the diol. In the case of zinc 2-ethylhexanoate, the ethylhexanoate ligands can chelate with the zinc cation, providing a larger and more stable coordination environment, with better miscibility with PET and promoting the activation of the ester bond.

To optimize the reaction conditions, the effect of solvent quantity and amount of catalyst added during polymerization (so-called external catalyst) on the time of full depolymerization in addition to the impact of time on % depolymerization were analyzed. By increasing the amount of excess methanol from 0.4 to 4.8 grams in depolymerization of S<sub>3</sub> at 170 °C, the rate of reaction was enhanced initially and reduced at some point, with the optimal amount of 1.6 to 2.4 grams (equal to MeOH:PET molar ratio of 32 to 48), *Figure 4- 5A*. Several studies suggested that a high amount of excess methanol (>50 MeOH: PET molar ratio) is crucial not only for the complete

dispersion of PET in the solvent medium but also for obtaining a high yield of dimethyl terephthalate (DMT) and suppressing the formation of byproducts [8], [9].

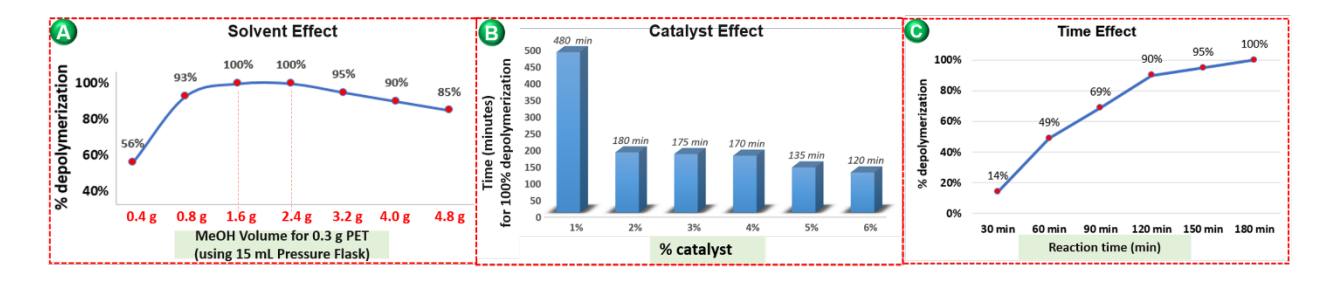


**Figure 4- 5.** A) Effect of methanol mass on the degree of depolymerization of  $S_3$  at 170 °C. B) Effect of weight% of catalyst added during depolymerization on time of full depolymerization time of  $S_3$  at 170 °C. C) Effect of the reaction time on rection progress for  $S_3$  at 170 °C.

Similarly, studying the effect of catalyst content, varying from 1 to 6 weight% of zinc acetate, on complete depolymerization of S<sub>3</sub> in 2.5 mL of methanol at 170 °C, indicated that employing 2 weight% of catalyst was efficient, with only slight acceleration of reaction when using higher catalyst percentage, *Figure 4-5B*.

Moreover, the impact of reaction time on the depolymerization rate was examined at 170°C in the presence of 2.5 mL methanol and 2 weight% zinc acetate, focusing on the S<sub>3</sub> sample due to its moderate rate of depolymerization. Results depicted in *Figure 4- 5C* present that after 30 minutes, only a 16% depolymerization percentage was achieved, which increased to 49% after 1 hour and it reached completion after 3 hours.

After optimizing the reaction condition, pretreated samples were analyzed using Differential Scanning Calorimetry (DSC) to assess the thermomechanical impact of pretreatment. The DSC thermograms exhibited that the glass transition temperature ( $T_g$ ), crystallization temperature ( $T_c$ ) and melting temperature ( $T_m$ ) of neat PET ( $S_0$ ) were ~81 °C, ~140 °C, ~250 °C, respectively, as can be seen in *Figure 4- 6A*. These values were reduced for the pretreated samples  $S_1$ ,  $S_2$ , and  $S_3$ , *Figure 4- 6B*. More specifically, the  $T_c$  for  $S_1$ ,  $S_2$ , and  $S_3$  were decreased drastically to 108, 113, and 127 °C, respectively. Additionally, the peaks corresponding to  $T_m$  of  $S_1$ ,  $S_2$ , and

 $S_3$  were broadened and less sharp as compared to peaks for  $S_0$ . The underlying reason for the broadened melting range is the expanded molecular weight distribution happening during the melt extrusion process where PET polymer chains were randomly cleaved through thermal degradation and shear stress, especially in the presence of zinc 2-ethylhexanoate catalyst. These thermal attributes explain the improved rate of depolymerization in samples  $S_2$  and  $S_3$  as compared to  $S_0$ .

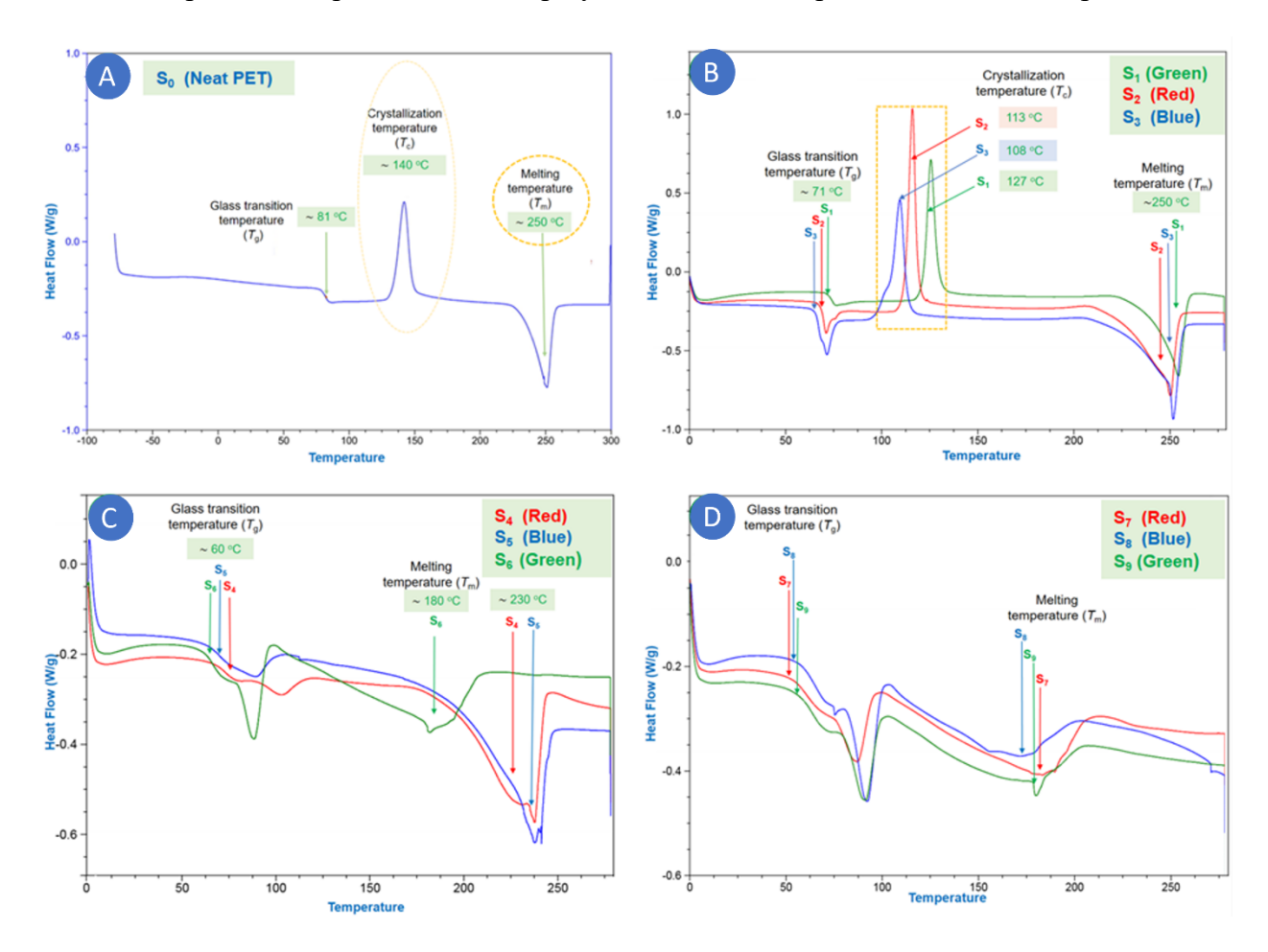


**Figure 4- 6.** A) DSC thermograms of neat PET  $(S_0)$  with highlighted  $T_g$ ,  $T_C$  and  $T_m$ . B) DSC thermograms of melt-pretreated PET with no catalysts and additives/diols  $(S_1)$ , pretreated PET carrying only catalysts  $(S_2$  and  $S_3)$ . C and D) DSC thermograms of samples melt-processed with both catalysts and diols/additives  $(S_4$  to  $S_9)$ .

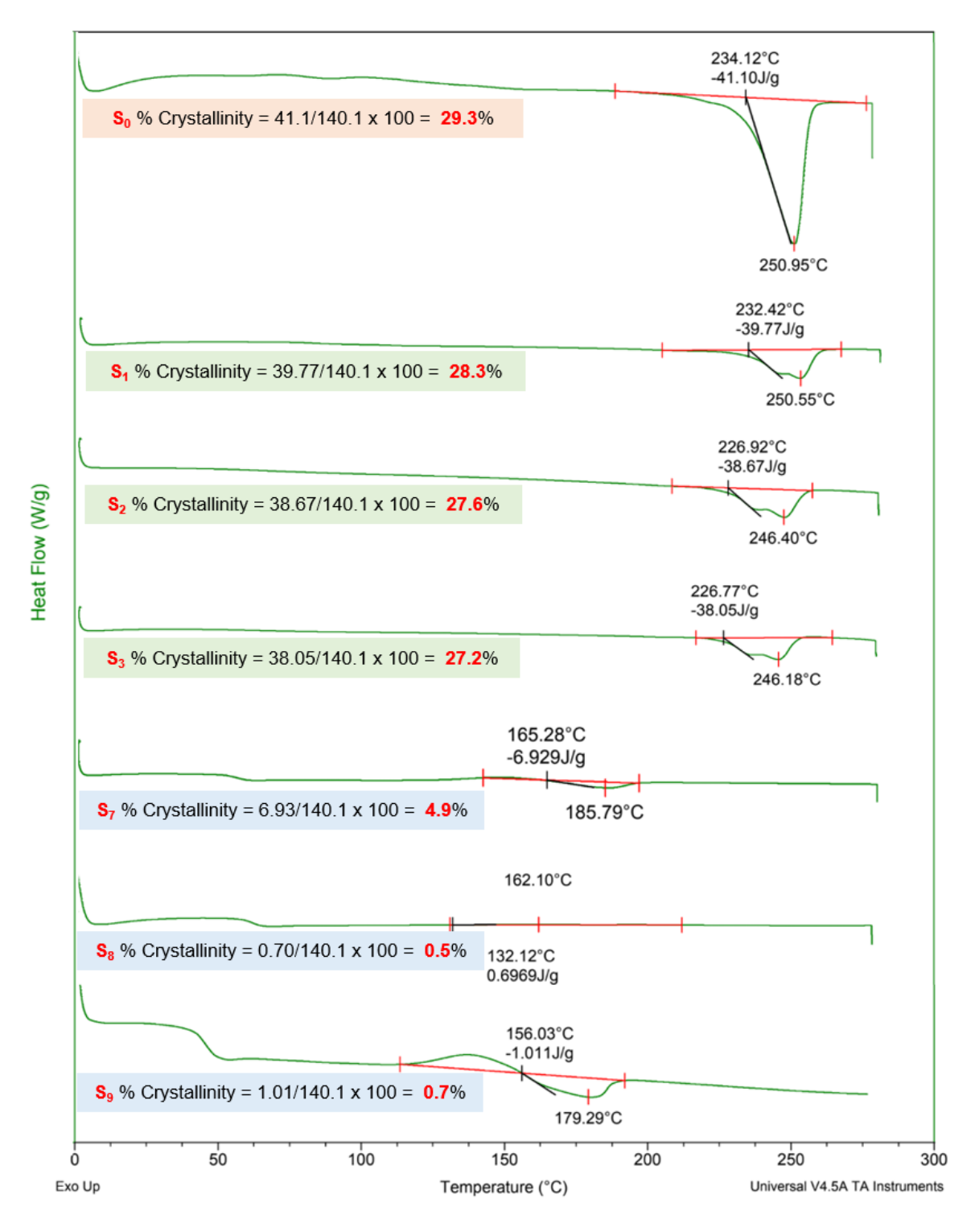


**Figure 4-** 7. Calculated % crystallinity for selected PET samples from the second heating cycle of DSC, depicting that the melt-treatment suppressed the crystal growth in PET.

A further decrease was observed in T<sub>g</sub>, T<sub>c</sub> and T<sub>m</sub> when comparing samples pretreated with

catalysts and diols to previous samples. For samples S<sub>4</sub> and S<sub>5</sub>, treated with BHET as the diol, the melting range was considerably reduced and widened due to significant chain scission caused by the presence of -OH group in BHET. This clarified the swift enhancement in the depolymerization rate of S<sub>4</sub> and S<sub>5</sub> compared to S<sub>2</sub> and S<sub>3</sub>, *Figure 4-6C* (red and blue thermograms). Incorporation of both CHDM and BHTD further decreases the T<sub>m</sub> to lower than 200 °C while broadening the melting range. This reduction lies in the irregularities that were introduced to PET molecular structure when CHDM and BHTD with different structures than the parent monomers of PET were incorporated, *Figure 4-6C* (green thermogram) and *Figure 4-6D*.

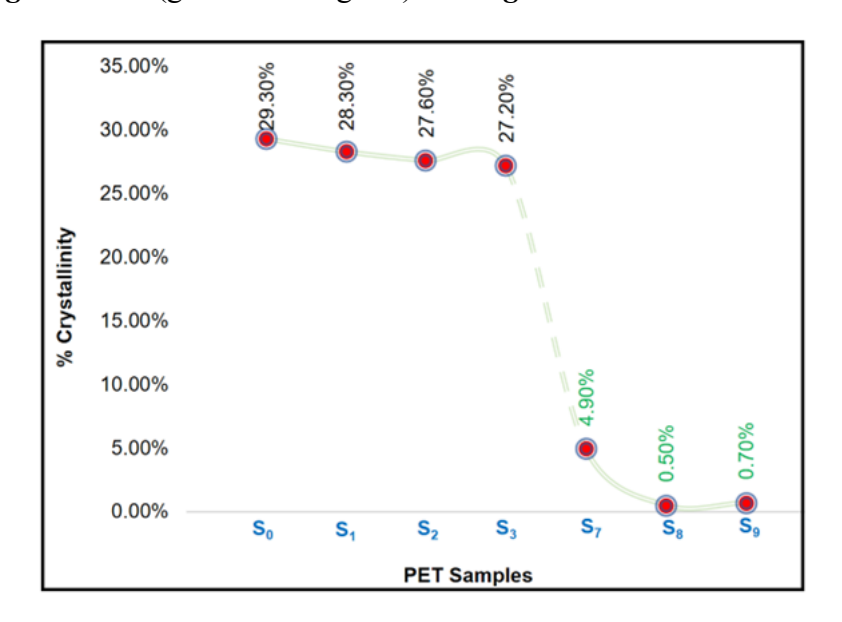


Figure 4-8. Decreasing degree of crystallinity after melt pretreatment.

To calculate the absolute mass crystallinity (degree of crystallinity), PET samples underwent a second cycle of heating that eliminated the processing history. The area between the thermograms and a random baseline before the cold crystallization peak to the end of melting, exhibited in *Figure 4-7*, represents the enthalpy of fusion for semi-crystalline PET samples. Percent crystallinity was determined by dividing this value by the theoretical enthalpy of fusion (140.1 J/g). The descending pattern of the degree of crystallinity after melt pretreatment in the absence and presence of the catalyst as well as when both catalyst and diols were used

simultaneously, as plotted in *Figure 4-8*, shows the effectiveness of this method on continuous elimination of crystalline regions in the PET samples. Additionally, the drastic reduction of percent crystallinity for samples S<sub>7</sub>, S<sub>8</sub>, and S<sub>9</sub> further confirms the role of active site formation along with increased chain scission and introduction of structural irregularity when diols and catalyst were incorporated at the same time.

After characterizing the pretreated samples, the depolymerized products were analyzed using  ${}^{1}$ H NMR and  ${}^{13}$ C NMR spectroscopy and GC-MS analysis. *Figure 4- 9A* and *Figure 4- 9B* illustrate the  ${}^{1}$ H NMR and  ${}^{13}$ C NMR spectra of the filtered solution revealing the presence of nearly 99% monomer (dimethyl terephthalate, DMT) in addition to ethylene glycol (EG) and 1% of byproducts (potentially consisting of dimers). In the  ${}^{1}$ H NMR spectra, singlets at  $\delta = \sim 8$  and  $\delta = \sim 3.9$  ppm correspond to the four aromatic protons (shown in red) and the 6 hydroxyl protons (shown in blue), respectively, confirming the presence of DMT. Additionally, the peak with the integration of  $\sim 3.7$  at  $\sim 3.8$  ppm (highlighted with green) is related to the four hydrogens of ethylene glycol (EG) *Figure 4- 9A*. The formation of DMT was further substantiated by the resonances at  $\delta = \sim 166$ ,  $\sim 134$ ,  $\sim 130$ , and  $\sim 53$  ppm in the  $^{13}$ C NMR spectra, *Figure 4- 9B*.

Similarly, GC-MS analysis of different samples proved the presence of the DMT monomer with a retention time of 9.73 minutes and EG with a retention time of 8.74 minutes, *Figure 4-9C*. The mass spectrum for the peak corresponding to DMT at 9.7 minutes revealed a m/z of 194.06, verifying the detected monomer with a molecular weight of 196.06 g/mol, as shown in *Figure 4-9D*.

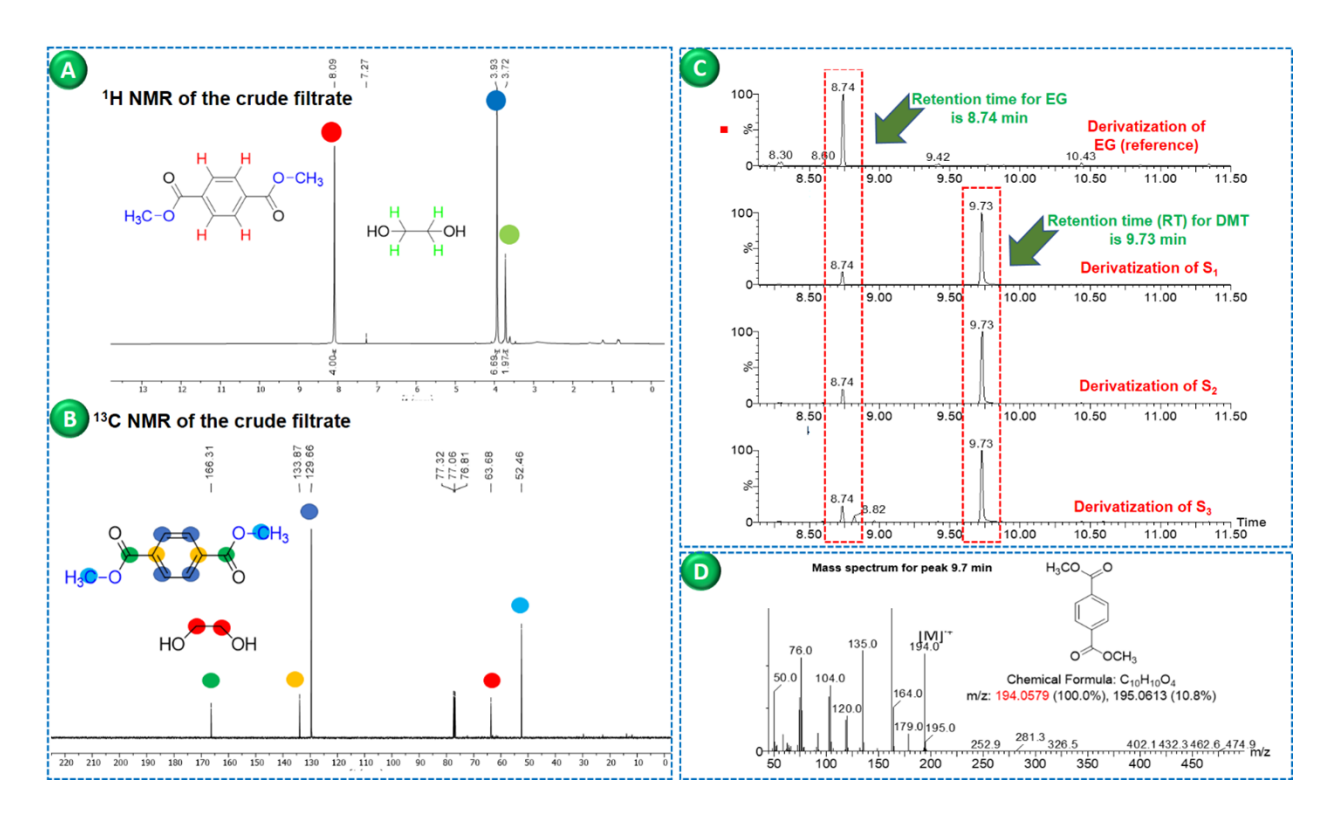


**Figure 4- 9.** Characterization of the products of depolymerization. **A)**  $^{1}H$  NMR and **B)**  $^{13}C$  NMR spectra of the crude filtrate after depolymerization, showing the high yield of DMT. **C)** GC chromatograms of derivatized EG (first from the top) and sample  $S_{1}$ , (second from top)  $S_{2}$  (third from top) and  $S_{3}$  (fourth from top, showing the purity of the depolymerized samples. **D)** Mass spectrum of DMT monomer as the only compound detected after depolymerization of PET.

After characterization of the pretreated samples and the products and investigating the impact of various parameters on the rate of depolymerization, it was concluded that sample S<sub>7</sub> has the highest performance at optimal conditions of 2.5 mL methanol, 2 weight% zinc acetate (as a so-called external catalyst) at 170 °C. Therefore, the energy demand for melt pretreatment and depolymerization of S<sub>7</sub> was compared to that of unpretreated PET. The energy requirement for each process was determined separately, the summation of which revealed the total energy demand at two temperatures of 170 and 200 °C.

Grinding (A): According to the specifications of the grinder, summarized in **Table 4-2**, the power of the grinder was calculated using the following equation:

$$P = V \times I = 115 V \times 4.8 A = 552 W$$

Assuming that 10 g PET could be ground at most within 20 min, the required energy was:

$$E_A = \frac{552 J}{s} \times 20 \min \times \frac{60 s}{\min} \times \frac{kJ}{1000 J} = 662.4 kJ$$

Table 4- 2. Specifications of the grinder.

Name	Wiley® Mini Cutting Mill	
Frequency	60 Hz	
Voltage	115 V	
Amps	4.8 A	

Extrusion (B): Considering that the extruder works 70% of the maximum temperature of the maximum power of the instrument for 4 minutes with 30 minutes of extruding LDPE for removing the residues of PET samples from the extruder, the overall time of extruding 12.225 grams of PET+ Zn-EH+ CHDM was ~4.5 min. According to the **Table 4-3**, the energy was calculated as follows:

*Table 4- 3. Specifications of the extruder.* 

Name	DSM 15cc mini-extruder Xplore	
Power	900 watts	
<b>Maximum Operating</b>	400 °C	
Temperature		

$$E_B = \frac{900 J}{s} \times \frac{70}{100} \times 270 s \times \frac{kJ}{1000 J} = 170.1 kJ$$

Depolymerization (C): Assuming power efficiency of 70% for the hot plate and linear correlation of power output with temperature, the energy demanded for depolymerization S7 was found as follows, using the specification of the hot plate listed in *Table 4- 4*.

Table 4- 4. Specifications of the hot plate.

Name	Corning® PC-420D
Voltage	120V/60 Hz
Power	698 watts
<b>Maximum Operation Temperature</b>	200 °C

$$E_C = P \times t \times = \frac{698 \, J}{s} \times \frac{100}{70} \times \frac{85}{100} \times 50 \, min \times \frac{60 \, s}{1 \, min} \times \frac{kJ}{1000 \, J} = 2542.7 \, kJ$$

Total energy requirement: The energy requirement for the melt pretreated PET was the summation energy consumed at each step.

$$E_{7,170} = \sum E = 3375.2 \, kJ$$

The required energy for depolymerization of the non-pretreated sample  $(S_0)$ , considering the same conditions for the depolymerization process, was calculated as follows:

$$E_{0,170} = P \times t = \frac{698 J}{s} \times \frac{100}{70} \times \frac{85}{100} \times 3360 \ min \times \frac{60 \ s}{1 \ min} \times \frac{kJ}{1000 \ J} = 170870.4 \ kJ$$

The energy demanded for depolymerizing PET with no pretreatment (S<sub>0</sub>) under the same reaction conditions using the same amount of zinc acetate and methanol was more than 50 times greater when compared to the two-step depolymerization route. Hence it is concluded that the pretreatment step enormously diminished the energy requirement for full depolymerization PET to its monomer, DMT, at a low temperature of 170 °C. To further investigate the energy efficiency of this process, analogous calculations were performed at 200 °C, for at higher temperatures depolymerization of non-pretreated PET was more accelerated compared to pretreated PET, leading to a smaller difference between the time of full depolymerization of S<sub>0</sub> and S<sub>7</sub>.

$$E_{C,200} = P \times t \times = \frac{698 \, J}{s} \times \frac{100}{70} \times \frac{100}{100} \times 7 \, min \times \frac{60 \, s}{1 \, min} = 418.8 \, kJ$$

$$E_{7,200} = \sum E = 662.4 + 170.1 + 418.8 = \mathbf{1251.3} \, kJ$$

$$E_{0,200} = P \times t = \frac{698 \, J}{s} \times \frac{100}{70} \times \frac{100}{100} \times 166 \, min \times \frac{60 \, s}{1 \, min} = \mathbf{9931.5} \, kJ$$

The results repeated at 200 °C exhibited that the required energy for depolymerization of neat PET ( $S_0$ ) is still ~8-fold greater than that of pretreated PET ( $S_7$ ). Nevertheless, it is important to acknowledge that energy estimates were derived from bench-top experiments and laboratory-scale instrumentation. On an industrial scale, the energy demand for the depolymerization reactor may not have the primary contribution to the overall energy consumption. Furthermore, the calculations are applicable only to lab-top scale experiments, where post-consumer PET bottles were manually washed and shredded while the energy required for material transfer between instruments was omitted. As a result, considering these factors could either augment or diminish the energy demand. In this thesis, the claim is that the incorporation of the melt pretreatment process before PET depolymerization lowered the overall energy requirement.

## **4.4 Conclusions**

The crystalline region of the semi-crystalline PET is one of the barriers to rapid depolymerization of PET by impeding the mass transfer of methanol (or other reagents such as glycols, water. etc.,) during depolymerization. Resultantly, the depolymerization processes for PET recycling are either energy-intensive or very slow. The primary goal of **this work** was to devise an energy-efficient process for the chemical recycling of PET by alleviating the presence of crystalline regions and creating active sites that enhance the depolymerization rate. Herein, a rapid energy-effective depolymerization technique for post-consumer PET was showcased. The time of full depolymerization of PET samples subjected solely to melt-extrusion-cold-quench pretreatment was reduced by 30-50%. Notably, incorporating 2.5 mol% catalyst and diol during pretreatment reduced the depolymerization time by 5-fold with decreased and widened melting

range showing broadened molecular weight distribution caused by chain scission. Another underlying reason was depolymerization both from the surface and from within the PET chains, where active sites carried catalyst and diol. Furthermore, a novel contribution to the field, the low-cost, environmentally friendly zinc 2-ethylhexanoate was used as a catalyst for PET chemical recycling. Noteworthy, energy assessments revealed that the two-step depolymerization saved up energy up to 50 times at 170 °C and 8 times at 200 °C compared to non-pretreated PET.

#### REFERENCES

- [1] R. Sharma, S. N. Maiti, R. Sharma, and S. N. Maiti, "Effects of Crystallinity of PP and Flexibility of SEBS- g-MA Copolymer on the Mechanical Properties of PP / SEBS-g-MA Blends Effects of Crystallinity of PP and Flexibility of SEBS-g-MA Copolymer on the Mechanical Properties of PP / SEBS-g-MA Blends," vol. 2559, 2014.
- [2] P. G. Karagiannidis, A. C. Stergiou, and G. P. Karayannidis, "Study of crystallinity and thermomechanical analysis of annealed poly(ethylene terephthalate) films," *Eur. Polym. J.*, vol. 44, no. 5, pp. 1475–1486, 2008.
- [3] Y. Kong and J. N. Hay, "The enthalpy of fusion and degree of crystallinity of polymers as measured by DSC," *Eur. Polym. J.*, vol. 39, no. 8, pp. 1721–1727, 2003.
- [4] Z. Yang, H. Peng, W. Wang, and T. Liu, "Crystallization behavior of poly(ε-caprolactone)/layered double hydroxide nanocomposites," *J. Appl. Polym. Sci.*, vol. 116, no. 5, pp. 2658–2667, 2010.
- [5] J. Spannhake, O. Schulz, A. Helwig, A. Krenkow, G. Müller, and T. Doll, "High-temperature MEMS heater platforms: Long-term performance of metal and semiconductor heater materials," *Sensors*, vol. 6, no. 4, pp. 405–419, 2006.
- [6] D. V. Zinov'ev and P. Sole, "Quaternary codes and biphase sequences from Z8-codes," *Probl. Peredachi Informatsii*, vol. 40, no. 2, pp. 50–62, 2004.
- [7] S. Santra *et al.*, "Post-CMOS wafer level growth of carbon nanotubes for low-cost microsensors A proof of concept," *Nanotechnology*, vol. 21, no. 48, 2010.
- [8] Y. Yang, Y. Lu, H. Xiang, Y. Xu, and Y. Li, "Study on methanolytic depolymerization of PET with supercritical methanol for chemical recycling," *Polym. Degrad. Stab.*, vol. 75, no. 1, pp. 185–191, 2002.
- [9] D. D. Pham and J. Cho, "Low-energy catalytic methanolysis of poly(ethyleneterephthalate)," *Green Chem.*, vol. 23, no. 1, pp. 511–525, 2021.

# Chapter 5. EFFICIENT CHEMICAL RECYCLING OF POLYETHYLENE TEREPHTHALATE (GLYCOLYSIS)

Part of this chapter is published as:

Aayanifard. Z., Khan. A., Naveed, N., J. Schager, J., Rabnawaz, M., "Rapid depolymerization of PET by employing an integrated melt-treatment and diols" *Polymer*, 265, p.125585, 2023.

Aayanifard, Z., Khan, A, Naveed, M, Saffron, C. M., Rabnawaz, M., "Enhanced Glycolysis of Post-Consumer Polyethylene Terephthalate: Synergizing Melt-Pretreatment with Organic Catalysis", *ACS Sustainable Chemistry and Engineering*, 2024.

# **5.1 Summary**

Previously, an energy-efficient route for the chemical recycling of post-consumer poly (ethylene terephthalate) (PET) was devised using methanol (MeOH) as the reagent, where the PET samples initially underwent a melt pretreatment followed by quenching and depolymerization to the parent monomer, dimethyl terephthalate (DMT). The optimal pretreatment involved the incorporation of zinc 2-ethylhexanoate (Zn-EH), as a so-called internal catalyst, and 1,4-Cyclohexanedimethanol (CHDM), as a diol, followed by depolymerization in the presence of 2.5 mol % zinc 2-ethylhexanoate and EG: PET molar ratio of 10 at 170 °C. The energy efficiency of the process was proved with an energy requirement analysis, comparing the required energy for the depolymerization of melt pretreated samples with that of neat PET under the same reaction conditions. In this chapter, the melt pretreatment methodology was used while the depolymerization reaction occurred using ethylene glycol (EG) as the reagent in depolymerizing post-consumer PET to the parent monomer, Bis (2-hydroxyethyl) terephthalate (BHET). Additionally, the addition of zinc acetate during the depolymerization process was eliminated. Herein, initially, the same pretreated samples were subjected to glycolytic depolymerization, the reaction conditions were optimized and both the pretreated samples and the depolymerization products were characterized. The results confirmed that the integration of the melt pretreatment could reduce the time of depolymerization due to the lowered crystallinity of the PET samples and the formation of active sites within the structure of PET. To move towards more environmentally friendly frameworks, the zinc 2-ethylhexanoate catalyst that was incorporated during melt extrusion was substituted with organic catalysts, 1,8-diazabicyclo[5.4.0]undec-7-ene (DBU) or 1,5,7-Triazabicyclo[4.4.0]dec-5-ene (TBD). Pretreatment of PET in the presence of solely 0.5 mol% of this catalyst and CHDM as the most effective diol could enable rapid glycolysis. For

characterizing the pretreated samples, in addition to thermal analysis using Differential Scanning Calorimetry (DSC), the molecular weight of the PET samples was indirectly measured through inherent viscosity measurement. The presence of a catalyst (zinc ion) within the structure of melt pretreated PET was explored using Energy Dispersive X-ray (EDX) analysis. The depolymerization reaction was monitored with in-line Fourier Transfer Infrared Spectroscopy-Attenuated Total Resonance (FTIR-ATR) to characterize the conversion of PET to its monomer, BHET. Products were analyzed using Nuclear Magnetic Resonance Spectroscopy (NMR) and Liquid Chromatography-Mass Spectrometry (LC-MS) to give insights to the depolymerization products. Exploring the energy efficiency of pretreating PET with TBD and DBU exhibited 37-60% less energy is required for depolymerizing melt-treated PET compared to neat PET.

## **5.2 Materials and Methods**

#### 5.2.1 Materials

PET Coke bottles (SP code #1) were purchased from a local Meijer store in Michigan, USA. Zinc acetate (Zn(OAc)<sub>2</sub>), Bis (2-hydroxyethyl) terephthalate (BHET), 1,4-Cyclohexanedimethanol (CHDM), 4,8-Bis(hydroxymethyl)tricyclo[5.2.1.0<sup>2,6</sup>]decane (BHTD), Methanol (MeOH, 99.8%), and Dimethyl terephthalate (DMT) were purchased from Sigma Aldrich. Zinc 2-ethylhexanoate (Zn-EH) was purchased from AlfaAesar. Phenol crystal (unstabilized, reagentplus, >99%), ethylene glycol (EG, 99.8%), 1,5,7-triazabicyclo[4.4.0]dec-5-ene (TBD, 98%), and 1,8-diazabicyclo[5.4.0]undec-7-ene (DBU, 96%) were purchased from Sigma Aldrich, and 1,1,2,2-tetrachloroethane (98.5+%) was from Thermo Scientific. DI water was used in all experiments. All chemicals were used as received.

# **5.2.2** Experimental

Melt pretreatment: The pretreatment method was as described in **Chapter 4**, starting from

washing the post-consumer PET bottles with water and detergent after removing caps and labels, shredding them into  $\sim$ 3 cm<sup>2</sup> pieces using scissors followed by washing with acetone, drying, and grinding into a size of  $\sim$ 1 mm<sup>2</sup>. For the metallic glycolysis, 300 mg ground PET was mixed with 0.25 g (1.35 mmol) of zinc acetate or 0.475 g (1.35 mmol) of zinc 2-ethylhexanoate of catalyst and 0.7 g (17.5 weight%) of diol according to *Table 5- 1*, and was fed into the extruder at 280 °C for 4 minutes.

For organic glycolysis, a new set of samples was prepared where initially 0.14 g (1 mol%) of 1,5,7-triazabicyclo[4.4.0]dec-5-ene (TBD), or 0.15 g (1 mol%) 1,8-diazabicyclo[5.4.0]undec-7-ene (DBU) was dissolved in solution, mixed with 300 g ground PET, and dried at room temperature. The catalyst dispersed within ground PET was melt-extruded with/without the addition of CHDM as diol in the extruder at 280 °C for 4 minutes. Additionally, ethylene glycol was used as a diol with EG: PET equimolar ratio, instead of CHDM, during the pretreatment of PET with 1 mol% of TBD/DBU. All melt-extruded samples were quenched in cold methanol to impede the crystal growth in PET. The composition of samples for organic glycolysis is listed in *Table 5- 1*.

# 5.2.2.1 Depolymerization reaction

Samples non-treated vs pretreated without any catalyst: Same with the initial studies in Chapter 4, the impact of reducing the crystallinity barrier on the glycolytic depolymerization of the first two PET samples, namely S<sub>0</sub> and S<sub>1</sub>, the neat and melt pretreated PET, respectively. ~300 mg of these samples was subjected to ethylene glycol (EG) for depolymerization in the presence of 2.5 mol % zinc 2-ethylhexanoate (previously referred to as "external catalyst") at 180 °C. When the medium was visually clear, the reaction was considered to be finished. The reaction flask was cooled down to room temperature for 5 to 10 minutes followed by the addition of boiling water to

dissolve BHET (and potentially some low-molecular-weight by-products) and the mixture was cooled down in the refrigerator. The crystallized products were filtered and tested.

Table 5-1. Summary of sample specifications for metallic glycolysis.

Sample	Formulation				
Code _	PET	Extruded	Catalyst (mol%)	Additives (weight%)	
Metallic ca	ntalysis				
$S_0$	10.0 g	NO	-	-	
$S_1$	10.0 g	YES	-	-	
$S_2$	10.0 g	YES	$^{42}$ Zn(AOc) <sub>2</sub> (2.5)	-	
$S_3$	10.0 g	YES	<sup>43</sup> Zn-EH (2.5)	-	
$S_4$	10.0 g	YES	$Zn(AOc)_2$ (2.5)	<sup>44</sup> BHET (17.5)	
$S_5$	10.0 g	YES	Zn-EH (2.5)	BHET (17.5)	
$S_6$	10.0 g	YES	$Zn(AOc)_2(2.5)$	<sup>45</sup> CHDM (17.5)	
$S_7$	10.0 g	YES	Zn-EH (2.5)	CHDM (17.5)	
$S_8$	10.0 g	YES	$Zn(AOc)_2(2.5)$	<sup>46</sup> BHTD (17.5)	
$S_9$	10.0 g	YES	Zn-EH (2.5)	BHTD (17.5)	
Organic ca	ntalysis				
$S_{10}$	10.0 g	YES	<sup>47</sup> TBD (0.5)	-	
$S_{11}$	10.1 g	YES	<sup>48</sup> DBU (0.5)	-	
$S_{12}$	10.0 g	YES	TBD (0.5)	CHDM (17.5)	
$S_{13}$	10.0 g	YES	DBU (0.5)	CHDM (17.5)	
$S_{14}$	10.0 g	YES	TBD (1)	CHDM (17.5)	

 <sup>&</sup>lt;sup>42</sup> Zinc acetate (used during the melt pretreatment, so-called "internal catalyst")
 <sup>43</sup> Zinc 2-ethylhexanoate (used during the melt pretreatment, so-called "internal catalyst")

<sup>&</sup>lt;sup>44</sup> Bis(2-hydroxyethyl) terephthalate (used during the melt pretreatment, so-called "internal additive")

<sup>&</sup>lt;sup>45</sup> 1,4-Cyclohexanedimethanol (used during the melt pretreatment, so-called "internal additive")

<sup>&</sup>lt;sup>46</sup> 4,8-Bis(hydroxymethyl)tricyclo[5.2.1.0<sup>2,6</sup>]decane (used during the melt pretreatment, so-called "internal" additive")

<sup>&</sup>lt;sup>47</sup> 1,5,7-triazabicyclo[4.4.0]dec-5-ene (TBD) (used during the melt pretreatment, so-called "internal catalyst")

<sup>&</sup>lt;sup>48</sup> 1,8-diazabicyclo[5.4.0]undec-7-ene (DBU) (used during the melt pretreatment, so-called "internal additive")

**Table 5- 1.** (cont'd)

$S_{15}$	10.0 g	YES	DBU (1)	CHDM (17.5)

Melt pretreatment in the presence of metallic catalysts and additives: The next set of experiments was focused on the impact of metallic catalysts, Zn(OAc)<sub>2</sub>, and Zn-EH, with or without the addition of 17.5 wight% of various diols, BHET, CHDM, and BHTD, during the melt-extrusion process. As mentioned earlier, zinc 2-ethylhexanoate was used **in this thesis** for the first time for the depolymerization of PET, with a 10 times lower price compared to zinc acetate and an environmentally safer alternative. For the glycolysis of these pretreated samples with a catalyst and/or diol (S<sub>3</sub> to S<sub>9</sub>) the presence and absence of a catalyst during the depolymerization (external catalyst) were also explored.

Melt pretreatment in the presence/absence of organic catalysts and diols: To move towards environmentally friendlier options for chemical depolymerization of PET, metallic catalysts were replaced with organic catalysts. Moreover, the simultaneous addition of 0.5 and 1 mol% an organic catalyst (TBD/DBU) and 17.5 and 10 weight% CHDM was explored. All compositions are listed in *Table 5-1* and a schematic of the process is depicted in *Figure 5-1*. The previously mentioned hypothesis was that through melt pretreatment in the presence of catalysts and diols, active sites would be created that accelerate the depolymerization in various ways, including facilitating depolymerization both from the surface and inside the bulk of PET chains, enhancing chain scission and broadening the molecular weight distribution, as well as formation of random copolymer to induce irregularity (in case of using CHDM as the diol) in the structure of PET.

## **5.2.2.2 Reaction optimization**

Solvent quantity: The effect of EG: PET molar ratio on the degree of depolymerization was investigated by subjecting ~300 g of the S<sub>3</sub> sample at 180 °C within 30 minutes. Furthermore, the role of the molar equivalent of EG to PET was examined in the conversion rate of the sample

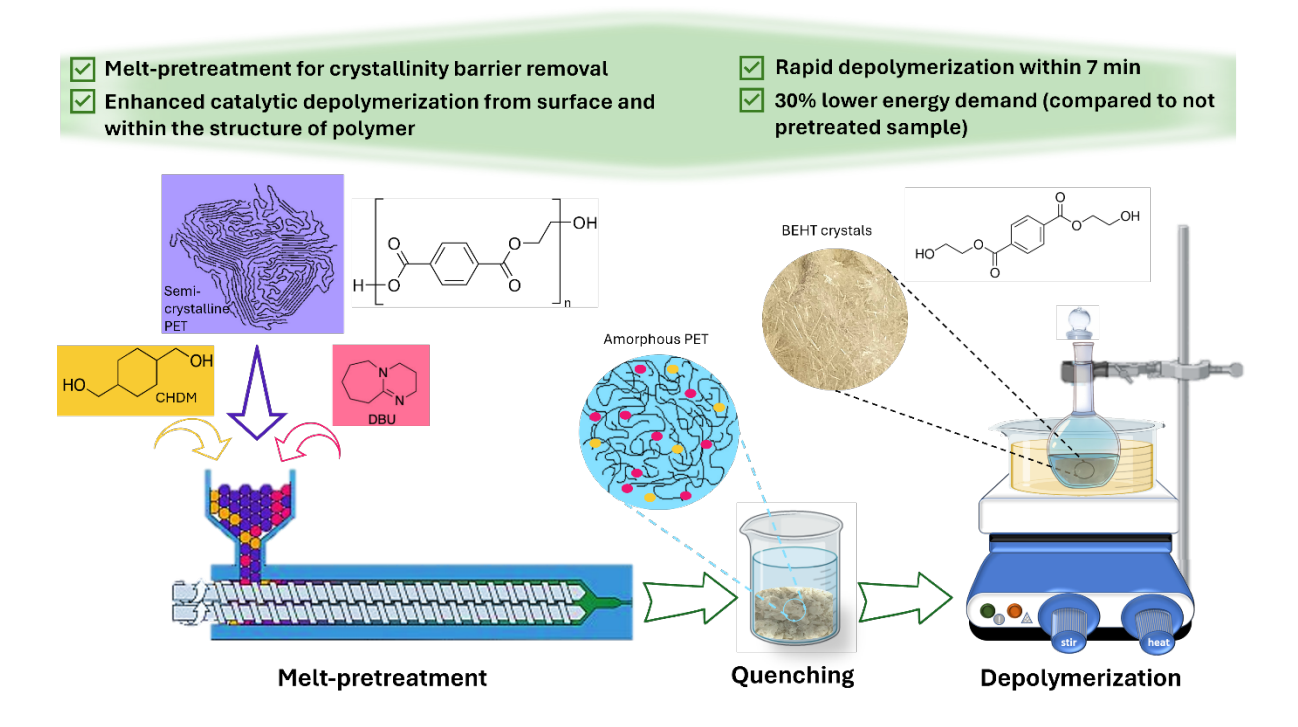


*Figure 5-1.* Schematic of the two-step depolymerization of post-consumer PET.

Effect of temperature: Samples containing metallic catalysts were examined at various depolymerization temperatures ranging from 160 to 200 °C in the presence of 10 molar equivalent of EG to PET and the absence of any catalyst during the glycolysis reaction. Additionally, for organic catalysis depolymerization reactions, S<sub>12</sub> was subjected to EG with EG to PET molar equivalents of 11 by varying the temperature from 170 to 200 °C.

# 5.2.2.3 Characterization

Energy Dispersive X-ray: To validate the distribution of catalysts inside the structure of melt pretreated samples, samples S<sub>0</sub> and S<sub>3</sub> underwent analysis using EDX.

Glass transition, crystallization, and melting temperature of non-pretreated/pretreated samples: Samples were characterized using Differential Scanning Calorimetry (DSC) using Q-100 TA Instruments, following the same previously described procedure. Two cycles of heating-cooling were run, during which samples in both cycles, samples were cooled down to 0 °C and

heated up to 270 °C with an equilibrium rate of 10 °C/min. Using the Universal Analysis 2000 software, glass transition temperature (T<sub>g</sub>), crystallization temperature (T<sub>c</sub>), and melting point temperature (T<sub>m</sub>) were determined.

Degree of crystallinity of pretreated samples: Using the data from the second cycle of the DSC analysis, the degree of crystallinity (% crystallinity) for selected PET samples was determined. The % crystallinity was calculated by integrating the area of the endothermic peak (enthalpy of fusion of the semi-crystalline PET) and a baseline drawn divided by the enthalpy of completely crystalline PET ( $\Delta m^{\circ} = 140.1 \text{ J/g}$ ) [1]–[4].

Inherent Viscosity of PET (non-treated and pretreated) samples: The inherent viscosities of samples S<sub>0</sub> to S<sub>15</sub> were measured, according to D4608-18 [5], to indirectly investigate the effect of melt treatment on the molecular weight of PET samples where higher inherent viscosity proportionate with higher molecular weight.

In-line Fourier Transfer Infrared Spectroscopy-Attenuated Total Resonance (FTIR-ATR) of reaction medium: The reaction progress was monitored by in-line FTIR-ATR. For this purpose, during the depolymerization of sample S<sub>3</sub> at 180 °C, a small amount of reaction from the clear layer was tested every 15 minutes.

Liquid Chromatography-Mass Spectrometry (LC-MS) of depolymerization products: To analyze the products of depolymerization, filtrates from the reactions were dissolved and diluted in methanol (MeOH). Using the data derived from MS, accurate mass, retention time, and fragmentation pattern, the compounds were identified, while Photodiode array (PDA) data was utilized for quantification of the identified compounds.

Nuclear Magnetic Resonance (NMR) of depolymerization reaction products: ~50 mg of selected crude PET samples were dissolved in deuterated chloroform and examined to obtain the

<sup>1</sup>H NMR spectra within chemical shifts of 0-14. The isolated monomers were also analyzed to confirm the high yield of the reactions.

## **5.2.3** Energy requirement calculation

The goal of this energy requirement assessment was to compare the energy demand for depolymerization of PET samples melt extruded with 0.5 mol% of organic catalyst (TBD/DBU) and 17.5 weight% CHDM versus that of non-pretreated samples depolymerized in the presence of 0.5 mol% of TBD/DBU under the same reaction conditions. For the pretreated samples, the total energy requirement was the summation of energy consumption for grinding PET (A), drying the ground PET mixed with catalyst (C), extrusion (D), depolymerization reaction (F), BHET crystallization (J), drying BHET (L), and drying undepolymerized by-products (I). Whereas the energy required for glycolysis of non-pretreated PET in the presence of 0.5 mol% TBD/DBU, only included the depolymerization reaction (F), drying of undepolymerized PET (I), crystallization of BHET (J) and BHET drying (L), and drying the undepolymerized by-products (I). In this laboratory-based analysis, energy for dissolving catalyst and mixing it with ground PET (B), quenching extruded samples (E), addition of boiling water to dissolve BHET (G), and filtration steps (H and K) were not included in the energy calculations. The process flow diagram (PFD) of the process is depicted in Figure 5-2. The table summary of the streams and the detailed calculations are included in APPENDIX A: ENERGY REQUIREMENT ASSESSMENT FOR DEPOLYMERIZATION OF POLYETHYLENE TEREPHTHALATE (PET).

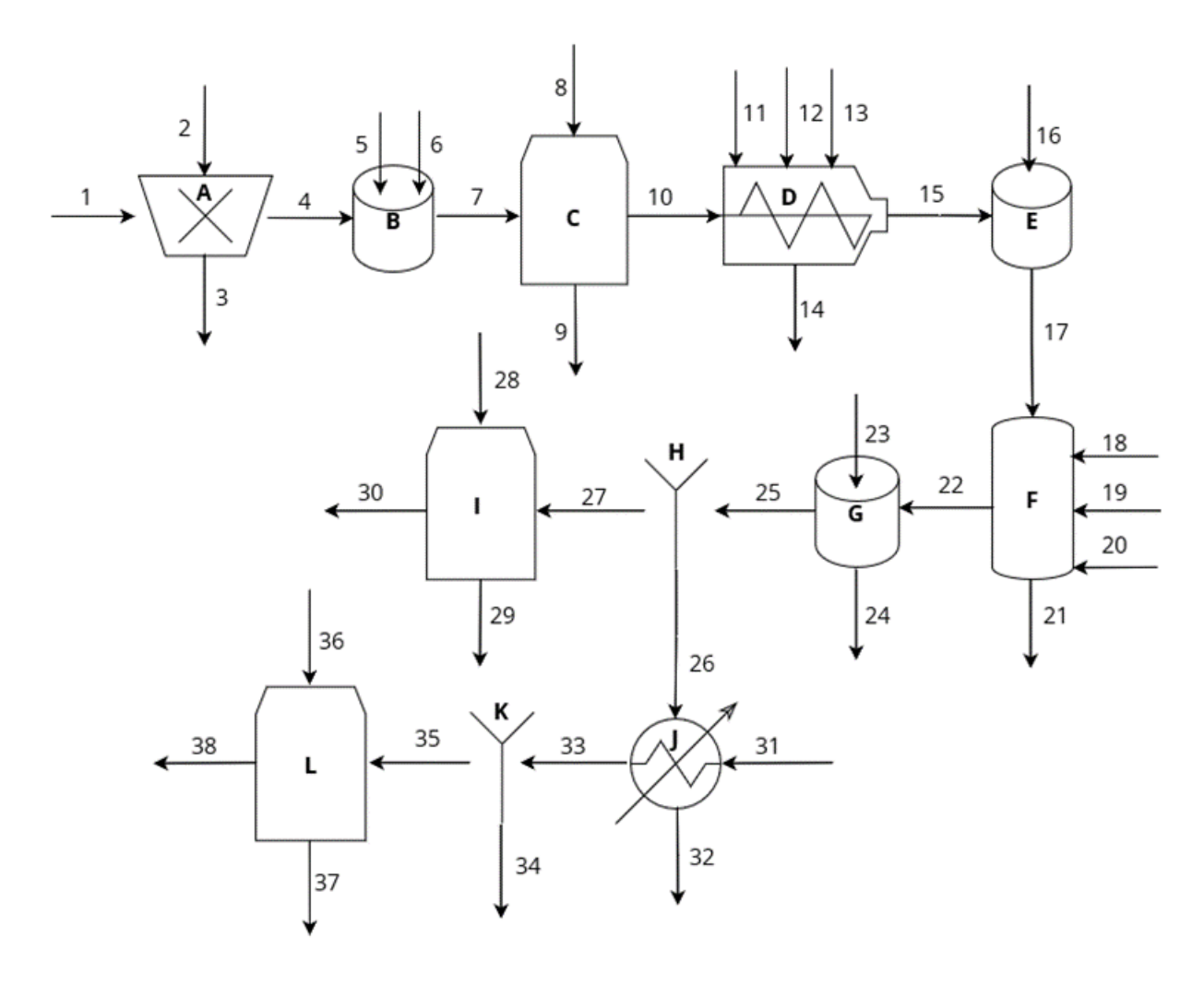


**Figure 5- 2.** Process flow diagram for the melt pretreatment and glycolytic depolymerization of PET.

Grinding (A): Hand-shredded PET was ground to a size of  $\sim 1 \text{ mm}^2$ . The energy requirement for this process was calculated as explained in **Chapter 4: 4.2.3 Energy requirement** calculation, according to the specifications of the grinder. It was assumed that 100 grams of PET was ground within  $\sim 120 \text{ min}$  and there was no material loss during the grinding process.

Dissolution of catalyst and mixing with ground PET (B): Both TBD and DBU are soluble in either water or acetone. Herein, we tried 500 mL water to dissolve 100 grams of ground PET mixed with TBD/DBU. The catalyst solution was mixed with ground PET and dried at 60 °C

temperature. The energy for drying 500 mL water was calculated from the energy required to evaporate the water, assuming 10% energy loss during this process.

Extrusion (D): The energy requirement for the extrusion process was calculated, assuming that the power of the extruder is linearly correlated with temperature [6]–[8], and the energy required for preheating is based on a heating rate of 5 °C/s and a minimum power output of 500 watts (corresponding to 222 °C). Additionally, with the lower boiling point of catalysts than 280 °C and close to the boiling point of CHDM (286 °C), some of the catalysts and additives were likely evaporated. consequently, it is reasonable to consider at least 10% of material loss through evaporation and solidification in the extruder and on the screws (106 grams exits the extruder). With a max capacity of extruder to be 20 grams per cycle and 30 seconds of extruding LDPE after each cycle, the extruder was run for ~22.5 minutes to extrude 100 grams of PET.

Quenching (E): The PET sample exiting the extruder was immediately quenched in cold methanol to stop the crystal growth in PET.

Depolymerization (F): The depolymerization reaction involved the addition of  $\sim$ 300 grams of the PET (untreated and pretreated) to a 15 mL pressure flask and subjection to glycolysis by immersion in an oil bath at 190 °C. For neat PET samples, S<sub>0</sub>, 0.5 mol% of TBD/DBU was used during the polymerization, while samples S<sub>12</sub> and S<sub>13</sub> were depolymerized in the absence of any additional catalysts. The reaction was assumed to be terminated when the medium went clear. Energy loss from the hot plate to the surroundings was calculated by the convection of heat from the surface of the hot plate that was in contact with the air. Additionally, assuming a ceramic top of  $\sim$ 0.5 kg on the hot plate, the energy required for preheating the hot plate was determined. With linearity of power with temperature [6]–[8], the energy requirement for the depolymerization was calculated.

Mixing with water (G): After cooling the reaction medium within 5-10 minutes, approximately 550 mL of distilled (DI) water, boiled, was added (approximately 6-7:1 water to BHET ratio) to separate water-soluble monomers from insoluble compounds.

Filtration of water-insoluble by-products (H): unpolymerized compounds were separated from the water-soluble polymerized products using a Büchner funnel.

Drying By-products (I): With  $\sim$ 300% water content in the by-products, the energy required to evaporate the water at 60 °C was calculated based on the enthalpy of water at 60 °C and a 90% dryer efficiency.

Crystallization (J): The water-soluble mixture was chilled to 4 °C to induce crystallization of BHET. The energy for boiling water and crystallizing BHET was determined using the specific heat of water and BHET. The energy needed to crystallize BHET that was produced from the depolymerization of the S<sub>0</sub> sample in the presence of 0.5 mol% TBD/DBU was calculated similarly.

Filtration of crystallized BHET (K): BHET was filtered from the water using a Büchner funnel.

Drying BHET monomers (I): Similar to the by-products, with  $\sim 300\%$  water content in filtered BHET, energy for drying the yielded BHET from both samples  $S_{11}$  and  $S_{12}$  was calculated using the heat of vaporization of water and considering 90% efficiency for the dryer. Analogous calculations were performed to find the energy required for drying BHET yielded from depolymerization of the  $S_0$  sample in the presence of 0.5 mol% TBD/DBU.

#### **5.3 Results and Discussion**

Another goal of **this thesis** was to extend the two-step energy-efficient process devised for methanolysis of PET to glycolic depolymerization in the presence of metallic and organic

catalysts. The melt-extrusion-cold-quench in the presence of catalysts and diols proved the success of this melt pretreatment process in lessening the crystallinity of PET and the formation of active sites that can enhance the depolymerization rate. Zinc 2-ethylhexanoate, used for the first time for chemical recycling PET, showed high performance in glycolytic depolymerization of PET, too. Samples pretreated according to *Table 5-1* were subjected to ethylene glycol in the presence and absence of a catalyst during the depolymerization process. The conditions were optimized for the glycolysis reactions. Additionally, the pretreated samples, as well as the depolymerized products, were characterized using various methods. Finally, the energy required for the two-step recycling of PET using organic catalysts during the melt treatment step was compared with that of non-pretreated PET depolymerization in the presence of TBD and DBU, as so-called external catalysts.

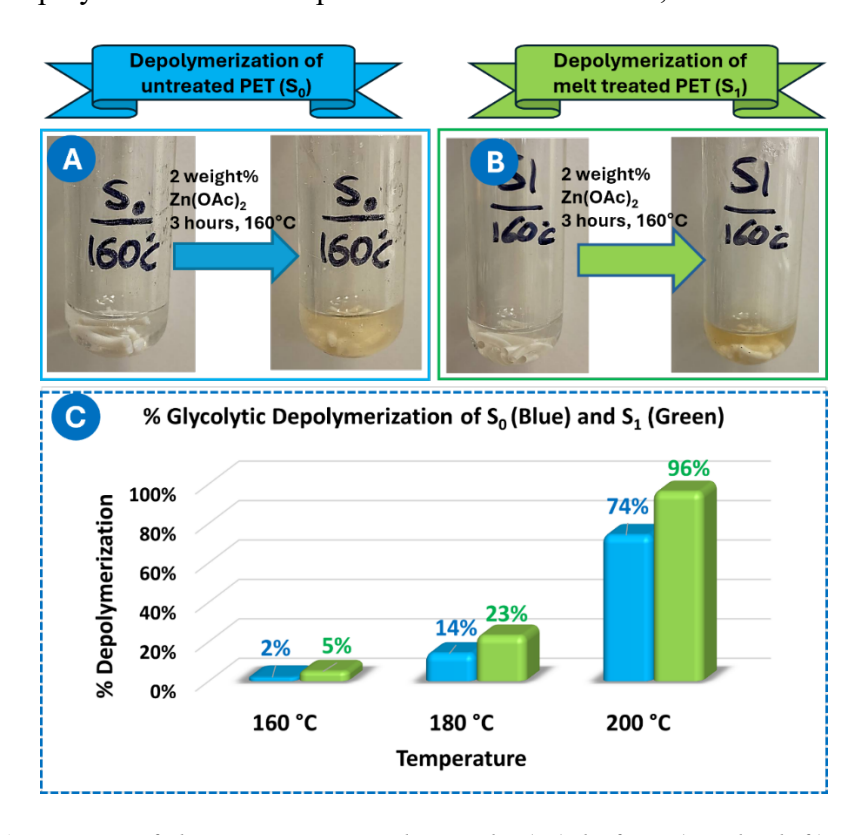


**Figure 5- 3.** A) Images of the non-pretreated sample  $(S_0)$  before (on the left) and after (on the right) the glycolytic depolymerization at  $160^{\circ}$ C for 3 hours. B) Images of the pretreated sample with no catalysts and additives/diols  $(S_1)$  before (on the left) and after (on the right) the glycolysis at  $160^{\circ}$ C for 3 hours. C) Depolymerization of  $S_0$  and  $S_1$  samples at various temperatures for 30 minutes.

Initially, the effect of melt pretreatment in the presence and absence of any catalysts and diols on the glycolytic depolymerization of PET was studied by subjecting two samples,  $S_0$  and  $S_1$  to ethylene glycol and 2 weight% zinc acetate at 160°C, as depicted in *Figure 5- 3A* and *B*. Since both  $S_0$  and  $S_1$  were fully depolymerized at 200 °C within 3 hours (with different times of depolymerization), the glycolysis reactions at different temperatures were performed within 30 minutes. Results revealed that the melt treatment accelerated the depolymerization at 180 and 200 °C by ~30 and ~40%, respectively, as depicted in *Figure 5-3C*.

Subsequently, the depolymerization time of melt pretreated samples,  $S_1$  to  $S_9$  with compositions according to *Table 5-1*, were examined. Same with neat PET  $(S_0)$ , depolymerization of the sample pretreated with no metallic catalyst or diol (S<sub>1</sub>) occurred in the presence of 2 weight% zinc acetate (as a so-called external catalyst), whereas other samples (S2 to S9) were glycolyzed without the addition of any further catalyst or diol. When the time of full depolymerization (when the sample was clear) of neat PET (S<sub>0</sub>) in the presence of 2.5 mol% (equal to 2 weight%) zinc acetate (more than 6 hours) was compared to that of S<sub>2</sub> (95 min), a ~4-fold acceleration was observed. Furthermore, the comparison of sample S<sub>1</sub> with S<sub>2</sub> exhibited a drastic acceleration (~2fold) when zinc acetate was incorporated during depolymerization versus during melt extrusion, (S<sub>1</sub> versus S<sub>2</sub>), refer to *Figure 5-4*. Further acceleration was observed when zinc acetate was replaced with zinc 2-ethylhexanoate (S<sub>3</sub>), from 95 minutes to 85 minutes. Another significant improvement was achieved when catalysts and diols were incorporated during the pretreatment at the same time. At 180 °C, while depolymerization of non-pretreated PET (S<sub>0</sub>) took over 6 hours, the melt pretreated PET with Zn-EH and CHDM (S<sub>7</sub>) only took 9 minutes. The same hypothesis was applied that the presence of a catalyst and a diol can enhance the rate of depolymerization via chain scission, formation of active sites, and introduction of irregularity in the structure of PET, in

addition to trapping the catalyst within the bulk of polymer that enables depolymerization not only from the surface but also from within the chains.

Similar to metallic methanolysis of PET, the presence of zinc-based catalysts during PET melt pretreatment could accelerate degradation through various means. If water traces are present, zinc can form complexes with PET's carbonyl oxygen, aiding water molecules' attack on the carbonyl carbon. This cleaves ester bonds, forming carboxylic acid and alcohol groups, therefore reducing the molecular weight of PET. The higher efficiency of zinc 2-ethylhexanoate (found in sample S<sub>3</sub>) over zinc acetate (in sample S<sub>2</sub>) is due to better mixing and miscibility of the former in PET, boosting its catalytic activity in PET degradation.

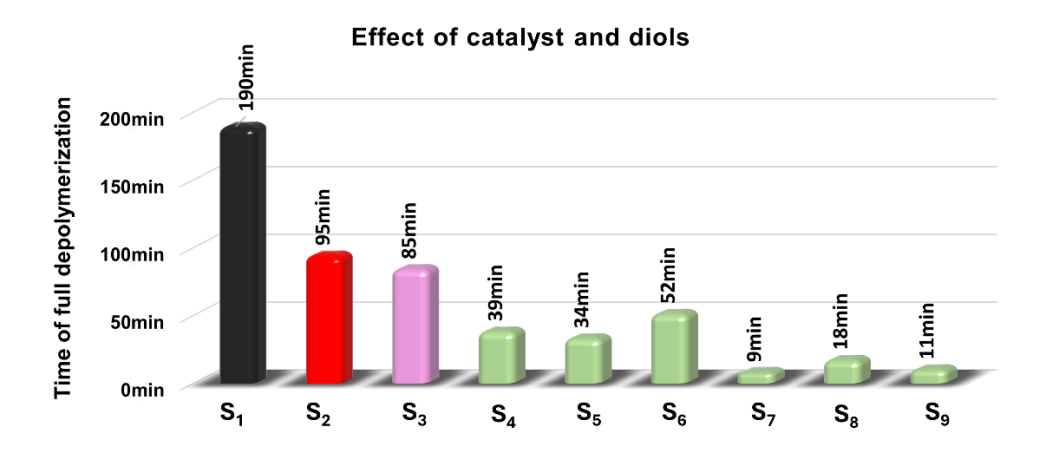


**Figure 5- 4.** Time for full depolymerization of samples pretreated with or without metallic catalysts. Lengthier depolymerization of pretreated samples in the absence of any catalysts or diol  $(S_1, black)$  compared to improved rate of depolymerization for samples containing only catalyst  $(S_2 \text{ and } S_3)$ , and samples carrying both catalyst and diol/additive  $(S_4 - S_9)$  in EG to PET molar ratio of 10:1 at 180°C. (sample  $S_0$  was depolymerized in the presence of 2 weight% zinc acetate while no catalysts were added during the glycolysis of samples  $S_2$  to  $S_9$ ).

Furthermore, in the presence of diols alongside zinc acetate or zinc 2-ethylhexanoate, the zinc catalyst can coordinate with the carbonyl oxygen of PET's ester bond, making the nucleophilic attack by the diols more favorable. This coordination, involving zinc cation acting as a Lewis acid, amplifies the electrophilic nature of the ester carbon, thereby attracting nucleophiles like the hydroxyl groups of the diol. In the case of zinc 2-ethylhexanoate, the ethylhexanoate ligands can

chelate with the zinc cation, creating a larger and more stable coordination environment. This enhances the catalyst's miscibility with PET and promotes the activation of the ester bond.

Extending the research to organic catalysis further confirmed the applicability of this two-step methodology for the chemical recycling of PET. For preparing the samples for melt extrusion, 0.5-1 mol% TBD/DBU was dissolved in water, mixed with ground PET, and fed into the extruder along with 17.5 weight% of CHDM. Herein, only CHDM was chosen out of the three examined diols, due to the higher performance of the sample pretreated with CHDM, S<sub>7</sub> [9], [10]. Initial screening was performed when solely 0.5 mol% of TBD/DBU was deployed, samples S<sub>10</sub> and S<sub>11</sub>. The results presented a slight decelerated rate of reaction with full depolymerization within 350 and 320 minutes in the presence of TBD and DBU, respectively (*Figure 5-5*).

At high temperatures, TBD or DBU may interact with functional groups in PET, such as hydroxyl or carboxyl groups. These interactions could potentially lead to coupling reactions, where they covalently bond to PET molecules, hence altering the structure of PET and influence its degradation behavior. Even if direct coupling doesn't occur, the basic properties of TBD and DBU can catalyze certain reactions within the PET matrix. This catalytic activity could enhance PET degradation by promoting reactions such as hydrolysis (in case traces of water were present), chain scission, or other degradation pathways. Meanwhile, the presence of even traces of water at high temperatures can hydrolyze TBD and DBU, leading to neutralizing their catalytic activity. On the other hand, TBD and DBU might also stabilize PET molecules under certain conditions, potentially inhibiting degradation. This stabilization could occur through hydrogen bonding interactions between TBD and functional groups in PET, which may hinder the mobility of polymer chains and reduce their susceptibility to degradation.

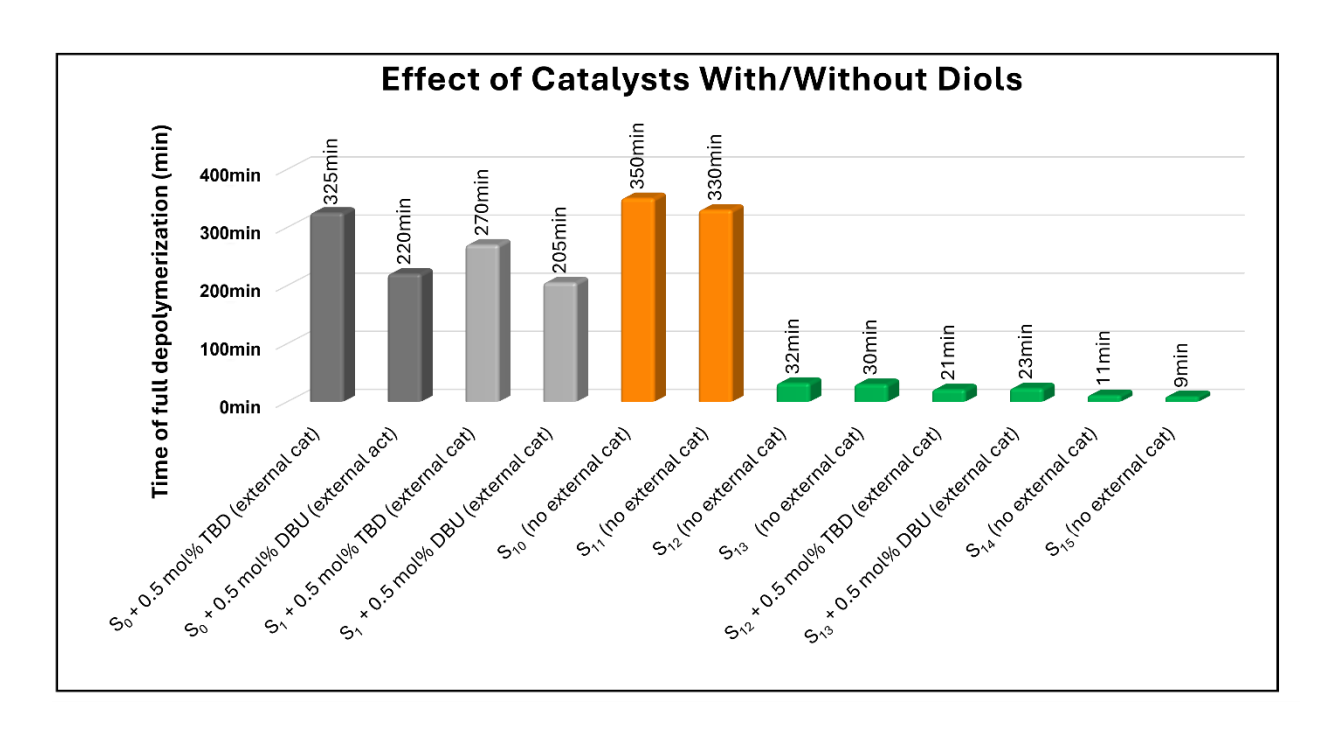


**Figure 5- 5.** Effect of the presence of catalyst with/without during the pretreatment versus during the depolymerization. All samples were glycolyzed in the presence of 10 molar equivalent of EG to PET at 190 °C.

When catalyst and diol, herein CHDM, were employed together during the melt-extrusion, the reaction rate accelerated significantly, by at least 7 to 8 times compared to S<sub>0</sub>, aligning with previous findings. When a diol is present, the hydroxyl groups that act as nucleophiles attack the carbonyl carbon of the ester bond in PET. The interaction between the diol and the catalyst can occur through coordination/hydrogen bonding with the nitrogen atoms of TBD or DBU, leading to the formation of a reactive complex. TBD and DBU can enhance the reactivity of the diol by activating its hydroxyl groups through hydrogen bonding and in turn increasing electron density of the Oxygen of the OH, thus increasing their nucleophilicity. Additionally, DBU or TBD catalysts can facilitate the attack of the diol on the ester bond by stabilizing transition states and lowering the activation energy barrier of the reaction. Consequently, PET acquired a broader molecular weight distribution, resulting in smaller chains that are more susceptible to glycolysis and leading to increased amorphization. Furthermore, CHDM, being a diol different from the PET

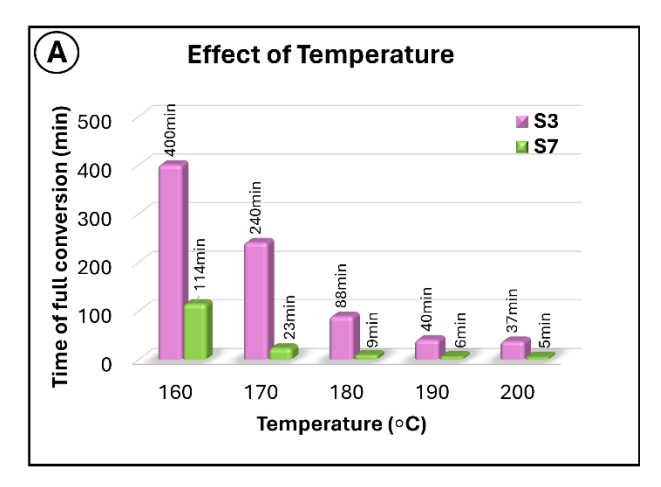
building block, could introduce irregularities in the PET chains, further enhancing amorphization. Moreover, active sites were hypothetically formed where the catalyst was dispersed within the structure of PET and could not only enable the depolymerization from the surface of the polymer but it could facilitate the attack to the ester bonds from within the structure of the polymer [10].

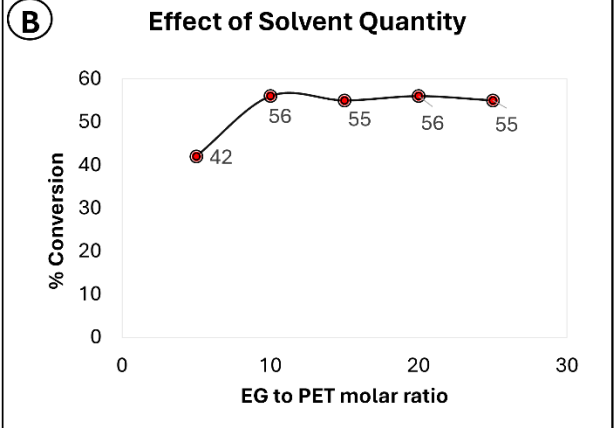
Comparison of the depolymerization rate of samples containing TBD (e.g., S<sub>12</sub>) to those having DBU (such as S<sub>13</sub>) revealed that despite the bifunctionality of TBD, capable of activating both esters and alcohols through hydrogen bonding, DBU presents more efficacy during the depolymerization. A computational study demonstrated that the excess EG can also serve as a cocatalyst during the glycolysis of PET, working synergistically with the catalyst to activate the ester carbonyl group via hydrogen bonding. This combined activation, particularly in the presence of excess short-chain diols, is more effective than activation by the bifunctional TBD catalyst [11].

Figure 5- 5 also revealed that when the catalyst content was increased from 0.5 mol% to 1 mol% in samples S<sub>14</sub> and S<sub>15</sub>, the reaction proceeded three times faster. Moreover, to examine the effectiveness of using catalysts both during pretreatment and depolymerization compared to using catalysts solely during extrusion, samples S<sub>12</sub> and S<sub>13</sub> were depolymerized in the presence of a 0.5 mol% external catalyst (added during depolymerization). Contrasting these results with samples S<sub>14</sub> and S<sub>15</sub>, containing 1 mol% TBD and DBU respectively, revealed that employing catalysts solely during extrusion is more effective than a partial addition during melt-extrusion and partial addition during depolymerization.

The effect of multiple parameters on the glycolytic depolymerization of PET was examined to find an optimal reaction condition. The impact of solvent quantity was studied on S<sub>3</sub> by altering the EG to PET molar ratio from 5 to 25 at 180°C and measuring % depolymerization within 30 minutes, *Figure 5-6*. The results showed that 10 molar equivalents of EG have a higher rate of

conversion of PET and the conversion rate will not increase by elevating the amount of EG.





**Figure 5- 6.** Effect of reaction conditions on PET depolymerization. **A)** Effect of temperature on the time of full depolymerization of  $S_3$  and  $S_7$ . **B)** Effect of solvent quantity on PET conversion of sample  $S_3$  at  $180 \, ^{\circ}$ C.

Additionally, to explore the impact of the temperature on the time of complete depolymerization, sample S<sub>3</sub> was subjected to 10 molar equivalents of EG and varying the temperature from 160 to 200°C. *Figure 5- 6* shows that for samples containing metallic catalysts, S<sub>3</sub> and S<sub>7</sub>, by increasing the temperature from 160 to 190°C significant improvements were observed. For sample S<sub>3</sub>, the time for 100% depolymerization was decreased from 400 minutes to 40 minutes, with a ~2-fold acceleration for each 10°C temperature elevation. Finally, the effect of time was explored on sample S<sub>3</sub> at 180C showing that a 90% conversion was achieved after 60 minutes, and the PET sample was fully depolymerized in less than 100 minutes.

Moreover, the reaction conditions for organic catalysis of PET were studied at various temperatures, EG to PET molar ratio, and the amounts of catalyst. To keep the catalyst content as low as possible, the amount of catalyst added during the melt pretreatment was increased from 0.5 to 1 mol% enabling 3 times faster depolymerization, but the reaction was still rapid at lower catalyst contents, suggesting that both 0.5% and 1% can be chosen as the optimal catalyst dosage owing to the ability to achieve desirable reaction kinetics without using excessive catalysts.

Studying the impact of temperature on the reaction kinetics proved that it is more pronounced. Below the temperature of 190 °C, the reaction proceeded at a low pace, while temperatures above 190 °C did not yield significantly faster reaction rates. For example, the depolymerization of sample S<sub>12</sub> at 170 °C took more than 23 hours. Increasing the temperature to 180 °C could drastically decrease the time of full depolymerization by up to 78 minutes. However, comparing the rate of depolymerization at 190 °C and 200 °C, it was observed a marginal difference of less than 9 minutes. Therefore, 190 °C was identified as the optimal temperature for maximizing reaction efficiency and PET conversion. Moreover, different EG to PET molar ratios were examined to find the optimal condition for a higher degree of degradation. It was observed that EG molar equivalents lower than 8 and more than 16 decelerate the glycolysis reaction with slight improvement when 24 molar equivalents were used with values around 10 to 12 producing the lowest amount of undepolymerized PET, being in line with many other investigations [11]–[14].

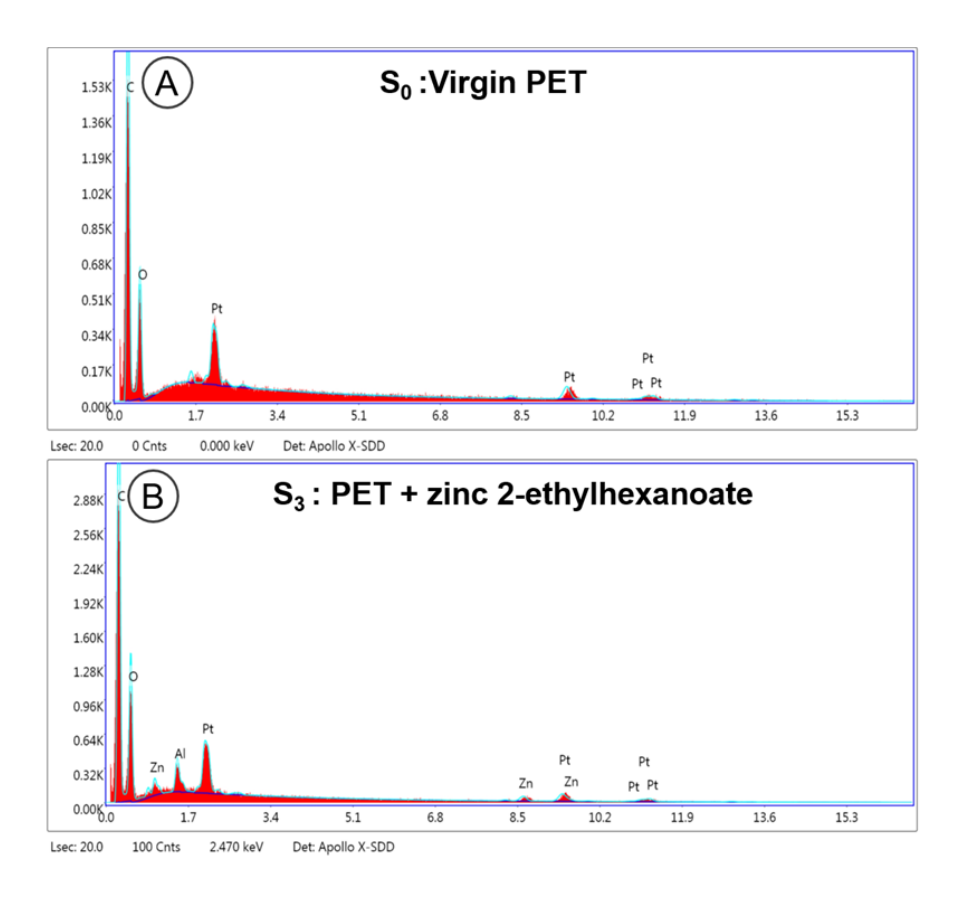


**Figure 5-** 7. EDX analysis of PET samples with no catalyst vs pretreated with zinc 2-ethylhexanoate. A) EDX analysis of virgin  $PET(S_0)$  with no peak appearance corresponding to zinc atom, and B) EDX of the PET sample pretreated with zinc 2-ethylhexanoate ( $S_3$ ) confirming the presence of zinc atom within the structure of the PET sample.

To track the catalyst during the pretreatment process, EDX analysis was performed on samples S<sub>0</sub> and S<sub>3</sub>. *Figure 5-7A* shows no traces of zinc atoms in the structure of neat PET, sample S<sub>0</sub>, whereas zinc atoms were found in the structure PET pretreated with zinc 2-ethylhexanoate, sample S<sub>3</sub>, *Figure 5-7B*. This validates the distribution of catalyst within the structure of PET during the pretreatment process, which enables the initiation of depolymerization within the bulk of polymer in addition to depolymerization from the surface, resulting in enhancing the rate of depolymerization.

The thermomechanical properties of samples pretreated with organic catalysts,  $S_{10}$  to  $S_{15}$  were also assessed using DSC. The results of the DSC analysis unveiled significant alterations in the PET samples with different compositions. The DSC thermogram of neat PET (*Figure 5- 9A*)

displayed distinctive thermal characteristics, with a glass transition temperature ( $T_g$ ) of approximately 80 °C, crystallization temperature ( $T_c$ ) of around 140 °C, and a melting point ( $T_m$ ) starting at about 227 °C, marked by a sharp peak at 253 °C. Following the melt pretreatment, significant changes emerged, as depicted in *Figure 5- 9B*. The  $T_c$  values for the treated samples  $S_{10}$  and  $S_{11}$  declined to 99 °C and 102 °C, respectively, revealing potential disruption in the crystalline structure. Moreover, the broader melting range ( $T_m$ ) for  $S_{10}$  and  $S_{11}$  initiated at 221 °C and 219 °C, respectively. This broadening suggests a wider distribution of molecular weights, attributed to chain scission due to extrusion. Notably, despite this broader distribution, the sharp peaks in  $T_m$  for both  $S_{10}$  and  $S_{11}$  shifted to approximately 258 °C, depicting the multiple ways TBD and DBU can impact the degradation pattern of PET by both facilitating or impeding it. This also confirms that the slight extension in the time of depolymerization for these samples are due to simultaneous chain scission and potential mobility hinderance in PET.

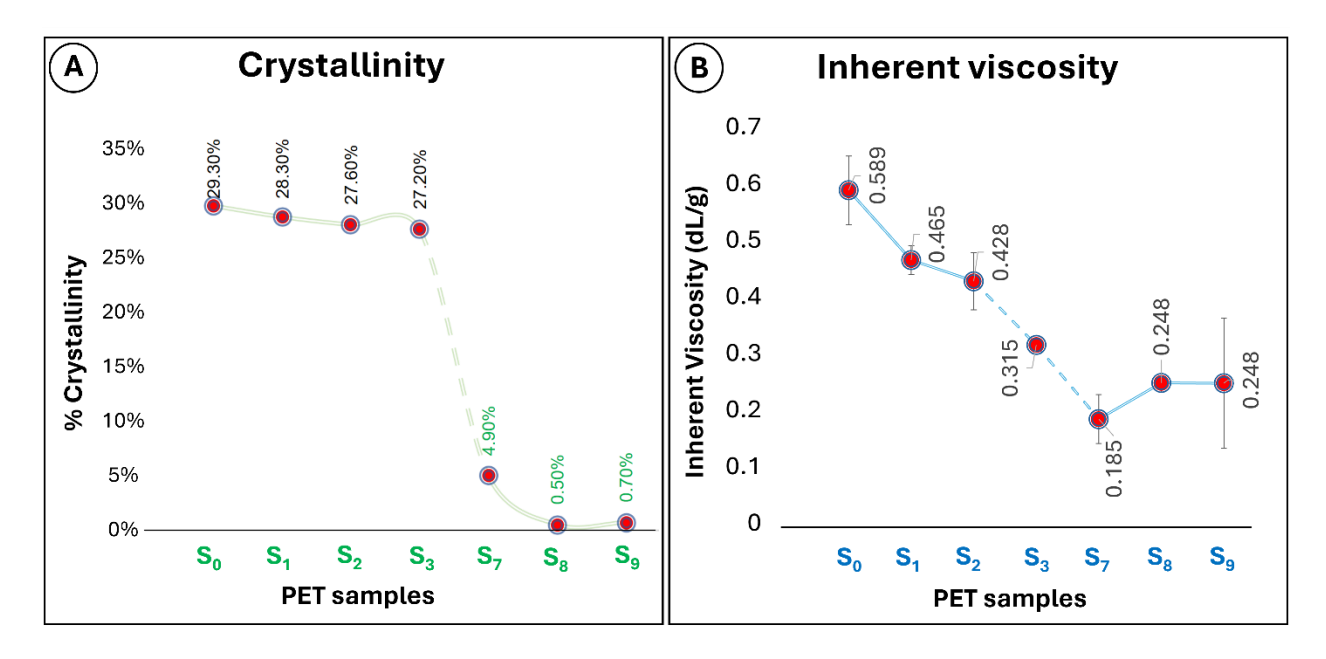


**Figure 5- 8.** Impact of pretreatment on degree of crystallinity and inherent viscosity of PET. **A)** % Crystallinity of selected samples indicating the descending crystallinity after pretreatment. **B)** Inherent viscosity of selected samples as an indirect measurement of molecular weight revealing decreasing molecular weight after pretreatment with S<sub>7</sub> having the lowest value.

To confirm the hypotheses of how pretreatment had impacted the PET polymer, Differential Scanning Calorimetry (DSC) was performed. Samples S<sub>0</sub> to S<sub>9</sub> were previously analyzed and the results were elaborated in *Chapter 4*. In this chapter, the crystallinity of the samples is compared alongside inherent viscosity. *Figure 5-8A* reveals the decreasing pattern of crystallinity after pretreatment, where extrusion with/without catalyst (S<sub>1</sub> to S<sub>3</sub>) slightly lowered the crystallinity, whereas when both catalyst and diols were incorporated (S<sub>7</sub>, S<sub>8</sub>, and S<sub>9</sub>) the samples became almost amorphous with less than 4.9% crystallinity. Similar pattern was observed in *Figure 5-8B* where the molecular weight of the samples was indirectly examined by measuring the inherent viscosity, except that while the inherent viscosity of S<sub>7</sub> is the lowest, the sample is still slightly crystalline (4.9%). This can be attributed to the not full homogeneity of the samples. While PET was fully immersed in the catalyst solution and were mixed with the diol before extrusion, the short period of extrusion process cannot guarantee the homogeneous distribution of catalyst and diols within the sample. This was also observed in the different time of depolymerization in each repetition.

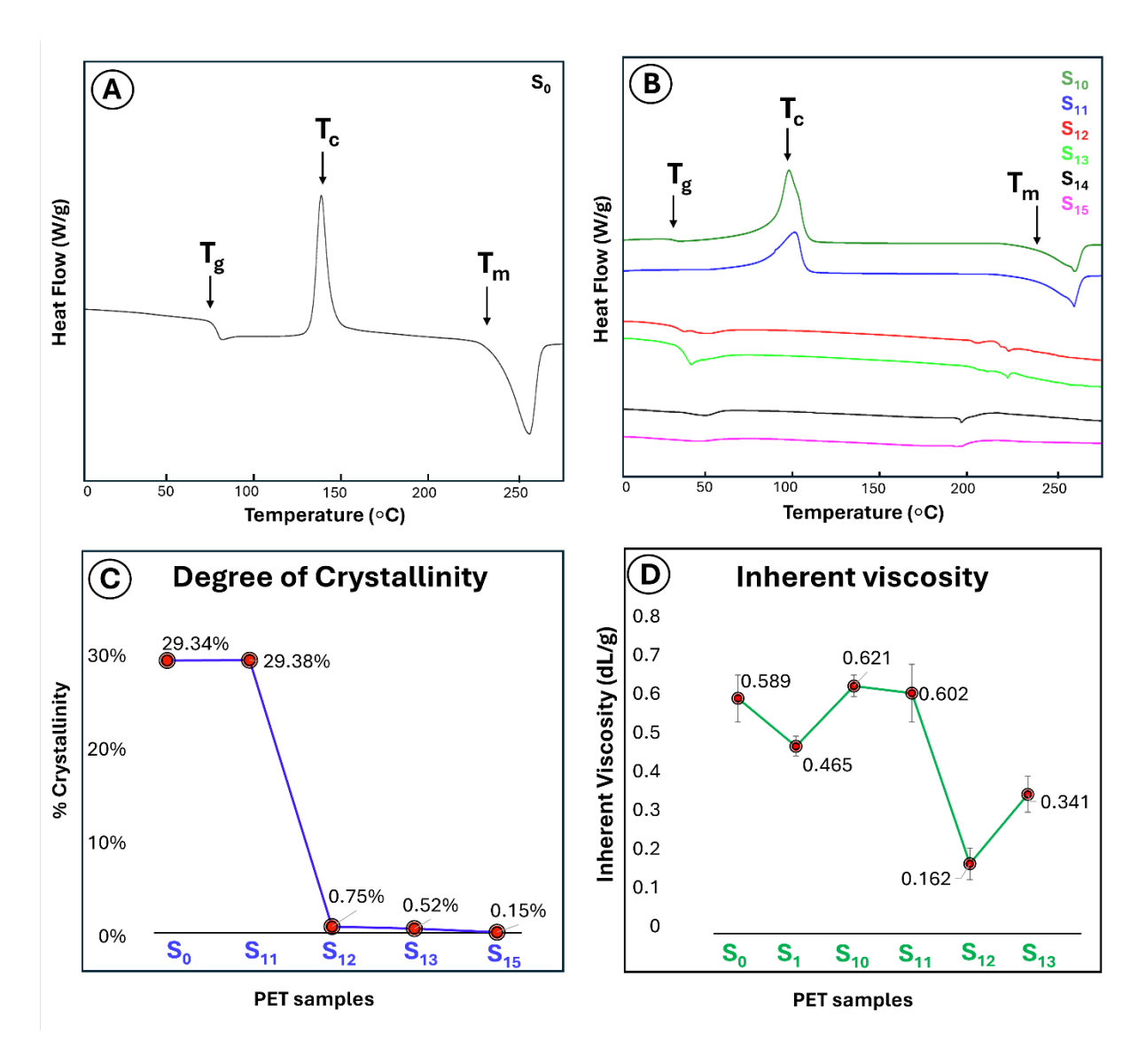


**Figure 5- 9.** DSC analysis, crystallinity, and inherent viscosities of the samples. **A)** DSC thermogram of neat PET  $(S_0)$  with identified  $T_g$ ,  $T_c$  and  $T_m$ . **B)** DSC thermograms of pretreated samples with catalyst with/without diols  $(S_{10}$  to  $S_{15})$ , presenting  $T_C$  and  $T_g$  and  $T_m$ . **C)** Degree of crystallinity of selected PET samples. **D)** Inherent viscosity of selected PET samples.

Furthermore, *Figure 5- 9B* exhibited that the incorporation of catalysts and diols in samples  $S_{12}$  to  $S_{15}$  induced drastic changes. DSC thermograms explained the rapid depolymerization, evident from lowered and broadened  $T_m$  values. The presence of -OH groups from the CHDM diols likely contributed to this effect by promoting chain scission. Consequently,  $S_{12}$  to  $S_{15}$  experienced accelerated depolymerization compared to  $S_{10}$  and  $S_{11}$ . These shifts in  $T_m$ 

correspond to irregularities in PET chains introduced by the presence of CHDM during extrusion, as a diol different from the building block of PET [10]. Additionally, the degree of crystallinity for sample containing only catalyst (S<sub>11</sub>) was very close to that of non-pretreated PET, *Figure 5-9C*, showing the minimal impact of DBU on disrupting the crystallinity of PET. This is also reflected in the inherent viscosities of sample S<sub>11</sub>, *Figure 5-9D*, where the average values are slightly higher than virgin PET, but the standard deviation is larger, exhibiting the complicated impact of DBU on the degradation of PET during melt-extrusion. This can also be attributed to the inhomogeneity of the samples that can be explained by the different time of full depolymerization in each repetition as well. The results of % crystallinity calculation and inherent viscosity on samples containing both catalyst and diol aligned with the previous hypothesis, revealing the extensive chain scission, complete elimination of crystalline regions, and lower and broadened molecular weight.

The PET depolymerization reaction progress towards the production of BHET was analyzed using FTIR-ATR spectroscopy. Samples were taken from the clear top layer of the reaction every 15 minutes and analyzed. BHET characteristic peaks of BHET [39] at 1718 cm-1 (C=O) and 1275 cm-1 (C=O) [15] became more defined in the first 60 minutes and no visible change was observed after that, showing consistency with the previous result of ~90% conversion in the first 60 minutes. consistent from 90 minutes to 120 minutes. Concurrently, the shift in the peak at 1718 cm-1 towards 1714 cm-1 is likely attributed to the involvement of distributed zinc atoms within the structure of PET that started the depolymerization process by attacking the carbonyl group.

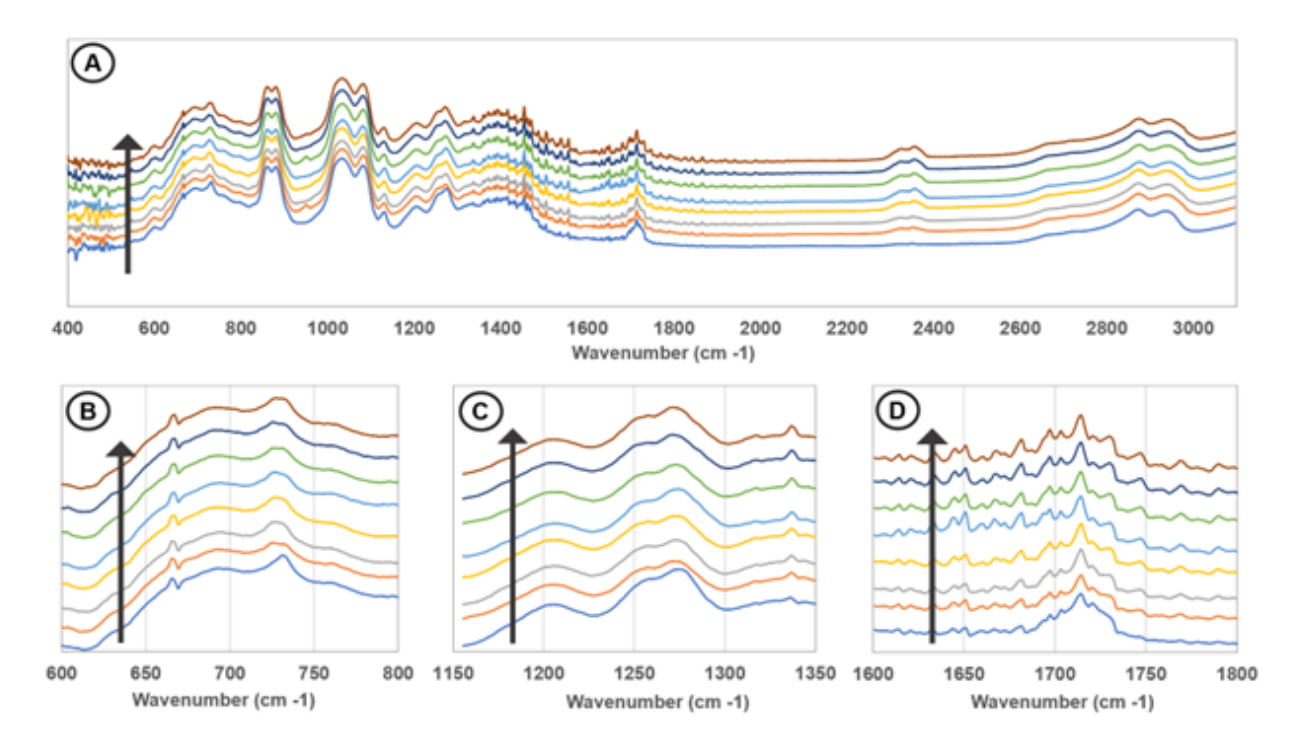


**Figure 5- 10.** FTIR spectra of the PET depolymerization reaction of sample  $S_3$ . **A)** full FTIR spectra of the reaction medium obtained at 15 min intervals from blue to brown lines being the first and last spectra. **B)** Magnified characteristic peak for C-H bond in BHET at 731 cm<sup>-1</sup>. **C)** Zoom-in characteristic peak at 1275 cm<sup>-1</sup> corresponding to C-O bond in of BHET. **D)** Magnified characteristic peak of C=O bond in BHET at 1718 cm<sup>-1</sup>. A considerable shift in the first 60 minutes and insignificant changes after 90 minutes were observed with a peak at 1718 cm<sup>-1</sup> shifting to 1714 cm<sup>-1</sup> that portrays the attack of  $Z_n$  to the carbonyl group.

Products of depolymerization were characterized using LC-MS analysis and <sup>1</sup>H NMR spectroscopy. Comparing the peaks that appeared in LC-MS spectra of depolymerized samples S<sub>1</sub>, S<sub>3</sub>, S<sub>7</sub>, S<sub>12</sub>, and S<sub>13</sub> with the standard spectra of BHET monomer and dimer, at 3.62 and 4.8 minutes, respectively, confirmed the presence of these two compounds in all samples, *Figure 5- 11A* and *11B*. Additionally, traces of BHET trimer and two new compounds were identified, the molecular structures of which are presented in *Figure 5- 11E*. These compounds were quantified using a photodiode array (PDA) and listed in *Figure 5- 11C*, while the yield of monomers and dimers are plotted The results from LC-MS revealed that, under the sample reaction conditions, glycolysis of sample S<sub>7</sub> yielded the highest amount of BHET (~85%), with all other samples yielding around 75

to 78% BHET monomer and up to 7.5% dimer.

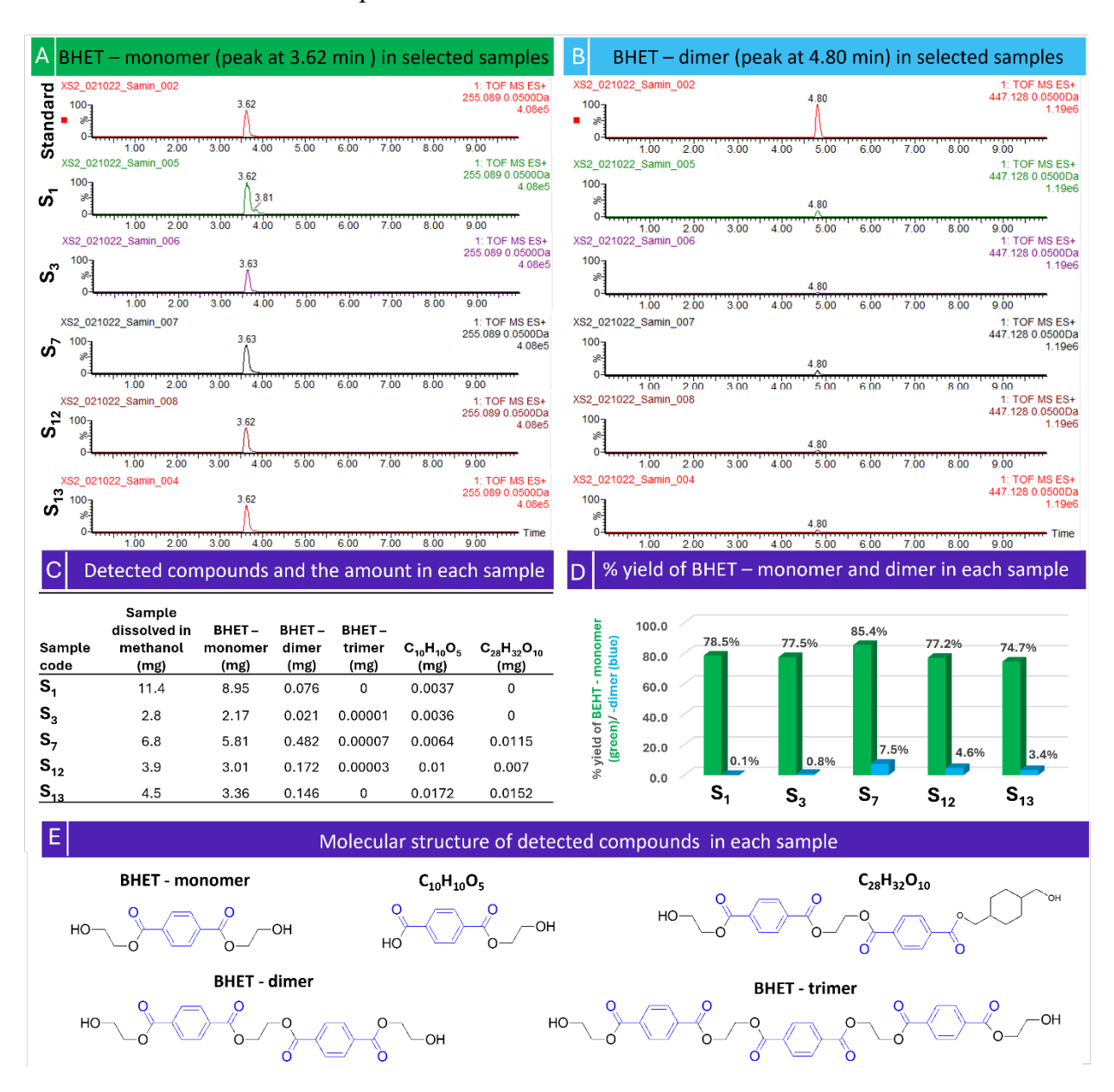


**Figure 5-11.** LC-MS analysis of depolymerized products and %yield of BEHT monomers and dimers. **A)** Peak at 3.62 min corresponding to the BEHT monomer in the standard and depolymerization products of selected samples. **B)** Peak at 4.8 min related to the BHET dimer in the standard and products of depolymerization of selected samples. **C)** Quantities of the compounds detected in each sample. **D)** % yield of BHET monomer and dimer in each sample. The highest yield of BHET was observed in sample S<sub>7</sub>.

The <sup>1</sup>H NMR spectra of the crude filtrate obtained from depolymerized samples S<sub>3</sub> and S<sub>7</sub> exhibited the presence of BHET monomer in addition to ethylene glycol (EG) and byproducts

(potentially consisting of dimers and monomers). In the  $^1H$  NMR spectra, the peak at  $\delta = \sim 8.1$  ppm corresponds to the four aromatic protons in BHET, and the two triplets at  $\delta = \sim 4.95$  ppm and  $\delta = \sim 4.3$  ppm are related to hydrogens in hydroxyl groups and methylene adjacent to the carboxylic groups, respectively, while the quadlet at  $\delta = \sim 3.8$  ppm is associated with the methylene adjacent to the hydroxyl protons, all confirming the presence of BHET.

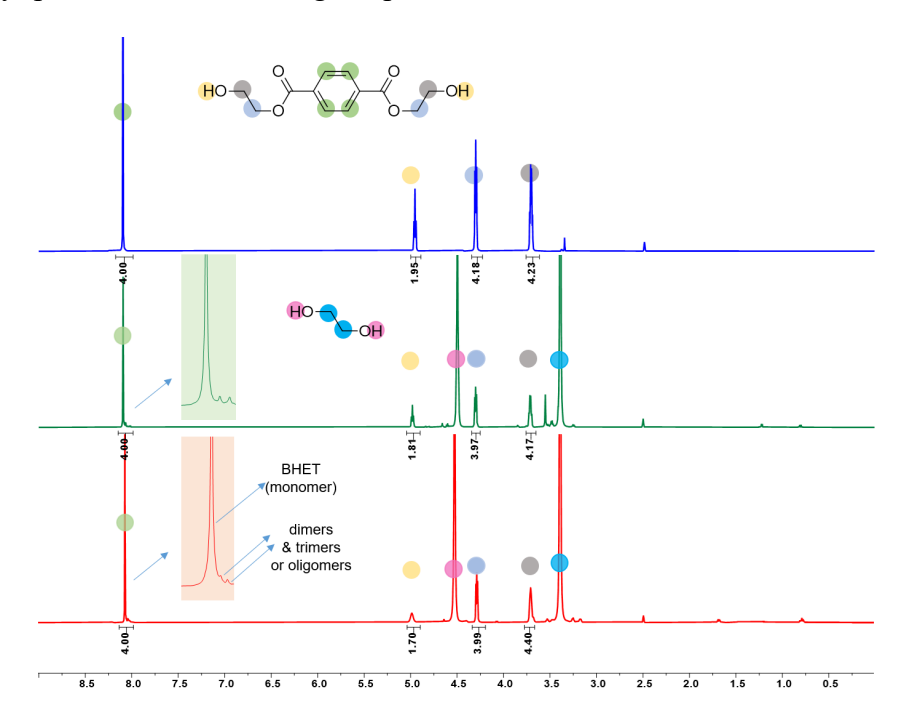
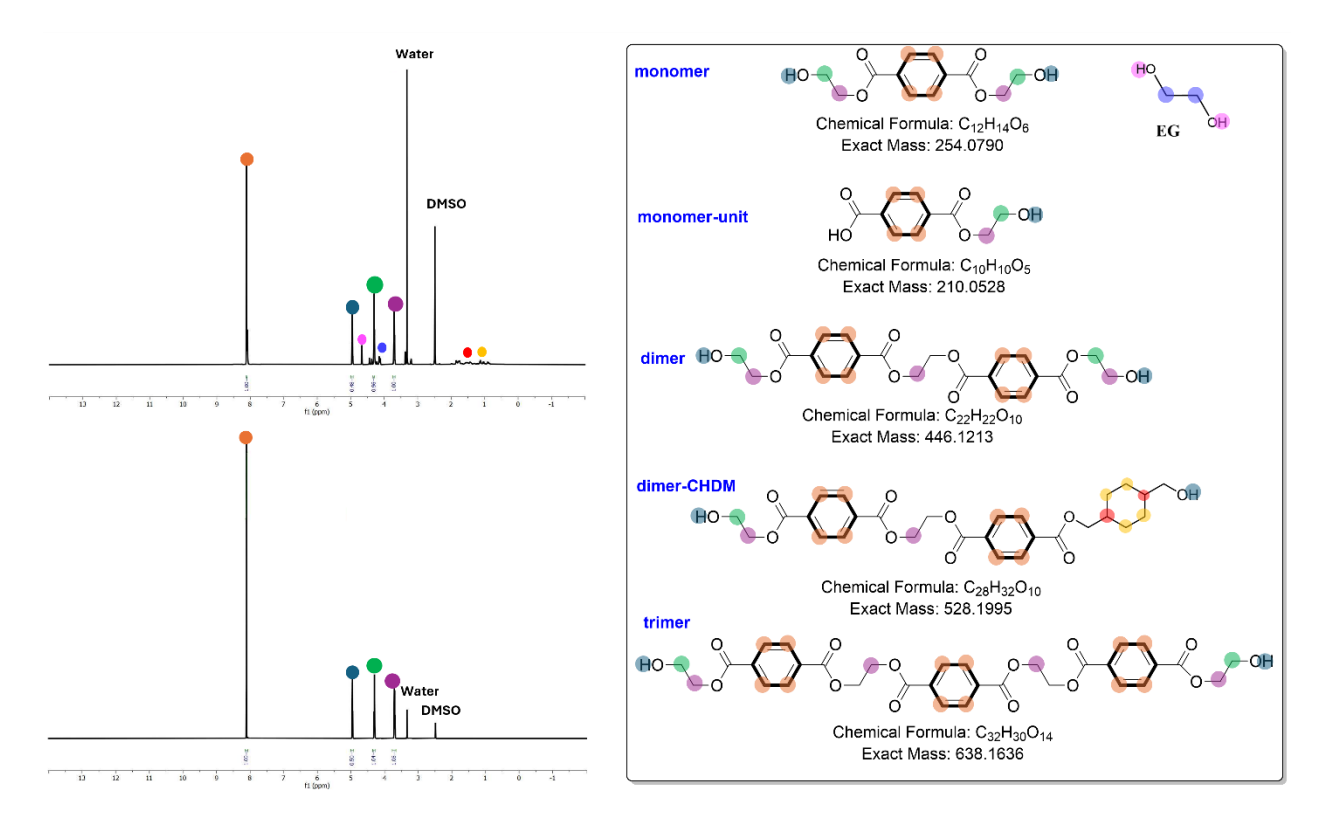


Figure 5- 12.  $^{1}H$  NMR spectra of products of  $S_{7}$  (blue), crude spectra of glycolysis of  $S_{3}$  (green) and  $S_{7}$  (red).  $S_{3}$  and  $S_{7}$  were exposed to ethylene glycol at 180  $^{\circ}C$  for 85 and 9 min respectively. Blue spectra show absence of any impurities except negligible amount of water. In the spectra of both  $S_{3}$  and  $S_{7}$  small peaks close to 8.1 ppm pertain to dimers, trimers and oligomers. Other small peaks in green and red spectra are assumed to be associated with zinc 2-ethylhexanoate and CHDM.

Similarly, when the <sup>1</sup>H NMR spectra of crude filtrated (after addition of hot water) and the crystallized BHET obtained from sample  $S_{12}$  were examined, the peaks associated with BHET were prominent. Because of the presence of high amount of water in the crude sample the peak associated with water at  $\delta = \sim 3.3$  ppm is more pronounced than the peaks corresponding to ethylene glycol, as depicted in *Figure 5-13* (the top spectra), whereas the same peak in the spectra

of isolated BHET is not very noticeable, *Figure 5-13* (the spectra on the bottom). In the <sup>1</sup>H NMR spectra of crude sample, resolving the peaks corresponding to the dimers, trimers, modified BHET, and dimer-CHDM, the structure of which are presented in *Figure 5-13* (on the right side), was very challenging due to the overlapping signals with the BHET monomer. Consequently, the peaks sharing similar chemical environments, although not precisely aligned in ppm, were assigned the same color. Additionally, the small peaks between 1 to 2 ppm most probably correspond to the cyclohexane group in CHDM, with the hydrogens attached to carbon atoms directly adjacent to OH- group (in red) being more deshielded compared to the hydrogens attached to carbon atoms further away from these groups (in yellow).



**Figure 5- 13.** Identification of present compounds in  $^{1}H$  NMR spectra of crude filtrate and crystallized BHET from sample  $S_{12}$ . Crude filtrate of samples  $S_{12}$ , glycolyzed at 190 °C for 32 minutes were mixed with hot water and the crystallized BHET of the same sample was isolated. The spectra on the top left shows the presence of BHET monomer peaks (overlapping with peaks of dimers and trimers), ethylene glycol, and water, and the small peaks corresponding to the detected compounds schemed on the right. The spectra of the isolated BHET on the bottom exhibits

Figure 5- 13. (cont'd).

the high purity of the BHET monomer with traces of water.

To compare the energy requirement for the pretreated samples with 0.5 mol% TBD or DBU and 17.5 weight% CHDM, S<sub>10</sub> and S<sub>11</sub>, with that of non-pretreated PET, S<sub>0</sub>, in the presence of 0.5 mol% TBD or DBU, an energy assessment was performed. For this purpose, energy consumption based on laboratory instrumentation was calculated according to the specifications of each equipment. The process flow diagram (PFD) is depicted in *Figure 5- 2* while the instrument specifications was listed in **Chapter 4.** Herein, the basis mass is 100 rams PET. The energy requirement for individual processes and overall energy are reported in *Table 5- 1*, assuming that both samples were depolymerized at 190 °C using 0.5 mol% TBD/DBU.

**Table 5-2.** Comparison of energy requirement for pretreated PET samples vs. neat PET.

Process	Energy for Two-Step  Depolymerization (kJ)		Energy for One-Step Depolymerization (kJ)	
	<sup>49</sup> <b>TBD</b>	<sup>50</sup> <b>DB</b> U	<sup>51</sup> <b>TBD</b>	<sup>52</sup> <b>DB</b> U
Grinding (A)	3,974	3,974	0	0
Catalyst	-	-	-	-
distribution in				
ground PET (B)				
Drying (C)	1,310	1,310	0	0
Extrusion (D)	892	892	0	0
Quenching (E)	-	-	-	-
Depolymerization	1273	1193	12930	8753
<b>(F)</b>				
<b>BHET</b> isolation	-	-	-	-
(G)				

<sup>&</sup>lt;sup>49</sup> TBD (0.5 mol%) added during the melt extrusion along with 17.5 weight% CHDM to prepare sample S<sub>10</sub>.

<sup>&</sup>lt;sup>50</sup> DBU (0.5 mol%) added during the melt extrusion along with 17.5 weight% CHDM to prepare sample S<sub>11</sub>.

<sup>&</sup>lt;sup>51</sup> TBD (0.5 mol%) added during the depolymerization of sample S<sub>0</sub>.

<sup>&</sup>lt;sup>52</sup> DBU (0.5 mol%) added during the depolymerization of sample S<sub>0</sub>.

**Table 5- 2.** (cont'd)

By-products	-	-	-	-
filtration (H)				
Drying by-	189	212	39	8
products (I)				
ВНЕТ	176	176	178	178
crystallization (J)				
BHET filtration	-	-	-	-
(K)				
BHET drying (L)	644	612	605	630
Total	8458	8378	13752	9569

For the grinding process, no energy and material loss were assumed, while in the drying steps 10% of the energy was lost to the environment. Additionally, for calculating the energy for the extrusion process, the energy for preheating of the instrument was taken into account, similar to including the energy for preheating the boiled water for the BHET crystallization process. In the depolymerization process, it was assumed that part of the energy loss was spent on preheating the hot plate, whereas it was partially lost from the surface of the hot plate that was transferring heat to the surroundings via convection. In the energy requirement calculation for the crystallization and drying the by-products and the BHET, the amount of water was considered based on the yield of BHET (obtained from LC-MS and based on results published by IBM [11]).

$$\% Energy saving_{TBD} = \frac{13752 - 8458}{13752} = 38.5\%$$

% Energy saving<sub>DBU</sub> = 
$$\frac{9569 - 8378}{9569} = 12.5\%$$

The results from the energy requirement revealed that the addition of the melt pretreatment step before the depolymerization of PET is 12.5% to 38.5% more energy efficient compared to when PET is directly subjected to depolymerization without pretreatment. However, it is important

to note that energy calculations were based on bench-top instrumentations where glassware apparatus was used, and the instruments were not insulated. While in this analysis the depolymerization step was the major contributor to the overall energy consumption, the analysis of the large-scale process might reveal different findings. Moreover, it is worth mentioning that washing post-consumer PET, shredding the washed bottles, transferring the materials between the processes and filtrations were all excluded, for they were all accomplished manually on the laboratory scale. As a result, the energy demand for the industrial scale can be higher or lower than what we report here. **In this thesis**, the claim is that the incorporation of the melt pretreatment process before PET depolymerization lowered the overall energy requirement.

## **5.4 Conclusions**

A melt pretreatment method is developed to decrease the crystallinity of PET for rapid depolymerization in a subsequent step. In some cases, catalysts with/without a diol were incorporated during the pretreatment step, which could further enhance the depolymerization rate via chain scission and introduce structural irregularity in PET that led to a further reduction of crystallinity (as low as 0.5%). The impact of melt pretreatment on the energy efficiency of PET depolymerization was assessed via glycolytic depolymerization of PET in the presence of Zn and organic base catalysts. Compared to untreated PET, the melt-pretreated PET in the absence of any catalysts or diols was depolymerized 17% faster, while the addition of only 2.5 mol% zinc 2-ethylehexanoate during the pretreatment, accelerated the reaction by 200%. Additionally, when the diols were added along with the catalysts, the rate of depolymerization was drastically improved due to the widened melting range, broader molecular weight distribution, and reduced crystallinity of the pretreated samples as well as the formation of active sites carrying catalyst and diol. The sample pretreated with the environmentally friendlier catalyst zinc 2-ethylhexanoate and

CHDM as a diol/additive outperformed when glycolyzed in a 10:1 molar ratio of EG to PET at 180 °C. Further studies on the replacement of metallic catalysts with two organic catalysts, TBD and DBU, exhibited the viability of this methodology in the presence of a trace amount of 0.5 mol% of catalyst. Melt-pretreated PET with only TBD/DBU (without diols and without external catalyst) experienced slightly longer depolymerization time due to alteration in the degradation pattern of PET caused by the TBD or DBU as well as potential neutralization of catalyst in the presence of traces of water. Furthermore, PET samples pretreated with CHDM were fully depolymerized within 11 to 32 minutes when TBD was added as a catalyst, whereas when DBU was incorporated complete depolymerization occurred within 9 to 30 minutes. Moreover, the energy requirement for the two-step glycolytic depolymerization of samples depicted more efficiency from ~12.5% to 38.5% compared to the one-step depolymerization of neat PET under the same reaction conditions.

## REFERENCES

- [1] Z. Yang, H. Peng, W. Wang, and T. Liu, "Crystallization behavior of poly(ε-caprolactone)/layered double hydroxide nanocomposites," *J. Appl. Polym. Sci.*, vol. 116, no. 5, pp. 2658–2667, 2010.
- [2] P. G. Karagiannidis, A. C. Stergiou, and G. P. Karayannidis, "Study of crystallinity and thermomechanical analysis of annealed poly(ethylene terephthalate) films," *Eur. Polym. J.*, vol. 44, no. 5, pp. 1475–1486, 2008.
- [3] Y. Kong and J. N. Hay, "The enthalpy of fusion and degree of crystallinity of polymers as measured by DSC," *Eur. Polym. J.*, vol. 39, no. 8, pp. 1721–1727, 2003.
- [4] R. Sharma, S. N. Maiti, R. Sharma, and S. N. Maiti, "Effects of Crystallinity of PP and Flexibility of SEBS- g-MA Copolymer on the Mechanical Properties of PP / SEBS-g-MA Blends Effects of Crystallinity of PP and Flexibility of SEBS-g-MA Copolymer on the Mechanical Properties of PP / SEBS-g-MA Blends," vol. 2559, pp. 229–238, 2014.
- [5] ASTM International, "Determining Inherent Viscosity of Poly (Ethylene iTeh Standards iTeh Standards," pp. 5–6.
- [6] J. Spannhake, O. Schulz, A. Helwig, A. Krenkow, G. Müller, and T. Doll, "High-temperature MEMS heater platforms: Long-term performance of metal and semiconductor heater materials," *Sensors*, vol. 6, no. 4, pp. 405–419, 2006.
- [7] D. V. Zinov'ev and P. Sole, "Quaternary codes and biphase sequences from Z8-codes," *Probl. Peredachi Informatsii*, vol. 40, no. 2, pp. 50–62, 2004.
- [8] S. Santra *et al.*, "Post-CMOS wafer level growth of carbon nanotubes for low-cost microsensors A proof of concept," *Nanotechnology*, vol. 21, no. 48, 2010.
- [9] A. Khan, M. Naveed, Z. Aayanifard, and M. Rabnawaz, "Efficient chemical recycling of waste polyethylene terephthalate," *Resour. Conserv. Recycl.*, vol. 187, p. 106639, Dec. 2022.
- [10] Z. Aayanifard, A. Khan, M. Naveed, J. Schager, and M. Rabnawaz, "Rapid depolymerization of PET by employing an integrated melt-treatment and diols," *Polymer (Guildf).*, vol. 265, p. 125585, 2023.
- [11] K. Fukushima *et al.*, "Unexpected efficiency of cyclic amidine catalysts in depolymerizing poly(ethylene terephthalate)," *J. Polym. Sci. Part A Polym. Chem.*, vol. 51, no. 7, pp. 1606–1611, 2013.
- [12] S. Nica *et al.*, "Functionalized 1,5,7-triazabicyclo [4.4.0] dec-5-ene (TBD) as Novel Organocatalyst for Efficient Depolymerization of Polyethylene Terephthalate (PET) Wastes," 2018.
- [13] C. Jehanno, I. Flores, A. P. Dove, A. J. Müller, F. Ruipérez, and H. Sardon,

- "Organocatalysed depolymerisation of PET in a fully sustainable cycle using thermally stable protic ionic salt," *Green Chem.*, vol. 20, no. 6, pp. 1205–1212, 2018.
- [14] Z. S. Baird *et al.*, "Physical Properties of 7-Methyl-1,5,7-triazabicyclo[4.4.0]dec-5-ene (mTBD)," *Int. J. Thermophys.*, vol. 40, no. 7, 2019.
- [15] A. H. Yasir, A. S. Khalaf, and M. N. Khalaf, "Preparation and Characterization of Oligomer from Recycled PET and Evaluated as a Corrosion Inhibitor for C-Steel Material in 0.1 M HCl," *Open J. Org. Polym. Mater.*, vol. 07, no. 01, pp. 1–15, 2017.

# Chapter 6. BIODEGRADABLE PAPER COATED WITH SYNTHETIC IONIC PBAT FOR PACKAGING APPLICATION: A TECHNOECONOMIC ANALYSIS

A version of this article is ready for submission as:

Aayanifard, Z., Saffron, C. M., Hamdani, S. S., Elkholy, H. M., Rabnawaz, M., "Technoeconomic Analysis for Biodegradable and Recyclable Paper Coated with Synthetic Ionic PBAT For Packaging Application," *ACS Sustainable Chemistry and Engineering*, 2024.

# **6.1 Summary**

In a previous investigation in the Sustainable Materials Lab, biodegradable Polybutylene adipate-co-terephthalate (PBAT) was ionized and utilized for paper coating applications with improved mechanical and barrier properties. In the synthesis of the ionized COOH-PBAT (CPBAT), PBAT was initially reacted with butanediol (BDO) to yield the lower molecular weight PBAT-diol, followed by reacting PBAT-diol with Meso-butane-1,2,3,4-tetracarboxylic dianhydride (MBTCA). The synthesized CPBAT was emulsified and coated on bare Kraft paper (CPBAT-K) and starch-coated Kraft paper (CPBAT-S). The CPBAT coated on Kraft paper exhibited higher mechanical properties compared to CPBAT coated on starch-coated Kraft paper, whereas the barrier properties of the starch-coated paper were higher. Additionally, the recyclability and repulpability of both of these coated papers were proved through analyses. Hence, either of these CPBAT coated papers could be used for packaging applications depending on the customers' demand. In this thesis, a technoeconomic analysis (TEA) was performed to investigate the industrial viability of the large-scale production of CPABT for coating applications. This TEA determined the capital investment, total operation costs, and minimum selling prices for a production capacity of 1 ton of CPBAT per day. The cost estimation analysis showed that the minimum selling price for CPBAT-K and CPBAT-S were \$1.327/m<sub>2</sub> and \$1.864/m<sub>2</sub>, respectively.

# **6.2 Methods**

## **6.2.1 Process overview**

In the bench-top experiments, synthetic steps were carried out using glass apparatus with the energy coming from electric hot plates. To scale up the process, a process flow diagram (PFD) was visualized using *Visio*, *Figure 6-1*, starting with drying PBAT in a rotary dryer, followed by high molecular weight PBAT undergoing treatment with 1,4-butanediol to yield PBAT-diols of

lower molecular weight. This reaction occurs in the presence of zinc acetate (0.5 wt.%) as a catalyst in a continuous stirred tank reactor (CSTR) to yield low-molecular weight PBAT-diol within 6 hours at 200°C. Subsequently, these PBAT-diols were subjected to ring-opening addition reactions with meso-butane-1,2,3,4-tetracarboxylic dianhydride (MBTCA), resulting in the synthesis of CPBAT polymers, which occurs in a CSTR at 170 °C for 30 min. To ionize CPBAT in water, CPBAT was mixed with ammonium hydroxide aqueous solution in a CSTR reactor for 45 min at 77 °C and transferred into a tank for storage. In the industrial setting, it is assumed that the energy needed for the reactions is generated by burning natural gas in the furnaces, while other electricity demands are supplied from mixed-grid electricity in the US.

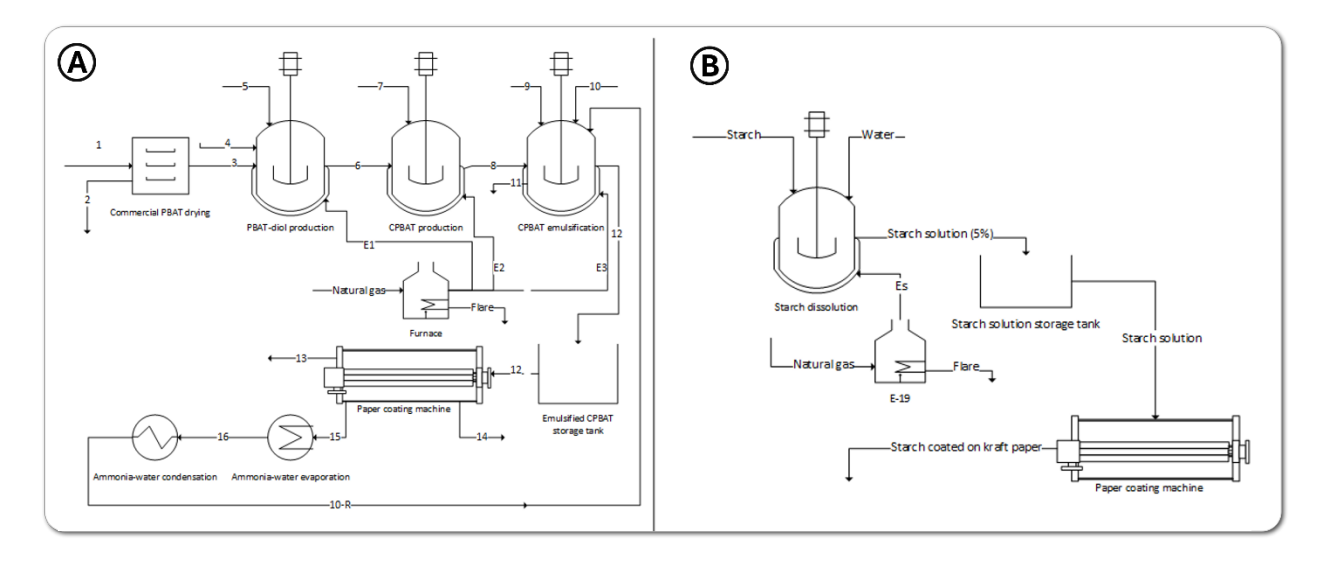


**Figure 6- 1.** Process Flow Diagram for kraft paper coated with CPBAT. **A)** PFD of CPBAT production and kraft paper coating. **B)** PFD of 5% starch dissolution in water and coating kraft paper.

In the laboratory-scale experiments, the ionized CPBAT was initially coated on Kraft paper using a silicone spatula, followed by drying in a small dryer at 130°C for 30-40 minutes to produce CPBAT-K. Additionally, starch-coated paper was prepared by applying 5% starch solution onto uncoated kraft paper using a multicoated machine (K303 Multi Coater), followed by air drying for 24 hours. Subsequently, CPBAT was coated on starch-coated paper to prepare CPBAT-S. It is

assumed that in the industrial setting, press rolling coating machines are employed to coat ionized CPABT and starch solution onto Kraft paper. As part of this project, the coating machines are equipped with integrated dryers. The assumptions for this technoeconomic analysis are listed in *Table* 6-1.

Table 6- 1. List of assumptions for TEA.

Description	Value	Unit	Reference
Plant capacity	1000	kg	
Time horizon	10	years	
Utility cost for mixed grid	0.1	USD kWh <sup>-1</sup>	[1]
Utility cost for natural gas	0.016	USD kWh <sup>-1</sup>	[2]
PBAT	3.1416	USD kg <sup>-1</sup>	[3]
1,4-butanediol (BDO)	1.95	USD kg <sup>-1</sup>	[4]
Zinc acetate	4	USD kg <sup>-1</sup>	[5]
MBCTA	6.39	USD kg <sup>-1</sup>	[6]
Ammonium hydroxide	0.159	USD kg <sup>-1</sup>	[7]
Starch	4.7	¢ kg <sup>-1</sup>	[8]
Fresh water price	1.08	¢ kg <sup>-1</sup>	[9]
Income tax	21	%	[10]
Salvage value	0	%	
Internal rate of return	0.1		

# **6.2.2** Total capital investment

To determine the total capital investments, it was necessary to estimate the equipment costs, which were contingent upon the size and stream flow rates. The equipments were designed using Aspen HYSYS and literature [11], [12]. Equipment costs were determined through quotations from suppliers and insights from [11]–[14]. Chemical engineering plant cost indices (CEPCI) were employed to adjust the equipment prices from previous years to the latest available

index (2022). By combining these temporal cost adjustments with the six-tenths rule, the equipment costs were adjusted with the equipment scale. In the estimation of overall capital investment, as listed in *Table 6-2*, the direct costs, including the instrumentation, piping, electrical systems, buildings, yard improvements, service facilities, land, and indirect expenses such as engineering, construction, legal fees, contractor charges, and contingency were estimated based on purchased equipment costs.

## **6.2.3** Operating cost estimation

Direct operating costs were estimated by combining calculated process flow rates with unitary costs of raw materials and utilities. Consequently, after estimating the raw material costs and utilities, fixed costs operating costs, including labor and benefits, supervision, laboratory expenses, consumables, insurance, taxes, depreciation, administrative overheads, and plant overheads, were derived from direct operating costs and capital investment values. For CBPAT production, two operators, one supervisor, and one laboratory technician were employed. For CPBAT-K production, two additional operators were hired for the coating process and methanol recovery. In the CPBAT-K production process, an additional operator and laboratory technician were employed for the starch coating process. Additionally, assuming zero salvage value, depreciation was calculated based on a 10-year life, by dividing the total capital investment by 10.

## **6.2.4 Profitability analysis**

To determine the minimum selling price, a profitability analysis was conducted to initially estimate the annual cash flow and annual net and gross profit considering the internal rate of return of 0.1. The cost and minimum selling price (MSP) of CPBAT production included all processes before CPABT emulsification and coating. While the cost and minimum selling price of CPBAT-K included the CPBAT coating on Kraft paper along with drying and recycling of the ionization

solvent, the additional coating and drying for preparing starch-coated paper was incorporated into the costs and minimum selling price of CPBAT-S.

## **6.2.5** Sensitivity analysis

Once the utility costs, total operating costs, total capital investment, and minimum selling prices (MSPs) for CPBAT, CPBAT-K, and CPBAT-S were determined, changes in MSP were assessed across various parameters, such as production capacity, raw material costs, price of PBAT, CPBAT reaction yield, energy required for coating and the reactions, internal rate of return (IRR), and rate of ionization solvent recovery. In the base case scenario, the production capacity was based on producing 1000 kg PCBAT per day, with a reaction yield of 100%, 40% recovery of the ionization solvent, and an IRR of 0.1. additionally, it was assumed that the energy of the exothermic reactions was not recovered, hence lost to the environment.

## 6.3 Results and Discussions

The stacked bar graph depicted in *Figure 6- 2A* shows the breakdown of the costs comprising the fixed capital investment, highlighting that equipment costs are the major component of the fixed capital investments. Since fixed capital investment is based on installed equipment costs, the summation of the equipment costs and installation costs contribute to 50% of non-normalized direct fixed capital investment and 39% after normalization to a total of 100%. Buildings (9%), piping (8%), and service facilities (8%) are the next largest contributors to direct costs, while other direct costs such as electrical systems (5%), instrumentation and controls (4%), yard improvement (2%), and land (1%) have lesser contributions. In terms of indirect costs, construction expenses, and contingency (8%) are the two largest contributors, while engineering and supervision (6%), legal expenses (2%), and contractor's fee (2%) make up the remaining contributors to the indirect cost portion of fixed capital investment. Additionally, the graph reveals

that the fixed capital investments for the production of CPBAT-S are more than that of CPBAT-K. The itemized costs are listed in *Table 6-2*.

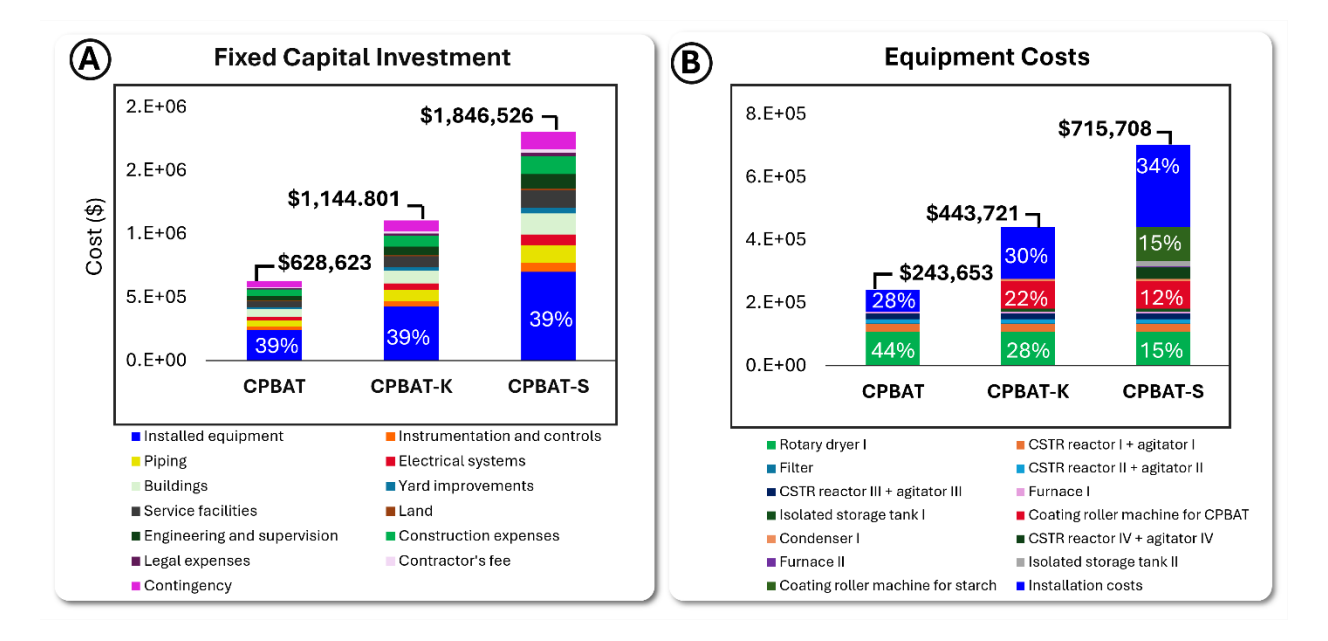


**Figure 6- 2.** Breakdown of **A)** fixed capital investment and **B)** equipment costs for CPBAT, CPBAT-K and CPBAT-S.

In *Figure 6-2B*, the breakdown of equipment costs for CPBAT is exhibited, in which the emulsification and coating steps were not considered, with total equipment costs amounting to \$174,620. However, the cost of one coating step in CPBAT-K production and two coating steps in CPABT-K increases the equipment costs to \$279,340 and \$432,759, respectively. This figure also reveals that while the rotary dryer for commercial PBAT drying constitutes the largest contributor to equipment costs of CPBAT and CPBAT-K, the two coating machines (total of 10) are the largest contributors to CPBAT-S.

Table 6- 2. Itemization of total capital investment.

	CPBAT	CPBAT-K	CPBAT-S
Direct costs			
Purchased equipment	\$243,653	443,721	688,935
Instrumentation and controls	\$24,365	44,372	68,894

**Table 6- 2.** (cont'd)

Piping	\$48,731	88,744	\$137,787
Electrical systems	\$29,238	\$53,247	\$82,672
Buildings	\$58,477	\$106,493	\$165,345
Yard improvements	\$14,619	\$26,623	\$41,336
Service facilities	\$48,731	\$88,744	\$137,787
Land	\$4,873	\$8,874	\$13,779
Indirect costs			
Engineering and supervision	\$38,984	\$70,995	\$110,229
Construction expenses	\$48,730	\$88,744	\$137,787
Legal expenses	\$9,746	\$17,748	\$27,557
Contractor's fee	\$9,746	\$17,748	\$27,557
Contingency	\$ 48,730	\$88,744	\$137,787
<b>Fixed Capital Investment</b>	\$628,623	\$1,144,801	\$1,777,453
(FCI)			

Figure 6-3 illustrates the production costs of CPBAT, CPBAT coated on Kraft paper (CPBAT-K), and starch-coated paper (CPBAT-S). CPBAT production involves drying and two production reactions, one that is highly exothermic. Hence, the primary operating costs are raw materials, capital recovery charges, labor, and maintenance. However, for the production of CPBAT-K and CPBAT-S, high utility expenses arise due to energy consumption during coating and paper drying. Additionally, the equipment cost for CPBAT-S production exceeds that of CPBAT-K production owing to five coating machines needed for the starch coating process and an extra reactor for starch dissolution in water. Figure 6-3 also shows the cost contributions of raw materials, revealing that PBAT is the key contributor to CPBAT, CPBAT-K, and CPBAT-S production followed by MBTCA as the second major contributor.

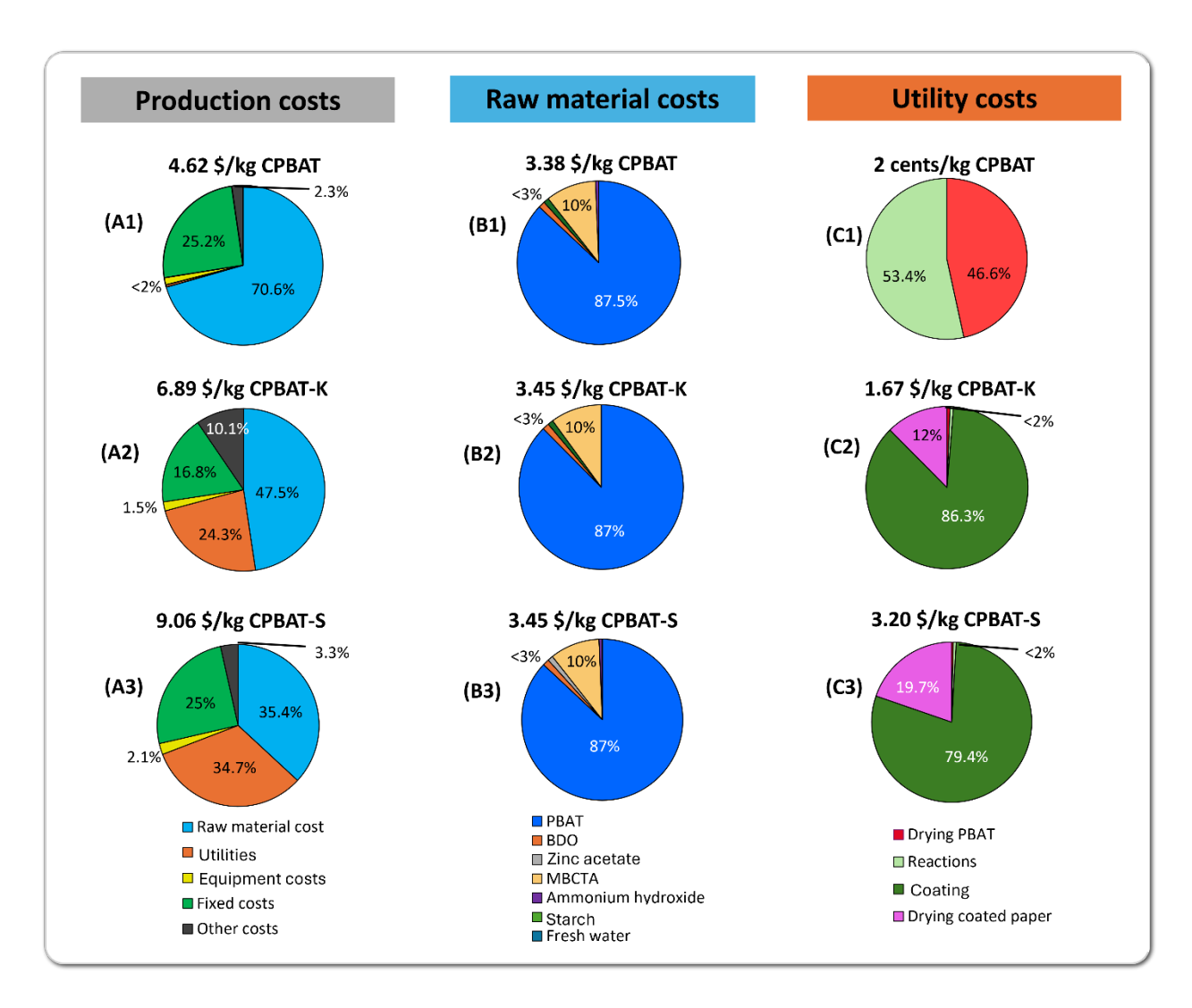
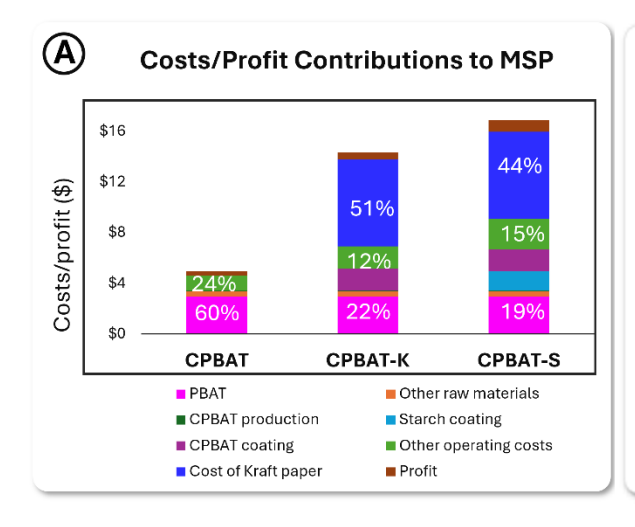


Figure 6-3. Utility, raw material, and production costs. Utility costs in (A1-3), production costs in (B1-3), and raw material costs in (C1-3). A1), B1), and C1): costs related to CPBAT production, A2), B2) and C2): costs of CPBAT coated on Kraft paper. A3), B3), and C3): costs associated with CPBAT coated on starch-coated paper.

The contrast in utility costs between CPBAT production and CPBAT-K and CPBAT-S production is remarkable. This difference primarily stems from the energy-intensive coating processes. In CPBAT production, part of the utility costs is attributed to the endothermic reaction of CPBAT production and partly to the drying process of commercial PBAT. Conversely, in the CPBAT-K utility cost breakdown, the contribution of the reaction is marginal, with coating processes accounting for over 86% of the total. Similarly, in CPBAT-S, the majority of utility costs

are linked to coating processes, while drying contributes to approximately 20% of the total utility cost.



B Economic			
contributors to MSP	CPBAT	CPBAT-K	CPBAT-S
PBAT	\$2.96	\$2.96	\$2.96
Other raw materials	\$0.42	\$0.42	\$0.42
CPBAT production	\$0.02	\$0.02	\$0.02
Starch coating	\$0.00	\$0.00	\$1.54
CPBAT coating	\$0.00	\$1.73	\$1.73
Other operating costs	\$1.21	\$1.76	\$2.38
Cost of Kraft paper	\$0.00	\$6.86	\$6.86
Profit	\$0.33	\$0.61	\$0.94
MSP (\$/kg)	\$4.95	\$14.34	\$16.86
MSP (\$/m <sub>2</sub> )	NA	\$1.327	\$1.864

**Figure 6- 4.** Itemization of costs and profit contributing to the minimum selling price (MSP) of CPBAT, CPBAT-K, and CPBAT-S. **A)** Stacked bar chart for the components of MSP. **B)** Values for the costs and profit, and MSP of CPBAT, CPBAT-K, and CPBAT-S.

Figure 6-4 gives insights into the costs and benefits contributing to the minimum selling price (MSP) of CPBAT, CPBAT-K, and CPBAT-S, emphasizing that while PBAT is the major contributor to the minimum selling price of CPBAT, the price of Kraft paper is the key contributor to the cost of both papers. With an internal rate of return (IRR) of 10%, the MSP per kilogram of CPBAT-K is \$14.41, while it amounts to \$16.86 for CPBAT-S. Additionally, the MSP per square meter of CPBAT-K and CPBAT-S stands at \$1.327 and \$1.846, respectively. Considering the production cost of CPBAT at \$4.62 (from Figure 6-3) and the MSP of \$4.95, this figure indicates that the main cost is associated with paper and coating costs. Optimizing the coating process by using a larger coating machine with higher production capacity and lower power consumption could reduce coated paper prices.

Once the utility costs, total operating costs, total capital investment, and minimum selling prices (MSPs) for CPBAT, CPBAT-K, and CPBAT-S were determined, changes in MSP were

assessed across various parameters, such as production capacity, raw material costs, price of PBAT, CPBAT reaction yield, energy required for coating and the reactions, internal rate of return (IRR), and rate of ionization solvent recovery. In the base case scenario, the production capacity was based on producing 1000 kg PCBAT per day, with a reaction yield of 100%, 40% recovery of the ionization solvent, and an IRR of 0.1. additionally, it was assumed that the energy of the exothermic reactions was not recovered, hence lost to the environment.

To analyze the sensitivity of the MSPs to the production capacity, the minimum selling prices for a larger plant with the capacity of producing 100,000 kg/day CPBAT were determined. For this purpose, the quantity of raw materials and required utility were scaled up while the equipment costs were adjusted based on the six-tenth rule. The result of sensitivity analysis, as depicted in *Figure 6-5*, revealed that the minimum selling price of CPBAT-K and CPBAT-S are highly sensitive to the production capacity, and expanding the plant size to 100,000 kg CPBAT production per day, the minimum MSPs dropped by 20%. Studies also confirm that a larger production capacity in a chemical plant can be more cost-effective for manufacturers, provided that there's sufficient demand to justify the initial investment. This is because larger plants benefit from economies of scale, efficiency improvements, and better purchasing power, which lower the cost per unit produced [15], [16].

Additionally, due to the large contributions of material costs (specifically the price of PBAT) to the operating costs of CPBAT-K and CPBAT-S, the dependency of MSPs on the raw material costs and price of PBAT alone, was examined by incorporating a 50% decrease/increase and recording the changes in the MSPs. The findings indicate that the minimum selling prices are highly influenced by raw material costs, particularly PBAT, which accounts for approximately 87% of the raw material costs. A 50% decrease in raw material costs could reduce the MSPs of

CPBAT-K and CPBAT-S by 16% and 11% respectively, while a corresponding increase could raise the MSPs by the same percentages. The changes in PBAT prices were closely associated with its contribution to overall raw material costs. Specifically, a 14% decrease and a 10% increase in MSPs were observed for CPBAT-K and CPBAT-S respectively, reflecting changes in PBAT costs relative to total raw material costs.

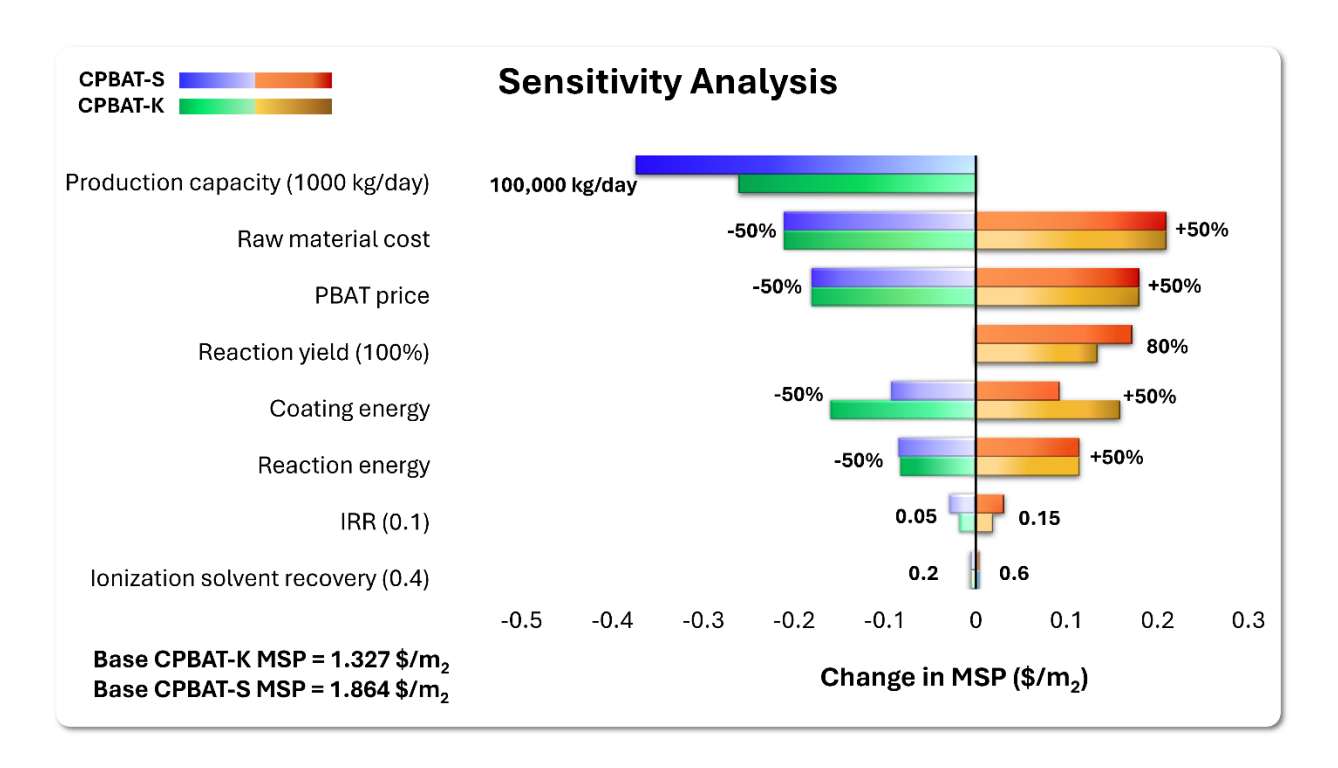


**Figure 6-5.** Sensitivity Analysis: Impact of changing various parameters on the MSPs of PBAT-K and PBAT-S, with the most sensitive parameter (production capacity) on the top to the least sensitive parameter at the bottom (ionization solvent recovery rate).

Moreover, a reduced reaction yield of 80% was factored with adjusted feed rates of raw materials into the reactors. Nevertheless, as the reactor sizes were initially overestimated to accommodate lower yields, the overall capital investment remained unchanged. The 80% yield decrease led to a 10% and 9% increase in MSPs for CPBAT-K and CPBAT-S respectively, highlighting the necessity of optimizing reactions to attain higher product yields and thereby lower selling prices.

As outlined in *Figure 6- 3C2* and *Figure 6- 3C3*, the energy requirement for the coating process was observed to have a considerable contribution to the utility costs of CPBAT-K and CPBAT-S. With a maximum coating rate of 7200 m/day (width of 55 cm), five coating machines were required for each coating step, resulting in high energy demand for coating processes. Hence, employing coating machines with greater capacity and/or enhanced energy efficiency can significantly influence costs and minimum selling prices (MSPs). Adjusting the energy demand to be 50% below and above the base case scenario resulted in a 12% decrease/increase in the MSP of CPBAT-K and a 5% change in the MSP of CPBAT-S.

As previously stated, the PBAT-diol production and CPBAT emulsification reactions are highly exothermic, generating recoverable energy for use in other process steps. However, a study on the depolymerization of polyethylene terephthalate (PET) suggested that despite the exothermic nature of the ester bond breakage reaction using a short diol, additional energy might be necessary to drive the reaction forward, as in the case of PBAT-diol production [13]. To ensure consistent calculations, the energy demand for PBAT-diol production was determined through bench-top experiment scale-up. For instance, scaling up the energy requirement for breaking ester bonds in PBAT to produce lower molecular weight PBAT-diol required 66577 MJ/day, compared to an estimate of around 99 MJ/day derived from large-scale energy requirements for breaking ester bonds in PET (as detailed in the supplemental information). Although the scale-up energy calculation was notably higher due to the use of glass apparatus in the laboratory with high energy loss, it's reasonable to consider a range of reaction energies between partial recovery of the produced energy in the exothermic reactions and partial energy demand calculated from the scaleup. As a result, modifying the reaction energy requirement from 50% energy recovery to 50% energy consumption led to a 6% to 9% decrease and increase in price for CPBAT-K, and a 5 to

6% reduction and increase in the price of CPBAT-S. The detailed calculations are included in APPENDIX C: TECHNOECONOMIC ANALYSIS CALCULATIONS.

Additionally, the internal rates of return (IRR) ranged between 0.05 to 0.15, resulting in varied shortened and extended periods of the expected return of the capital investment and hence profitability level and the minimum selling prices. Results exhibited a price elevation of 1% and 2% for CPBAT-K and CPBAT-S respectively when IRR increased to 0.15, and similar price decreases when IRR decreased to 0.05. With a lower IRR, a longer time for the return on investment for investors is expected which leads to a reduction in the minimum selling price as profits decrease [17].

In this analysis, the sensitivity of minimum selling prices to the recovery of the ionization solvent was investigated, as well. Elevating the recovery rate and reintroducing the recycled solvent into the emulsification step reduces raw material costs and harnesses energy from solvent condensation. However, this approach requires larger equipment with increased equipment costs, thereby raising capital investment. The results revealed that the dependency of MSPs on the recovery rate of the ionization solvent was marginal, with variations of less than 1% for both CPBAT-K and CPBAT-S.

Based on the results of the sensitivity analysis, a secondary scenario was formulated to explore the opportunities of lowering the minimum prices of CPBAT-K and CPBAT-S. In this scenario, the production capacity increased to 100,000 kg of CPBAT per day, with 50% lower-priced feedstock and 50% more energy-efficient coating machines. Additionally, insulated jacketed reactors with minimal energy loss were utilized, enabling 50% of the energy to be recovered and either redirected into other processes or sold at the same price as electricity generated from burned natural gas. With a reduced internal rate of return (IRR) of 0.05 and 20%

recovery of ionization solvent, the minimum prices dropped significantly to \$0.588/m² for CPBAT-K and \$0.914/m² for CPBAT-S, as can be seen in *Figure 6- 6*. Comparing these prices with that of commercial PE paper (also known as Poly coated paper) from *Uline*, priced at \$0.95/m², reveals a feasible opportunity for CPABT-K and CPBAT-S to achieve cost competitiveness, while offering added benefits of biodegradability and recyclability.

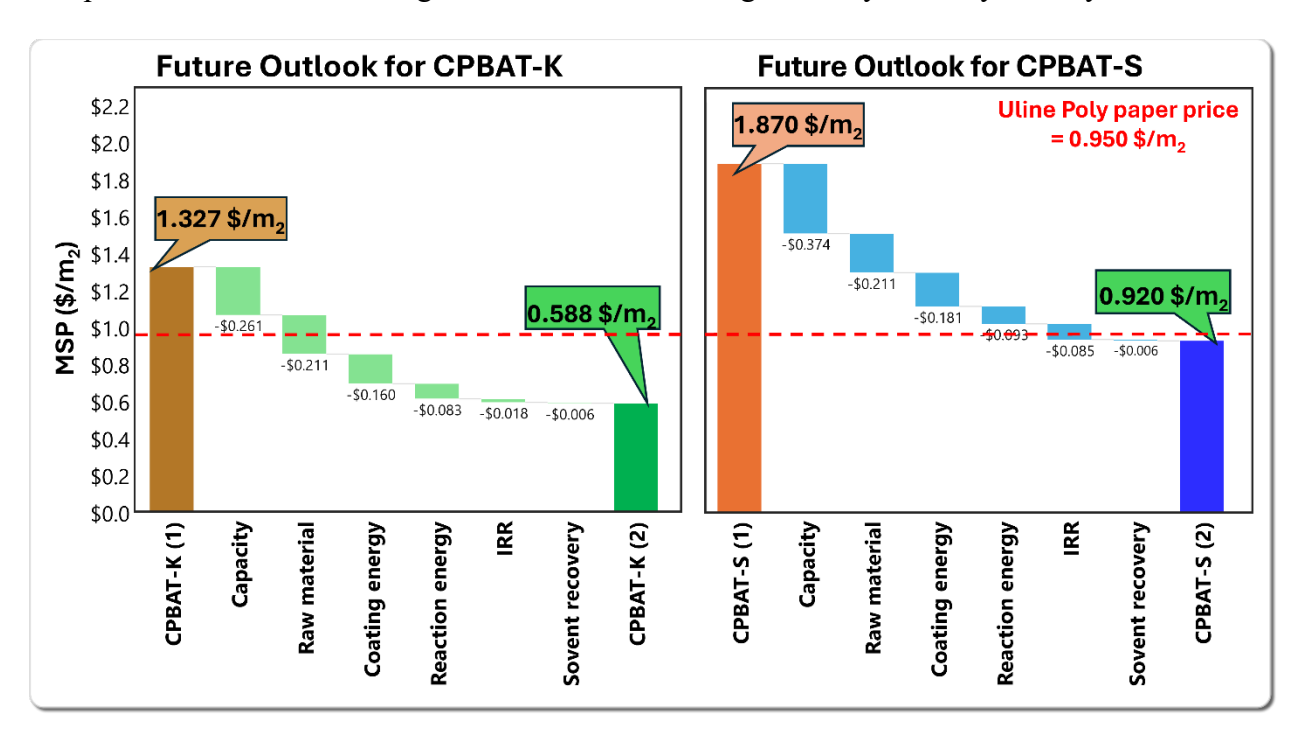


**Figure 6- 6.** Future outlook for MSPs of CPBAT-K (on the left) and CPBAT-S (on the right): waterfall chart displaying cost-saving opportunities to reduce the minimum selling price of CPBAT-K and CPBAT-S.

Although the initial cost of CPBAT-based papers is higher than Poly coated paper, it is important to consider their recyclability and biodegradability, in contrast to the non-biodegradable Poly coated paper. Furthermore, our technoeconomic analysis is based on small-scale production of 1 ton per day, and scaling up the production capacity could significantly reduce costs. With the potential cost reduction by increasing production scale and improved efficiency of the processes, CPBAT-K and CPBAT-S are promising alternatives for sustainable packaging solutions, filling a crucial gap in the market for environmentally friendly materials.

## **6.4 Conclusions**

In this project, the economic feasibility of a novel ionic PBAT (CPBAT) as a paper coating material was investigated through technoeconomic analysis (TEA). In a previous experimental study, CPBAT was initially applied to bare Kraft paper (CPBAT-K), demonstrating superior mechanical and good barrier properties (details are submitted in a separate article). Additionally, when applied to starch coated paper (CPBAT-S), it exhibited enhanced barrier properties compared to CPBAT-K. Importantly, both variants proved to be biodegradable and recyclable. This TEA determined total capital investment, operating costs, and minimum selling prices for a production capacity of 1 ton of CPBAT per day. The total capital investments were estimated at approximately \$1.14M for CPBAT-K and \$1.78M for CPBAT-S. The estimation of operating costs highlighted significant contributions from raw material costs, particularly the cost of PBAT, and the energy requirements for the coating machines. Additionally, the estimated minimum selling prices for CPBAT-K and CPBAT-S are \$1.327/m2 and \$1.864/m2, respectively. A sensitivity analysis was conducted to provide insights into the dependency of minimum selling prices on various parameters, revealing the high sensitivity of MSPs to plant production capacity, raw material costs, energy efficiency of the coating process, energy required or released from reactions, and reaction yield. Furthermore, it is worth noting that the recovery of ionization solvent and its reuse in the emulsification step only marginally increases the selling prices of CPBAT-K and CPBAT-S while saving energy and materials, making it highly recommended. In this scenario, the price of CPBAT-K is approximately 40% higher, and CPBAT-S is about 96% higher than that of commercial polyethylene-coated paper (PE Paper/Poly coated paper), priced at \$0.95/m<sup>2</sup>. With increased production capacity, lower raw material costs, utilization of more energy-efficient coating machines, and partial recovery of energy produced from reactions, the MSPs can be

reduced to \$0.588/m² and \$0.914/m² for CPBAT-K and CPBAT-S respectively. In conclusion, with comparable mechanical and barrier properties to PE paper and the added benefits of biodegradability and recyclability, CPBAT offers an economically feasible and sustainable alternative to current coated paper packaging.

#### REFERENCES

- [1] "Illinois Electricity Rates," 2024. [Online]. Available: https://www.energybot.com/electricity-rates/illinois/.
- [2] "US Energy Information Association," 2024. [Online]. Available: https://www.energybot.com/electricity-rates/illinois/.
- [3] S. J. Xiong *et al.*, "Economically Competitive Biodegradable PBAT/Lignin Composites: Effect of Lignin Methylation and Compatibilizer," *ACS Sustain. Chem. Eng.*, vol. 8, no. 13, pp. 5338–5346, 2020.
- [4] "Track Butanediol Price Trend in Top 10 Leading Countries Worldwide," 2023. [Online]. Available: https://www.chemanalyst.com/Pricing-data/butanediol-54.
- [5] "Zinc Acetate 99.9% Granular (Powder) ACS Grade," 2023. [Online]. Available: https://www.laballey.com/products/zinc-acetate-granular-acs?variant=42654366531739&currency=USD&utm\_medium=product\_sync&utm\_sourc e=google&utm\_content=sag\_organic&utm\_campaign=sag\_organic&gad\_source=1&gclid=Cj0KCQiAr8eqBhD3ARIsAIe-buNNULfcuh-3UyZWP7z0OuI6k.
- [6] "meso-Butane-1,2,3,4-tetracarboxylic Acid, 98% purity," 2023. [Online]. Available: https://www.aladdinsci.com/m158399.html?gclid=Cj0KCQiAj\_CrBhD-ARIsAIiMxT8YsGQ4uJkxaQpTUfP030xeN4mjaBhUi7y3nFLga-mUghvMJbUAuQcaArkbEALw wcB.
- [7] "Ammonium Hydroxide Prices Current and Forecast," 2019. [Online]. Available: https://www.intratec.us/chemical-markets/ammonium-hydroxide-price.
- [8] "Industrial Grade Starch Powder Manufacturer Price," 2024. [Online]. Available: https://www.alibaba.com/product-detail/Industrial-Grade-Corn-Starch-Powder-Manufacturer 1600696058510.html?s=p.
- [9] Y. Jadidi, H. Frost, S. Das, W. Liao, K. Draths, and C. M. Saffron, "Comparative Life Cycle Assessment and Technoeconomic Analysis of Biomass-Derived Shikimic Acid Production," *ACS Sustain. Chem. Eng.*, vol. 11, no. 33, pp. 12218–12229, 2023.
- [10] "Corporate Tax Rates 2023," 2023. [Online]. Available: https://www2.deloitte.com/content/dam/Deloitte/global/Documents/Tax/dttl-tax-corporate-tax-rates-2019-2023.pdf.
- [11] M. S. Peters and K. D. Timmerhaus, *Plant design and economics for chemical engineers*. Journal of Chemical Education, 1958.
- [12] A. Singh *et al.*, "socioeconomic impact analysis of enzymatic recycling of poly (ethylene terephthalate) of poly (ethylene terephthalate)," *Joule*, vol. 5, no. 9, pp. 2479–2503, 2021.
- [13] P. Huang et al., "Peng Huang, Ashiq Ahamed, Ruitao Sun, Guilhem X. De Hoe, Joe Pitcher,

- Alan Mushing, Fernando Lourenc, o, and Michael P. Shaver \*," 2023.
- [14] T. Uekert *et al.*, "Technical, Economic, and Environmental Comparison of Closed-Loop Recycling Technologies for Common Plastics," *ACS Sustain. Chem. Sci. Eng.*, vol. 11, no. 3, pp. 965–978, 2023.
- [15] C. I. Hsu and H. C. Li, "An integrated plant capacity and production planning model for high-tech manufacturing firms with economies of scale," *Int. J. Prod. Econ.*, vol. 118, no. 2, pp. 486–500, 2009.
- [16] H. Radatz, K. Kühne, C. Bramsiepe, and G. Schembecker, "Comparison of capacity expansion strategies for chemical production plants," *Chem. Eng. Res. Des.*, vol. 143, pp. 56–78, 2019.
- [17] J. Jurčević, I. Pavić, N. Čović, D. Dolinar, and D. Zoričić, "Estimation of Internal Rate of Return for Battery Storage Systems with Parallel Revenue Streams: Cycle-Cost vs. Multi-Objective Optimisation Approach," *Energies*, vol. 15, no. 16, 2022.

### **Chapter 7. CONCLUSIONS AND FUTURE DIRECTIONS**

### 7.1 Conclusions

The primary goal of this thesis was to devise an energy-efficient process for the chemical recycling of polyethylene terephthalate (PET). Furthermore, we aimed to perform a technoeconomic analysis (TEA) to analyze the economic feasibility of recyclable, biodegradable material for paper coating applications.

We demonstrated melt-pretreatment process for the methanolic depolymerization of PET was investigated, an energy-efficient process was developed to enhance the depolymerization of semi-crystalline PET by disrupting the crystalline regions and forming active sites in the structure of PET. PET samples underwent melt-extrusion in the presence of 2.5 mol% (1.35 mol) catalysts with/without shot diols followed by cold quenching in methanol. Under optimal conditions of 170°C, 32 molar equivalents of methanol, and the presence of 1.35 mol zinc acetate as a so-called external catalyst, the melt pretreated sample containing 1.35 mol zinc 2-ethylheaxanoate and 1,4cyclohexanedimethanol (CHDM) was depolymerized within 50 minutes (5-fold faster than nonpretreated PET). This was facilitated by a broadened melting range and broadened molecular weight distribution caused by chain scission, as well as the formation of active sites, carrying catalyst and diol that enabled depolymerization not only from the surface but also from within the PET chains. Low-cost, environmentally friendly zinc 2-ethylhexanoate was used for the first time as a catalyst for PET chemical recycling. Noteworthy, energy assessments revealed that the twostep depolymerization saved up energy up to 50 times at 170 °C and 8 times at 200 °C compared to non-pretreated PET. This approach proved to be an efficient chemical recycling approach for PET, surpassing conventional chemical recycling methods without melt pretreatment.

We also demonstrated melt-pretreatment process for the glycolytic depolymerization of PET was investigated. The same pretreated PET samples underwent glycolytic depolymerization, in the absence of any external catalyst when catalyst with/without were deployed during the melt-extrusion. Under optimal conditions of 180 °C and 10:1 molar ratio of ethylene glycol to PET, sample containing zinc 2-ethylhexanoate and CHDM, S<sub>7</sub>, was depolymerized within only 9 minutes. The underlying reasons were chain scission during melt extrusion, inducing structural irregularities in PET due to the presence of diols, particularly those with a structure different from PET monomers, that could reduce the crystallinity of PET to as low as 0.5%.

Furthermore, we tested organic catalysts such as 1,5,7-triazabicyclo[4.4.0]dec-5-ene (TBD), 1,8-diazabicyclo[5.4.0]undec-7-ene (DBU) as alternative to Zn catalyst for the chemical recycling of melt-treated PET. PET samples pretreated with CHDM achieved complete depolymerization within 11 and 30 minutes, respectively, when TBD was used as catalyst. In the case of DBU catalyst for CHDM assisted melt-treated PET achieved complete depolymerization within 9 and 30 minutes. Moreover, energy assessment analysis depicted 12.5% to 38.5% energy saving compared to one-step depolymerization of neat PET under identical reaction conditions.

In summary, our developed methodology for the methanolysis of PET using zinc-based catalysts not only proved to be effective for glycolytic depolymerization at a lower dosage of catalyst but also when traces amount of more environmentally sound organic catalysts was used.

The economic feasibility of a novel ionic polybutylene adipate-co-terephthalate (CPBAT) as a paper coating material was validated through technoeconomic analysis. CPBAT coated on bare Kraft paper (CPBAT-K) with superior mechanical and good barrier properties, and CPBAT coated on starch-coated paper (CPBAT-S) with enhanced barrier properties both proved to be biodegradable and recyclable. The TEA determined total capital investment, operating costs, and

minimum selling prices for a production capacity of 1 ton of CPBAT per day. Total capital investments were estimated at approximately \$1.14M for CPBAT-K and \$1.78M for CPBAT-S, while the minimum selling prices for CPBAT-K and CPBAT-S are \$1.327/m<sub>2</sub> and \$1.864/m<sub>2</sub>, respectively. In the initial scenario, the price of CPBAT-K is approximately 40% higher, and CPBAT-S is about 96% higher than that of commercial polyethylene-coated paper (PE Paper/Poly coated paper), priced at \$0.95/m<sub>2</sub>. With increased production capacity, lower raw material costs, utilization of more energy-efficient coating machines, and partial recovery of energy produced from reactions, the MSPs can be reduced to \$0.588/m<sub>2</sub> and \$0.914/m<sub>2</sub> for CPBAT-K and CPBAT-S respectively. In conclusion, with comparable mechanical and barrier properties to PE paper and the added benefits of biodegradability and recyclability, CPBAT offers an economically feasible and sustainable alternative to current coated paper packaging.

#### 7.2 Future Directions

Our two-step hot-melt-extrusion-cold-quench methodology for the chemical recycling of PET was found to be both rapid and energy efficient, with the organic glycolysis of pretreated PET being more environmentally sound and comparably rapid. However, there are challenges associated with organic catalyst-based glycolysis. Firstly, the yield of monomer is not as high as methanolysis and Zn-catalyzed glycolysis. Secondly, the scope of the study was limited to bench-top experiments only. Large-scale testing will be necessary to investigate the industrial viability of this approach. In addition, instead of two step hot-melt-extrusion-cold-quench methodology, one step approach where melt-treated PET is directly feed to the depolymerization reactor need to be investigated.

The Technoeconomic Analysis (TEA) of the ionic PBAT demonstrated the economic viability of the production of CPBAT for paper coating applications when Kraft paper and starch-

coated Kraft paper were used as the substrates. However, other papers, such as acrylic-based paper, are also recyclable and biodegradable. Therefore, conducting a TEA with other industrially applicable substrates would provide insights into the broader applicability of CPBAT in packaging. Additionally, this study was carried out using a constant thickness of the coating material. It is anticipated that if lower thicknesses could maintain the mechanical and barrier properties, the price of the coated paper would be reduced, rendering it economically competitive. Furthermore, the same synthesis approach could be extended to other polymers lacking water miscibility and therefore exhibiting lower adhesion to paper, yet cheaper than PBAT. This has the potential to enhance the economic competitiveness of these biodegradable and recyclable coated papers compared to currently commercially available polyethylene-coated paper (Poly coated paper).

# APPENDIX A: ENERGY REQUIREMENT ASSESSMENT FOR DEPOLYMERIZATION OF POLYETHYLENE TEREPHTHALATE (PET)

**Table A- 1.** The stream table for the energy analysis of methanolysis of sample pretreated with zinc 2-ethylehexanoate and 1,4-cyclohexanedimethanol (CHDM).

Streams	Content	Mass	Energy	Temperature	Pressure
		(g)	(kJ)	(°C)	(bar)
1	PET flakes into grinder	10		25	1
2	Grinding work in	10	662.4	25	1
3	Grinding heat loss			25	1
4	Grinded PET	10		25	1
5	Internal catalyst	0.475		25	1
6	Additive	1.75		25	1
7	Extrusion work in		170.1	280	1
8	Extrusion heat loss			280	1
9	extruded additive/catalyst-containing PET	12.225		280	1
10	Methanol	300		25	1
11	Amorphous pretreated PET (feed)	12.225		25	1
12	External catalyst	0.244		25	1
13	Reagent (methanol)	3		25	1
14	Depolymerization heat in		2542.7	170	1
15	Depolymerization heat loss			170	1
16	product (Unpolymerized			170	1
	PET+DMT+EG+catalyst+additive)				
17	Chloroform	2		25	1
18	Unpolymerized PET			25	1
19	PET+DMT+EG+catalyst+additive			25	1

Energy assessment for glycolysis of pretreated PET samples ( $S_{12}$  and  $S_{13}$ ):

**Table A- 2.** The stream table for the energy analysis of methanolysis of sample pretreated with zinc 2-ethylehexanoate and 1,4-cyclohexanedimethanol (CHDM).

Streams	Content	Mass (g)	Energy <sub>T</sub>	Energy <sub>D</sub>	Temperature	Pressure
			(kJ)	(kJ)	(°C)	(bar)
1	PET flakes into grinder	100			25	1
2	Grinding work in	100	3974	3974	25	1
3	Grinding heat loss	-	-	-	-	-
4	Ground PET	100	-	-	25	1
5	Catalyst (added during pretreatment)	0.5	-	-	25	1
6	Water	500	-	-	25	1
7	Ground PET in Catalyst-containing	600.5	-	-	100	1
	Solvent					
8	Drying Heat Input	-	1310	1310	60	-
9	Drying Heat Loss	-	131	131	60	-
10	Ground PET and Homogenous	100.5	-	-	25	1
	Catalyst					
11	Additive	17.5	-	-	25	1
12	Extrusion Work Input	-	892	892	280	1
13	Extrusion Heat Input	-	-	-	-	-
14	Extrusion Heat Loss	-	42	42	280	-
15	Extruded Additive/Catalyst-	106	-	-	280	1
	containing PET					
16	Methanol	400	-	-	25	1
17	Pretreated PET (feed)	106	-	-	25	1
18	Catalyst* (added during	-	-	-	-	-
	depolymerization)					
19	Reagent	517	-	-	25	1
20	Depolymerization Heat Input	-	438	358	190	1
21	Depolymerization Heat Loss	-	133	114	190	1
22	Product (Depolymerized	-	-	-	190	1
	PET+reagent+catalyst+additive)					
23	Water	550	-	-	25	1
24	Product Heat Loss	-	-	-	25	1
25	Product + Water	-	-	-	25	1
	1	ı		1		1

**Table A- 2.** (cont'd)

26	Filtrate	-	-	-	-	-
27	Wet Filtered Solid	96/108	-		25	1
28	Drying Heat Input	-	189	212	60	-
29	Drying Heat Loss	-	19	21	60	-
30	Dried Oligomers	24/27	-		60	1
31	Refrigerator Work Input	-	3		4	1
32	Refrigerator Heat Loss		1		4	1
33	Crystallized BHET + Water	560/548	-		4	1
34	Water	232	-		4	1
35	Wet BHET	328/316	-		4	1
36	Drying Heat Input	-	644	621	60	-
37	Drying Heat Loss	-	64	62	60	-
38	Dried BHET	82/79	-		60	1

Grinding (A): PET flakes with 2 to 4 cm<sup>2</sup> were ground to 1 mm diameter grains using Wiley® Mini Cutting Mill. Work energy is input to reduce the PET size based on the instrument's power. The energy transferred to the environment was counted as heat loss. The grinding power was calculated as:

$$P = V \times I = 115V \times 4.8A = 552 W$$

Given that the instrument grinds 50 g PET in an hour, grinding 100 g PET takes 120 minutes, and the required energy is:

$$E_A = \frac{552 J}{s} \times 120 \ min \times \frac{60 \ s}{min} \times \frac{kJ}{1,000 \ J} = 3,974 \ kJ$$

Drying (C): The catalyst solvent (either water or acetone) was evaporated in a simple oven at 60 °C. Heat of vaporization for water at 60 °C (2,357.7 J/g) was used to calculate the heat energy needed for water removal. As  $\sim$ 10% of the energy can be lost through the oven walls, the required energy is calculated as follows:

$$E_C = (m_w \times h_v) = \frac{2,357.7 \, J}{g} \times 500 \, g \times \frac{100}{90} = 1,310 \, kJ$$

The energy lost by transferring through the was 10% of the total energy requirement for this step.

$$E_{C.loss} = 0.1 \times 1310 = 131 \, kJ$$

Extrusion (D): In the extrusion process, the long PET chains were broken into smaller PET chains, while the catalyst and additives were trapped within the structure of PET. Since the boiling point of the volatile catalysts is low (e.g., 263 °C for TBD), some molecules were evaporated during extrusion at 280 °C and the actual catalyst content was lower than the theoretical percentage (less than 0.5%). CHDM is also an additive with a boiling point of 286 °C. It was very probable that some amount of this molecule also evaporated during extrusion; however, tracking the content was not possible due to extruded polymer waste that is formed in small batches. Overall, it is fair to assume that at least 10% of all the input is wasted through evaporation and solidification in the extruder and on the screws.

The work of the extruder on the PET was calculated based on the power of the extruder. The power output and temperature were assumed to be linearly correlated in the extruder, meaning that 70% of the maximum power of the instrument was used for extruding the samples at 280 °C [1]–[3]. The heat loss of the instrument was ignored due to the short period of the extrusion process. The extruder could process 20 grams of PET in each batch. After each extrusion process, LDPE was extruded to purge the extruder for 30 seconds. Hence, extrusion time was assumed to be 22.5 min for 100 g PET.

$$E_{D1} = \frac{900J}{s} \times \frac{70}{100} \times 270 \, s \times 5 = 850 \, kJ$$

Moreover, preheating from room temperature to 280 °C was calculated based on a heating rate of 5 °C/s and a minimum power output of 500 watts (corresponding to 222 °C). Calculating

the time it took to reach 222 °C:

$$t_1 = \frac{222 \text{ °C} - 25 \text{ °C}}{5 \text{ °C/s}} = 39.4 \text{ s}$$

$$t_2 = \frac{400 \text{ °C} - 222 \text{ °C}}{5 \text{ °C/s}} = 35.6 \text{ s}$$

$$E_{D,loss} = \left[ \frac{500J}{s} \times 39.4 \text{ s} + \frac{\left[ \frac{900}{400} (280 - 222) + 500 \right] J}{s} \times 35.6 \text{ s} \right] = 42 \text{ kJ}$$

$$E_D = 850 \text{ kJ} + 42 \text{ kJ} = 892 \text{ kJ}$$

During the extrusion, it is assumed that 10% of the material is lost, therefore out of 118 g PET, additive, and catalyst, ~106 g leaves the extruder.

Depolymerization (F): The pretreated PET, EG, and in some cases, external catalyst, were added to the pressure flask at 25 °C. The pressure flask was put in an oil bath on a hot plate until the solution became clear at a high temperature. The energy was transferred from the hot oil to the reaction chamber through convection. The source of the energy was a hot plate, which does not efficiently transfer heat to the oil bath, resulting in heat transfer to the environment. The amount of energy loss in the power was also dependent on the temperature of the hot plate. The energy loss was transferred from the walls and surface of the oil bath. Additionally, energy output at 190 °C for a hot plate with a maximum temperature of 200 °C was 95% of the maximum power based on previous studies where power was almost linearly related to a temperature lower than 600 K [1]–[3].

$$E_{F,S12,1} = P \times t = \frac{698 J}{s} \times \frac{95}{100} \times 32 \times 60 \ s = 1273 \ kJ$$

$$E_{F,S13,1} = P \times t = \frac{698 J}{s} \times \frac{95}{100} \times 30 \times 60 \ s = 1193 \ kJ$$

The energy requirement for preheating the hot plate with a ceramic top of at most 0.5 kg

can be calculated as follows:

$$E_{F,loss1} = mC_p(T - T_\infty) = 0.5 \ kg \times \frac{0.325 \ J}{kg} \times (463.15 - 398.15) \ K = 27 \ kJ$$

The amount of energy that was lost from the hot plate to the surrounding environment during the depolymerization correlated with the average heart capacity of the air ( $h_{avg}$ =50 W/m<sup>2</sup>K) and the surface of the hot plate that was in contact with air.

$$\begin{split} E_{F,S12,loss2} &= q \times t = hA(T - T_{\infty})t \\ &= \frac{50J}{sm^2K} \times \left[ (7 \times 0.0254)^2 - \left( \pi \times \frac{0.15^2}{4} \right) \right] m^2 \times (463.15 - 298.15) \, K \times 32 \\ &\times 60s = 221 \, kJ \\ E_{F,S12,loss} &= 221 + 27 = 248 \, \mathrm{kJ} \end{split}$$
 
$$E_{F,S13,loss2} &= q \times t = hA(T - T_{\infty})t \\ &= \frac{50J}{sm^2K} \times \left[ (7 \times 0.0254)^2 - \left( \pi \times \frac{0.15^2}{4} \right) \right] m^2 \times (463.15 - 298.15) K \times 30 \\ &\times 60s = 207 \, kJ \\ E_{F,S13,loss} &= 207 + 27 = 234 \, \mathrm{kJ} \end{split}$$

**Note:** At large scale, the depolymerization reactor would be insulated, and the fraction of energy that is lost could be smaller.

Crystallization (J): The flask was cooled to room temperature, then was mixed with  $\sim$ 5500 g of DI water at 100 °C to separate water-soluble monomers from insoluble compounds (ratio of water to BHET of 7:1 was optimal [4], [5]). Results from LCMS showed that  $\sim$ 77% of product mass for  $S_{12}$  and  $\sim$ 75% for  $S_{13}$  were BHET while the rest were dimers, trimers, oligomers, and other compounds. BHET was dissolved in water and other compounds were filtered and dried at

60 °C for 24 hours. The filtrate was cooled at 4 °C to crystallize BHET. Assuming similar crystallization heat of BHET to PET, crystallization energy was calculated as follows:

$$E_{J1,S12} = 38 \frac{kJ}{kg} \times 0.077 \ kg = 3 \ kJ$$

$$E_{J1,S13} = 38 \frac{kJ}{ka} \times 0.075 \ kg = 3 \ kJ$$

The energy for heating water from 25 °C to 100 °C should also be added.

$$E_{J2} = mC_p(T - T_\infty) = 0.550 \ kg \times \frac{4.2 \ kJ}{kg \ K} \times (373.15 - 298.15) \ K = 173 \ kJ$$

$$E_{J,S12} = 3 + 173 = 176 \ kJ$$

$$E_{J,S13} = 3 + 173 = 176 \ kJ$$

Drying of co-products (I): Weighing the sample before and after drying showed  $\sim 300\%$  water content. Hence, energy was required to evaporate 72 and 81 g water for  $S_{12}$  and  $S_{13}$ , respectively. Heat input was determined using the enthalpy of water at 60 °C and 90% efficiency.

$$E_{I,S12} = 0.072 \ kg \times 2357.7 \frac{\text{kJ}}{\text{kg}} \times \frac{100}{90} = 189 \ \text{kJ}$$

$$E_{I,S12,loss} = 19 \ kJ$$

$$E_{I,S13} = 0.081 \ kg \times 2357.7 \frac{\text{kJ}}{\text{kg}} \times \frac{100}{90} = 212 \ \text{kJ}$$

$$E_{I,S13,loss} = 21 \ kJ$$

Drying crystallized BHET (L): Same as co-products, the crystallized BHET monomers contained an average water content of 300%. To obtain 82 and 79 grams of dried BHET, 246 and 237 grams of water should have been evaporated. To evaporate the water, the sample was placed at 60 °C for 24 hours, avoiding higher temperatures to minimize the loss of volatile BHET monomers.

$$\begin{split} E_{L,S12} &= 0.246 \ kg \times 2357.7 \frac{\text{kJ}}{\text{kg}} \times \frac{100}{90} = 644 \ \text{kJ} \\ E_{L,S13} &= 0.237 \ kg \times 2357.7 \frac{\text{kJ}}{\text{kg}} \times \frac{100}{90} = 621 \ \text{kJ} \\ E_{L,S12,loss} &= 0.1 \times 613 = 64 \ \text{kJ} \\ E_{L,S13,loss} &= 0.1 \times 613 = 62 \ \text{kJ} \end{split}$$

Energy assessment for depolymerization of non-pretreated PET ( $S_0$ ):

The energy calculation for the two-step chemical recycling process including pretreatment and depolymerization and the depolymerization of non-pretreated PET is similar for mutual processes; however, energy requirements might differ due to different yields of BHET. The pretreatment step which includes grinding, drying, and extrusion is excluded from the process. Although the reason why PET flakes were ground was to use the extruder available in our lab; as such, this grinding step can be eliminated at the process scale. It is included at the bench scale to provide a conservative estimate of the pretreated PET depolymerization to the non-retreated counterparts. Additionally, the catalyst-PET homogenization step can be avoided in the industrial scale. Energy demand for depolymerizing 100 grams of virgin PET (S<sub>0</sub>) in the presence of 0.5 mol% TBD consists of the following terms:

Depolymerization (a): The depolymerization of the virgin PET (S<sub>0</sub>) occurred within 325 min with 100% conversion and BHET yield of 95 weight% and 99% for TBD- and DBU-catalyzed processes. Considering the same instrument being used for this process, the energy required for the depolymerization process is as follows:

$$E_{a,TBD,1} = P \times t \times = \frac{698 J}{s} \times \frac{95}{100} \times 325 \times 60 s = 12930 kJ$$

$$E_{a,DBU,1} = P \times t \times = \frac{698 J}{s} \times \frac{95}{100} \times 325 \times 60 \ s = 8753 \ kJ$$

Energy demand for preheating the same hot plate and energy loss to the surroundings are as follows:

$$E_{a,loss1,2} = mC_p(T - T_{\infty}) = 0.5 kg \times \frac{0.325 J}{kg} \times (463.15 - 398.15) K = 27 kJ$$

$$E_{a,TBD,loss2} = q \times t = hA(T - T_{\infty})t$$

$$= \frac{50J}{sm^2K} \times \left[ (7 \times 0.0254)^2 - \left( \pi \times \frac{0.15^2}{4} \right) \right] m^2 \times (463.15 - 298.15) K$$

$$\times 325 \times 60 s = 2242 kJ$$

$$E_{a,TBD,loss} = 3132 + 27 = 3159 kJ$$

 $E_{a,DBU,loss2} = q \times t = hA(T - T_{\infty})t$   $= \frac{50J}{sm^2K} \times \left[ (7 \times 0.0254)^2 - \left( \pi \times \frac{0.15}{4} \right) \right] m^2 \times (463.15 - 298.15) K \times 220$   $\times 60 s = 1518 kJ$ 

$$E_{F,DBU,loss} = 87 + 27 = 114 \text{ kJ}$$

Crystallization (b): Since, in their article, IMB scientists only reported on the yield when 10 mol% catalyst was used, we'd proceed with the same yields. Crystallization of 95 and 99 g BHET was performed under the same condition using 650 mg water.

$$E_{b1,T} = 38 \frac{kJ}{kg} \times 0.095 \ kg = 3.6 \ kJ$$

$$E_{b1,D} = 38 \frac{kJ}{kg} \times 0.099 \ kg = 3.8 \ kJ$$

$$E_{b,2} = mC_p(T - T_\infty) = 0.550 \ kg \times \frac{4.2 \ kJ}{kgK} \times (373.15 - 298.15) \ K = 173 \ kJ$$

$$E_{b,T} = 3.6 + 173 = 178 \ kJ$$

$$E_{b,D} = 3.8 + 173 = 178 \ kJ$$

Drying co-products (c): 5 grams and 1 gram of co-products were dried at 60 °C to remove 15 and 3 grams of water using the same oven.

$$E_{c,T} = 0.015 \, kg \times 2357.7 \, \frac{\text{kJ}}{\text{kg}} \times \frac{100}{90} = 39 \, \text{kJ}$$

$$E_{c,T} = 0.003 \, kg \times 2357.7 \, \frac{\text{kJ}}{\text{kg}} \times \frac{100}{90} = 8 \, \text{kJ}$$

Drying BHET (d): 285 and 297 grams of water were removed from BHET using the same drier and under the same conditions.

$$E_{d,T} = 0.285 \, kg \times 2357.7 \, \frac{\text{kJ}}{\text{kg}} \times \frac{100}{90} = 605 \, \text{kJ}$$

$$E_{d,D} = 0.297 \ kg \times 2357.7 \frac{\text{kJ}}{\text{kg}} \times \frac{100}{90} = 630 \ \text{kJ}$$

The total energy requirements for the samples  $S_{12}$  and  $S_{13}$  depolymerization processes are:

$$E_{S12} = 3974 + 1310 + 892 + 1273 + 176 + 189 + 644 = 8458kJ$$

$$E_{S13} = 3974 + 1310 + 892 + 1193 + 176 + 212 + 621 = 8378 \, kJ$$

While the energy demand for the non-pretreated PET is:

$$E_{S0,T} = 12930 + 178 + 39 + 605 = 13752 \, kJ$$

$$E_{S0,T} = 8753 + 178 + 8 + 630 = 9569 \, kJ$$

$$\frac{E_{S0,T}}{E_{S12}} = \frac{13752 - 8458 \, kJ}{13752 \, kJ} = 38.5\%$$

$$\frac{E_{S0,D}}{E_{S13}} = \frac{9569 - 8378 \, kJ}{9569 \, kJ} = 12.5\%$$

# APPENDIX B: ANALYSIS OF GLYCOLYSIS PRODUCTS OF POLYETHYLENE TEREPHTHALATE (PET)

Characterization of all present compounds present in the depolymerized products of PET glycolysis:

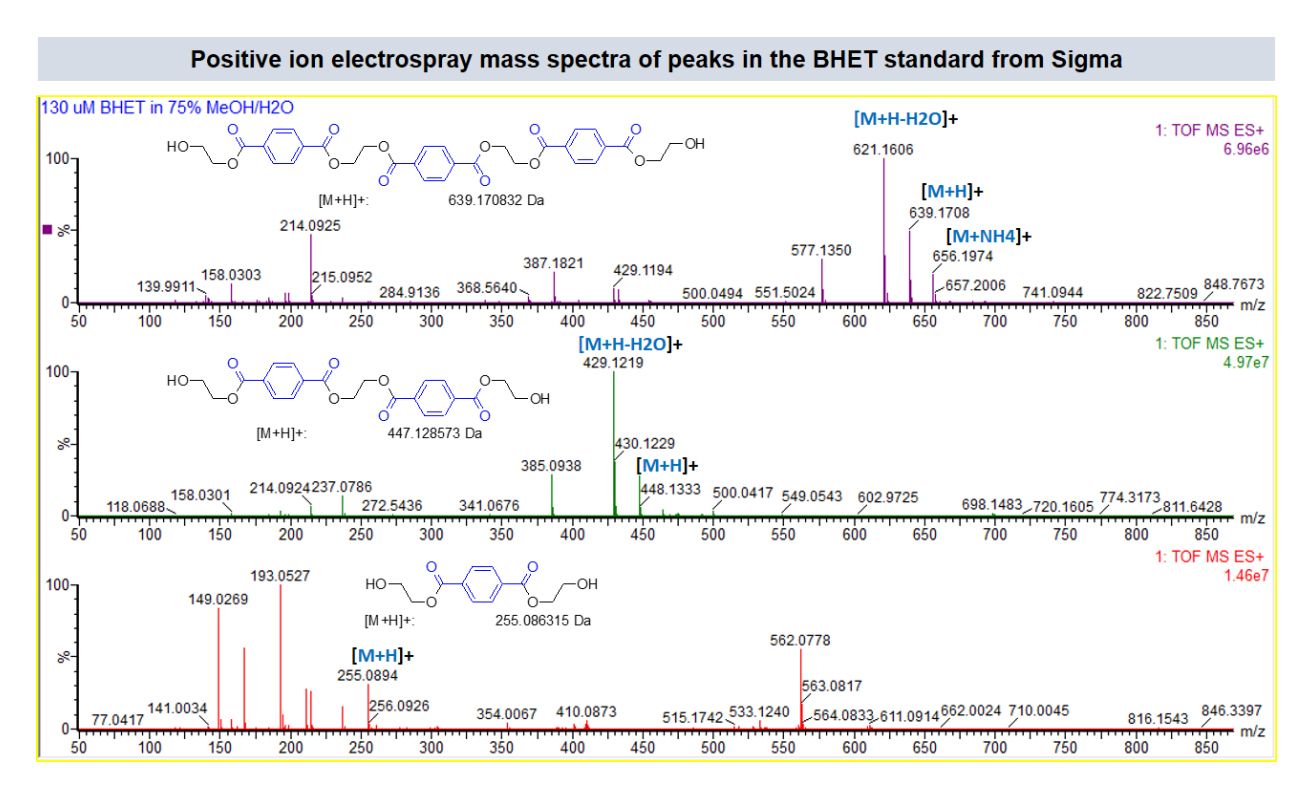


**Figure B- 1.** Mass spectra of peaks associated with the BHET, dimer and trimer, standard using positive ion electrospray.

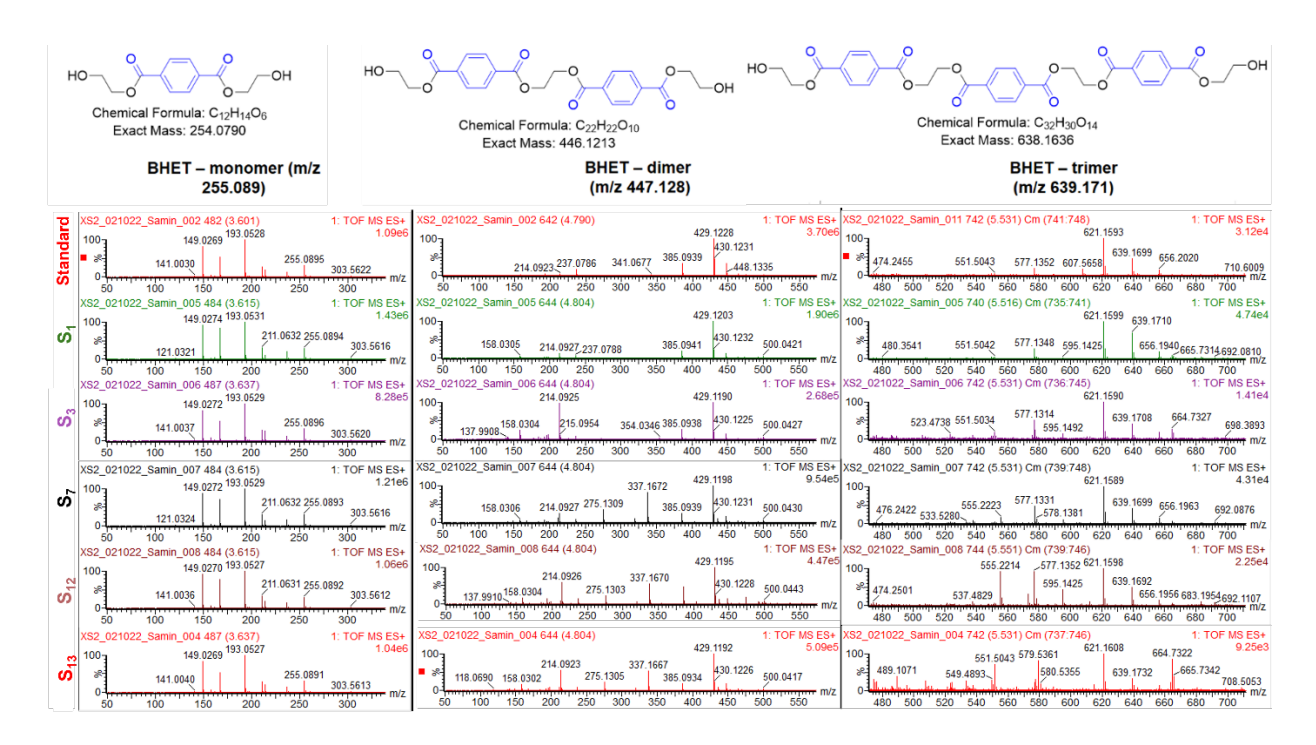


**Figure B- 2.** Mass spectrum fragmentation patterns of the standard, monomer, dimers, and trimers.

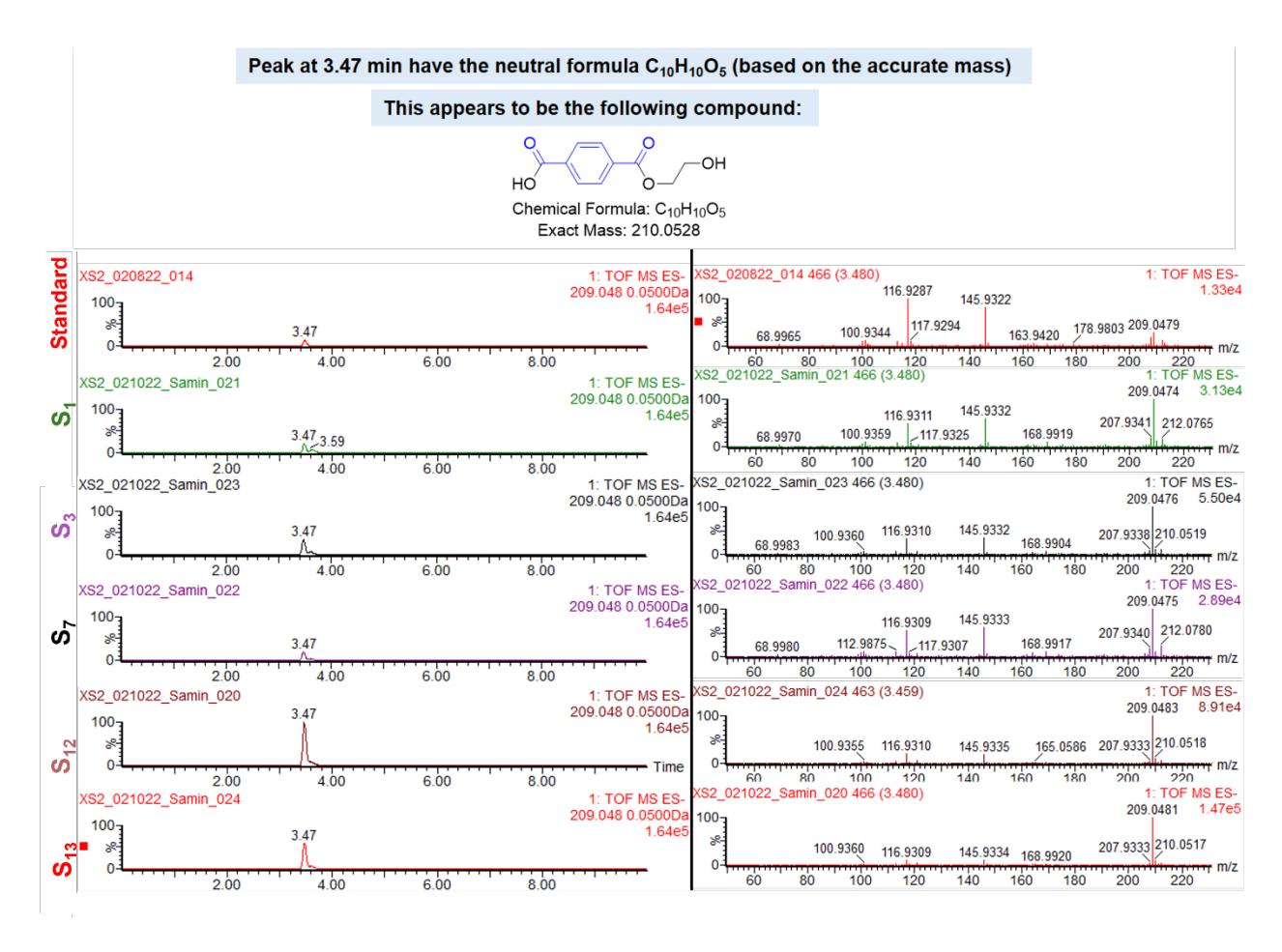


**Figure B- 3.** Peak at 3.47 minute potentially belongs to a neutral formula of  $C_{10}H_{10}O_5$ . The accurate mass and fragmentation pattern, the structure of the compound is a modified PET monomer which is consistent with the expected compounds in depolymerization of PET.

# Examination of peaks in PET-5 sample attempts to identify related compounds that are not BHET or the oligomers

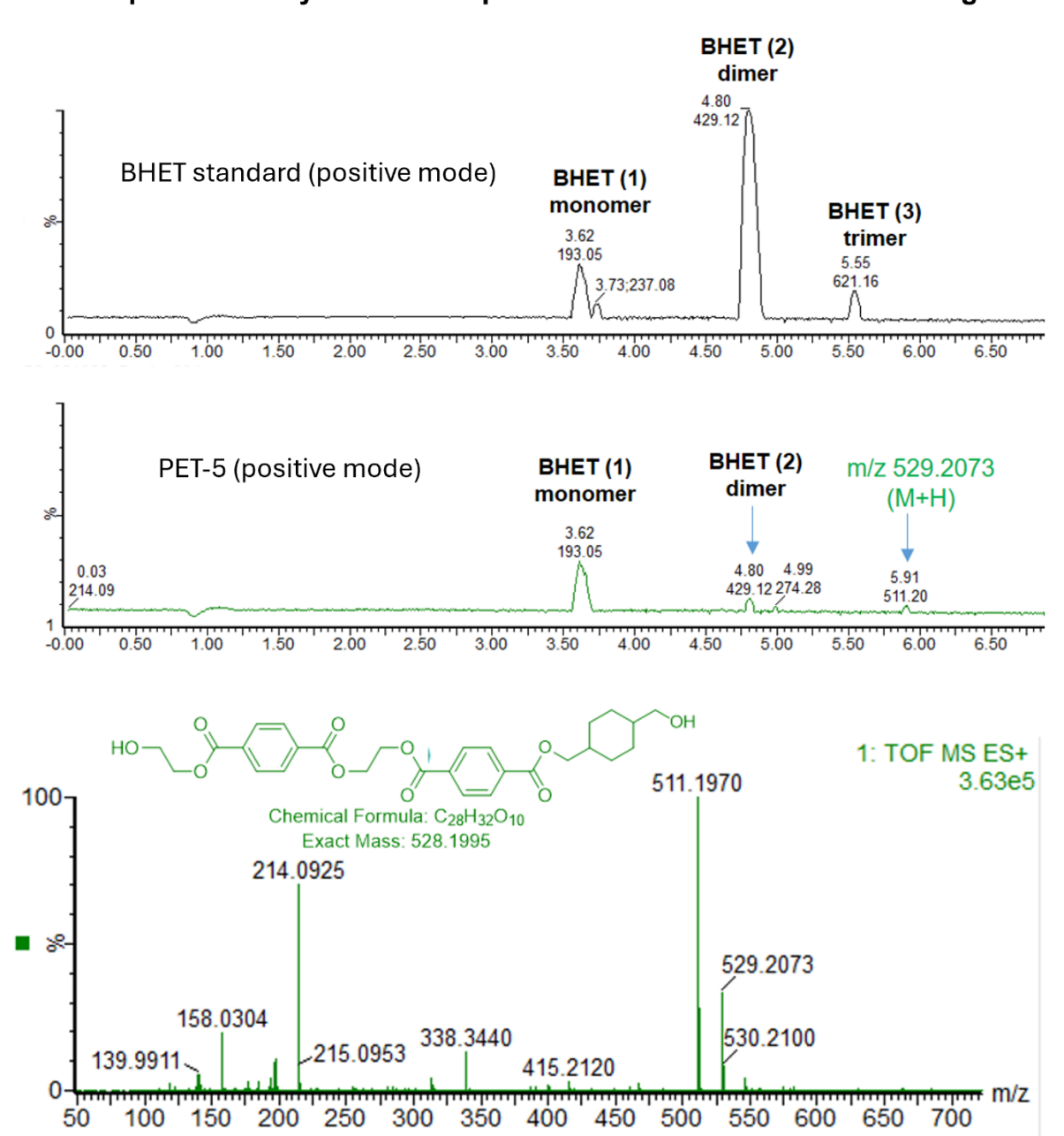


**Figure B- 4.** Identification of peaks in depolymerization products of pretreated PET sample containing DBU and CHDM  $(S_{13})$  to that are neither BHET nor the oligomers.

## APPENDIX C: TECHNOECONOMIC ANALYSIS CALCULATIONS

**Table C- 1.** Label definitions for the process flow diagram of CPBAT, CPBAT-S, and CPBAT-S production.

EQUIPMENT	PROCESS				
CPBAT PRODUCTION AND COATING PROCESS (A)					
FIRST DRYER	Drying commercial PBAT				
FIRST REACTOR	PBAT-diol production reaction				
SECOND REACTOR	CPBAT production reaction				
THIRD REACTOR	CPBAT emulsification reaction				
<b>FURNACE</b>	Natural gas combustion				
TANK	CPBAT emulsion storage				
<b>COATING MACHINE</b>	Coating CPBAT emulsion				
SECOND DRYER/BOILER	Drying CPBAT-coated paper				
(BUILT IN COATING					
MACHINE)					
CONDENSER	Condensation of water-ammonium mixture				
STARCH (	COATING PROCESS (B)				
REACTOR	Starch dissolution				
FURNACE	Natural gas combustion				
TANK	Starch solution storage				
COATING MACHINE WITH	Drying Starch coated paper				
BUILT-IN DRYER					

**Table C- 2.** Stream table associated with process flow diagram of CPBAT, CPBAT-K and CPBAT-S production.

$\mathcal{S}_{\mathcal{C}}$	25	20	20	25	25	200	25	25	25	25		77	77	7.0		7.0	091	25	25	06
																				101
,																				278.8
																				•
Kg/day	18.9	18.9	;	1	1	ŀ	ŀ	1	1	1923.1	1	1	1	384.6	1538.5	1538.5	1538.5	ł	5297.2	5297.2
Kg/day	+	1	;	;	;	;	<b>¦</b>		692.3	;	;	;	;	138.5	553.8	553.8	553.8	1	ŀ	
Kg/day	+	;	;	;	;	;	;	1000	;	;	;	;	1000	;	;	;	;	1	ŀ	
Kg/day	:	;	;	1	;	1	53.2	;	;	;	;	;	:	;	ŀ	;	1	1	1	
Kg/day	:	;	;	1	1	946.8	;	;	;	1	;	1	;	;	ŀ	;	1	1	ŀ	
Kg/day	1	ł	ł	1	9.2	1	ł	ł	1	<b>!</b>	9.2	<b>!</b>	1	ŀ	<b>!</b>	ł	1	1	1	
Kg/day	ŀ	ł	;	22.7	;	;	ŀ	ŀ	1	ŀ	ŀ	ŀ	ŀ	ŀ	;	;	;	1	1	
Kg/day	924.1	1	924.1	1	;	1	;	<b>!</b>	;	1	;	1	;	ł	;	;	1	1	1	
	Kg/day Kg/day Kg/day Kg/day Kg/day Kg/day Kg/day Kg/day Kg/d ay	Kg/day Kg/day Kg/day Kg/day Kg/day Kg/day Kg/d 18.9 18.9	Kg/day Kg/day Kg/day Kg/day Kg/day Kg/day Kg/d 18.9 18.9	Kg/day         Kg/day<	Kg/day         Kg/day<	Kg/day         Kg/day<	Kg/day         Rg/day         Rg/day<	Kg/day         Rg/day         Rg/day<	Kg/day         Rg/day         Kg/day         Kg/day<	Kg/day         Kg/day<	Kg/day         Kg/day<	Kg/day         Lg         Lg	Kg/day         Lg         Lg	Kg/day         Lg           122.7   -	Kg/day         Lg           122.7  <	Kg/day         Lg	Kg/day         Kg/day<	Kg/day         Kg/day<	Kgylday         Kg/day         Kg/day	Kgylday         Kgylday <t< th=""></t<>

Drying commercial PABT: Commercial PBAT usually has 1-2% water. Herein, it is assumed that the commercial PBAT has 2% water. The energy for drying PBAT goes both for evaporating water and preheating PBAT to the reaction temperature in reactor I. Ideally, moisture content was reduced to 0%. Energy for drying commercial PBAT is calculated by energy required for heating and evaporating the water and heating PBAT up to the reaction temperature, considering information in *Table C-3*. Additionally, for designing the dryer using hot air, the data in *Table C-4* was used.

**Table C- 3.** Dryer (A) specifications.

Parameter	Value	Unit
Input to dryer	Wet PBAT	
Wet moisture % (X <sub>i</sub> )	2	%
Dried moisture % (X <sub>o</sub> )	0	%
Air moisture in (Y <sub>i</sub> )	1.5	%
Air moisture out (Y <sub>0</sub> )	3.2	%
$C_{p,w}$	4.19	kJ/kg °C
$\Delta H_{\rm w}^{\rm vap}$ (at 120 °C)	2.05	MJ/kg
Mass flow rate of water (Ls)	18.86	kg/day
Mass flow rate of gas (G <sub>s</sub> )	1087.60	kg/day
$C_{p,PBAT}$	1.5	kJ/kg °C
hwater (at 120 °C)	2.05	MJ/kg
Energy requirement for preheating water	7.50	MJ/day
<b>Energy requirement for water evaporation</b>	38.69	MJ/day
h <sub>PBAT</sub>	1.50	kJ/kg °C
T <sub>rxn</sub>	200	°C
<b>Energy requirement for preheating PBAT</b>	242.58	MJ/day
Dryer efficiency	0.5	NA
Total dryer energy requirement	327.46	MJ/day

**Table C- 4.** Parameters for designing the dryer (A).

Parameter	Value	Unit
Wet moisture % (X <sub>i</sub> )	2	%
Dried moisture % (X <sub>0</sub> )	0	%
Air moisture in (Y <sub>i</sub> )	1.5	%
Air moisture out (Y <sub>0</sub> )	3.2	%
T <sub>PBAT-in</sub>	25	$^{\circ}\mathrm{C}$
T <sub>PBAT-out</sub>	120	$^{\circ}\mathrm{C}$
T <sub>air-in</sub>	120	$^{\circ}\mathrm{C}$
Tair-out	60	$^{\circ}\mathrm{C}$
h <sub>PBAT-in</sub>	39.64	kJ/kg °C
h <sub>PBAT-out</sub>	180.05	kJ/kg °C
h <sub>air-in</sub>	264.11	kJ/kg °C
h <sub>air-out</sub>	144.80	kJ/kg °C
$ m V^h_{air-in}$	1.14	$m^3/kg_{\ dry\ air}$
$ m V^h_{air-out}$	0.922	$m^3/kg_{dry\;air}$
$ m V_{air}$	2	m/s
Gas flux (G's)	0.455	$kg/m^2s$
Heat coefficient (U)	151.926	$W/m^3K$
Length (H) theoretical	3.141	m
Length (H) Actual	1.98	m

### Reaction Calculation Method:

- A. Mass Balances: The mass values for each stream were reported in units of kg/day.
- B. Reference state: the reference state for energy calculations was selected to be 25  $^{\circ}$ C and 1 bar pressure.
- C. Higher Heating Values: The higher heating values (HHV) required for calculating the heat of reactions, were calculated using the Gaur and Reed formula [6].

$$HHV = (0.3491 \ X_C) + (1.1783 \ X_H) + (0.1005 \ X_S) - (0.0151 \ X_N) - (0.1034 \ X_O)$$

Eq A1. Gaur and Reed Expression for calculation of HHV

 $(X_i = mass percentage and HHV is in MJ/kg)$ 

- D. Thermophysical Properties: The thermophysical properties like specific heat and latent heat of vaporization were extracted from the NIST database in Aspen or Polymer handbook [7].
- E. Sample Calculation: A sample calculation is shown below for the energy balance around the PBAT-diol reactor where the following equation applies:
- (a) PBAT-diol production reaction from PBAT and butanediol:

$$\begin{split} [C_{22}H_{28}O_8]_{124} + 124\ HO - (CH_2)_4 - OH &\rightarrow 10.3\ [C_{26}H_{38}O_{10}]_{12} \\ \Delta \boldsymbol{H_{rxn}} &= n_{PBAT-diol} \times \Delta H_{PBAT-diol}^f - n_{BDO} \times \Delta H_{BDO}^f - n_{PBAT} \times \Delta H_{PBAT}^f \\ &= 10.3 \times (-374.579) - 124 \times (-505.3) - 1 \times (-2401.925) \\ &= -1406.075\ \frac{MJ}{mol} \div 6940 \frac{g}{mol} \times 946.8\ \frac{kg}{day} \times \frac{1000\ g}{kg} \\ &= -191.824\ \frac{MJ}{day} \end{split}$$

For calculating the energy for PBAT-diol production from PBAT and butanediol, heat of formation of PBAT and butanediol are required. Additionally, for finding the heat of formation of PBAT and butanediol, heat of combustion of PBAT can be calculated and heat of formation of carbon dioxide and water be deducted. Same with butanediol formation, heat of carbon dioxide and water should be deducted from heat of combustion of butanediol.

(a.1) PBAT formation:

$$2728 C + 1736 H_2 + 496 O_2 \rightarrow [C_{22}H_{28}O_8]_{124}$$

$$\Delta H_{PBAT}^f = \Delta H_{CO2-H2O}^f - \Delta H_{PBAT}^{comb} = -2401.925 \frac{MJ}{mol}$$

(a.1.1) PBAT combustion:

$$[C_{22}H_{28}O_8]_{124} + 3100 O_2 \rightarrow 2728 CO_2 + 1736 H_2O_1$$

$$\Delta H_{PBAT}^{comb} = MW_{CPBAT} \times \Delta h_{PBAT}^{comb} = 31230 \frac{g}{mol} \times \frac{26.6 \ kJ}{g} \div 1000 = 832.202 \ \frac{MJ}{mol}$$

(a.1.2) Carbon dioxide and water formation:

$$2728 \ C + 3596 \ O_2 + 1736 \ H_2 \ \rightarrow 2728 \ CO_2 + 1736 \ H_2O$$

$$\begin{split} \Delta H_{CO2-H2O}^f &= n_{CO2} \Delta H_{CO2}^f + n_{H2O} \Delta H_{H2O}^f \\ &= 2728 \ mol \times (-393.52) \frac{KJ}{mol} + 1736 \ mol \times \frac{(-285.83) \frac{kJ}{mol}}{1000} \\ &= -1569.723 \ \frac{MJ}{mol} \end{split}$$

(a.2) PBAT-diol formation:

$$312\ C + 228\ H_2 + 60\ O_2 \rightarrow [C_{26}H_{37}O_{10}]_{12}$$

$$\Delta H_{PBAT-diol}^{f} = \Delta H_{CO2-H2O}^{f} - \Delta H_{PBAT-diol}^{comb} = -374.579 \frac{MJ}{mol}$$

(a.2.1) PBAT-diol combustion:

$$[C_{26}H_{37}O_{10}]_{12} + 366\ O_2 \rightarrow 312\ CO_2 + 228\ H_2O$$

$$\Delta H_{PBAT-diol}^{comb} = MW_{BDO} \times \Delta h_{PBAT-diol}^{comb} = 6940 \frac{g}{mol} \times \frac{26.9 \ kJ}{g} \div 1000 = 186.631 \ \frac{MJ}{mol}$$

(a.2.2) Carbon dioxide and water formation:

$$312 C + 426 O_2 + 228 H_2 \rightarrow 312 CO_2 + 228 H_2 O_2$$

$$\Delta H_{CO2-H2O}^{f} = n_{CO2} \Delta H_{CO2}^{f} + n_{H2O} \Delta H_{H2O}^{f}$$

$$= 312 \, mol \times (-393.52) \frac{kJ}{mol} + 228 \, mol \times \frac{(-285.83) \, \frac{kJ}{mol}}{1000}$$

$$= -187.947 \, \frac{MJ}{mol}$$

While this reaction is exothermic, some energy input is required to move the reaction forward. This energy is estimated based on the energy requirement for the bench-top experiments, scaled up to industrial production capacity.

The energy from a hot plate goes partly to the reaction and partly lost to the environment through convection. Several studies have shown that the power was almost linearly related to the temperature below 600 K. Hence energy requirement for the samples at 200 °C with the maximum temperature of the instrument (200 °C) power demand is (200/200x100)% of the maximum power of the instrument. Specifications of the hot plate is listed in *Table 4- 4* and the schematic of the hot plate is shown in *Figure C-1*.

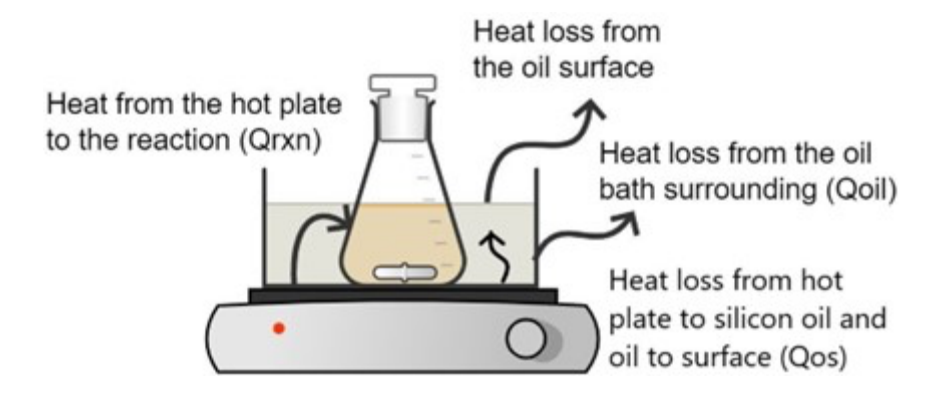


Figure C- 1. Schematic of the hot plate and the energy inputs and energy loss.

The maximum energy output of the hot plat working at 200 °C is as follows:

$$Q_p = 668 \frac{J}{s} \times \frac{200}{200} \times 6 h \times 3600 \frac{s}{h} \times \frac{kJ}{1000 J} = 15076.8 kJ$$

Energy loss to the surrounding from a 20 cm by 20 cm square hot plate and a 5 cm tall oil bath with 15 cm diameter is as follows:

$$Q_{loss,1} = 2.5 \frac{W}{m^2 K} \times (182 - 25) K \times (3.14 \times 0.15 \times 0.05) m^2 \times 6 \times 3600 s \times \frac{kJ}{1000J}$$
$$= 962.7 kJ$$

$$Q_{loss,2} = 2.5 \frac{W}{m^2 K} \times (200 - 25) K \times \left(0.2 \times 0.2 - 3.14 \times \frac{0.15 \times 0.15}{4}\right) m^2 \times 6 \times 3600 s$$

$$\times \frac{kJ}{1000 J} = 289.6 kJ$$

$$Q_{loss,3} = 2.5 \frac{W}{m^2 K} \times (182 - 25) K \times (0.15 \times 0.15) m^2 \times 6 \times 3600 s \times \frac{kJ}{1000 J} = 190.7 kJ$$

$$Q_{loss,4} = 0.6 \frac{W}{m^2 K} \times (200 - 25) K \times \left(3.14 \times \frac{0.15 \times 0.15}{4}\right) m^2 \times 6 \times 3600 s \times \frac{kJ}{1000 J}$$

$$= 40 kJ$$

$$Q_{rxn} = (15076.8 - 926.7 - 298.6 - 190.7 - 40) = 13620 kJ$$

This energy was required to produce 0.2 kg of PBAT-diol, for production of 946.8 kg/day of PBAT-diol we should scale up the numbers to:

$$Q_{rxn,PBAT-diol} = 13620 \ kJ \times \frac{1}{0.2 \ kg} \times 946.8 \frac{kg}{day} \times \frac{MJ}{1000 \ kJ} = 64477 \ MJ$$

This energy is much higher than the energy requirement for industrial setting due to the large heat requirement for glassware with no insulation while an adiabatic reaction in an insulated reactor can be used. Herein, in our base case scenario, we have considered the energy from the exothermic is not used elsewhere and in our sensitivity analysis, we assumed the maximum energy requirement is the scale up from the bench-top experiment is demanded. All other energy input to the reactors is calculated in the same way and summarized in *Table C- 5*.

**Table C-5.** Summary of reactions and the energy requirement for each reaction.

Reaction	Heat of	Energy from	Reaction	Reaction
	reaction	scale-up	duration	temperature
	(MJ)	(MJ)	(min)	(°C)
PBAT-diol production	-191824	64477	360	200
<b>CPBAT</b> production	2715	5015	30	170
<b>CPBAT</b> emulsification	-3555	2820	45	77

Starch dissolution	 6607	45	90

The energy requirement for PBAT-diol production is the highest as the energy loss correlates with the temperature and duration of the reaction in bench-top experiments. Similarly, the energy requirement for the reaction with lower temperature, e.g. CPBAT emulsification at 77 °C is much lower.

To compare how much this method of energy calculation can be higher than industrial scale, a study was found for calculating the breaking the ester bonds in PETG. In this investigation, the energy for 1000 kg PETG cards containing 920 kg PETG reaction with EG is estimated to be 800 MJ. Considering 18.57 wt% of PETG is the CHDM molecule, the rest has similar structure to PET and the number of ester bonds should be the same. Hence, the mass of PET is 749.16 kg which equals 3824.5 mol PET. In each repeating unit of PET, there are two ester bonds, therefore, there are 7648 mol ester bonds present. It is assumed that 49.16/1000 of total energy for the reaction goes to breaking the ester bond and the energy for breaking one ester bond is as follows:

$$m_{PET} = 920 \times (1 - 0.1857) = 749.16 \, kg$$
  $n_{PET} = 749.16 \, kg \times \frac{1000 \, g}{1 \, kg} \times \frac{1 \, mol}{192 \, g} = 3910.87 \, mol$  
$$E_{ester-PET} = \frac{800 \, MJ}{3910.87 mol} = 0.2046 \, \frac{MJ}{mol}$$

The number of ester bonds cleaved in reaction of PBAT with BDO can be estimated by knowing the mols of BDO. With 38 kg BDO that equals 422mol and each PBAT monomer having three ester bonds, energy required for PBAT-diol production can be estimated as follows:

$$n_{BDO} = \frac{38 \ kg}{day} \times \frac{1000 \ g}{1 \ kg} \times \frac{1mol}{92.12 \ g} = 422 \ \frac{mol}{day}$$

$$n_{eater-PBAT} = 422 \times 3 = 1266 \frac{mol}{day}$$

$$E_{PBAT-diol} = \frac{0.2046 \, MJ}{mol} \times 1266 \, \frac{mol}{day} = 259.02 \, \frac{MJ}{day}$$

Energy for rection comes from burning natural gas in a furnace. Composition of natural gas is up to 97% methane [8], hence it is assumed that it is only composed of methane. The furnace was designed in HYSYS Aspen software with the following information.

$$1CH_4 + 2(O_2 + 3.76N_2) \rightarrow CO_2 + 2H_2O + 7.52 N_2$$

$$\Delta H = -393.5 + 2 \times (-285.83) - (-74.6) = -890.57 \frac{kJ}{mol} \times \frac{1 \ mol}{16 \ g} \times \frac{1 \ MJ}{1000 \ kJ}$$

$$= -55.66 \frac{MJ}{kg}$$

When the total amount of energy from scale up of bench-top experiment is found, for the furnace designed in HYSYS Aspen, the natural gas enters the furnace at 200 °C with flow rate of 12.5 kg/h while air is flowed to the furnace at the rate of 225.3 kg/h at 25 °C. The flare gas leaves the furnace at 505.5 °C. In this situation the shell overall volume is 9.7 m<sup>3</sup>.

Reactor Design: For designing the reactor, 1st order reaction is assumed for all reactions. The graph below shows the reaction rate for PBAT-diol production that is 1st order with respect to PBAT concentration. For converting mol of PABT to concentration, melt density of PBAT and density of butanediol were used from Perry's handbook [9].

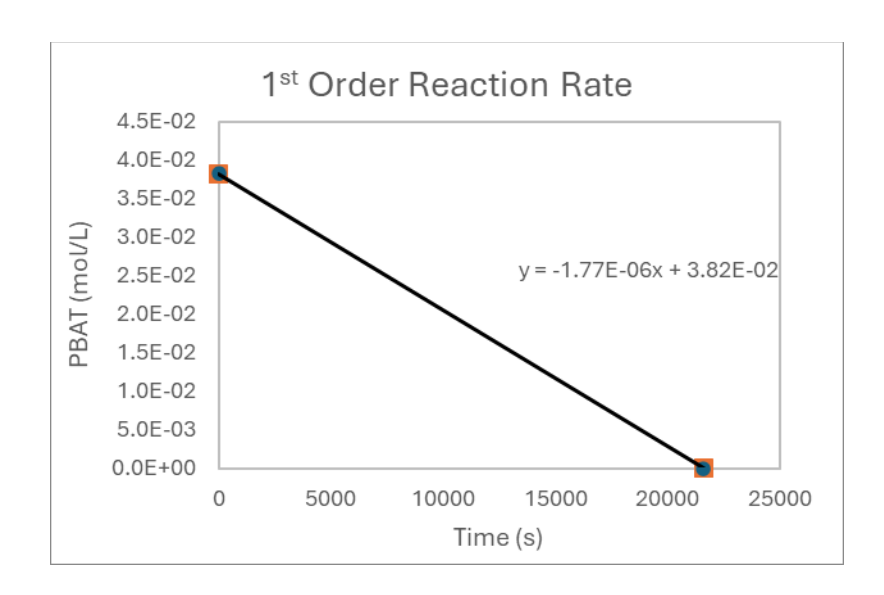


Figure C- 2. Reaction rate for PBAT-diol production from PABT and butanediol.

$$n_{PBAT} = \frac{924.1 \, kg/day}{36230 \, \frac{g}{mol} \div 1000 g/kg} = 29.59 \, mol/day$$

$$n_{PBAT} = \frac{22.7 \, kg/day}{90.12 \, \frac{g}{mol} \div 1000 g/kg} = 251.74 \, mol/day$$

$$V_{tot} = \frac{924.1 \, kg/day}{1.23 \, kg/L} + \frac{22.7 \, kg/day}{1.02 \, kg/L} = 773.61 \, L/day$$

$$C_{PBAT,0} = \frac{29.59 \, mol/day}{773.61} = 0.038 \, mol/L$$

$$V_{rxn,t} = \frac{C_{PBAT}V_{tot}}{-r} = \frac{0.038 \, \frac{mol}{L} \times 773.61 \, \frac{L}{day}}{-(-1.77 \times 10^{-6}) \, \frac{mol}{L \, s} \times \frac{3600 \, s}{h} \times \frac{24 \, h}{day}} = 190.4 \, L$$

Assuming that only 2-3<sup>rd</sup> of the reactor is filled, the actual volume would be:

$$V_{rxn,t} = \frac{3}{2} \times 190.4 = 290 L$$

The cost of the reactor is found from *Figure 13-15* of the book Plant Design and Economic for Chemical Engineers [10].

*Table C- 6.* Specifications of the coating machine.

Company	Coating machine	Equipment	Power	Coating	Temp	coating max
	type	price (\$)	(kW)	width	(°C)	speed
				(cm)		(m/min)
Xiamen	Customizable	17500	30	55	180	5
Simy	Coating Line					
Equipment	Solvent Coater					
	Machine with Oven					

 Table C- 7. Data for CPBAT-coated unbleached Kraft paper from Uline (75 lb).

Parameter	Value	Unit
Paper basis weight	0.122	kg/m <sup>2</sup>
coating weight/area	0.060	$kg/m^2$
Total weight/area	0.182	$kg/m^2$
Coating area	16694.5	$m^2$
Length of the coated paper	29811.6	m
max length per day	7200	m
number of coating machine	5	NA
<b>Energy for coating CPBAT</b>	53660.9	MJ/day

Table C- 8. Data for starch coated on unbleached Kraft paper from Uline (75 lb).

Value	Unit
0.017	kg/m <sup>2</sup>
278.8	kg
16694.5	$m^2$
29811.6	m
7200	m
5	NA
47435.0	MJ/day
	0.017 278.8 16694.5 29811.6 7200 5

Table C- 9. Specification and price of Kraft paper and Poly paper (50 lb and 75 lb) from Uline.

Poly paper type	Kraft paper	Kraft paper	Uline poly coated	Poly coated
	(50 lb)	(75 lb)	paper (50 lb)	<b>paper</b> (75 lb)
Basis weight (kg)	50	75	50	50
Length (m)	219.5	144.8	182.9	182.9
Width (cm)	56	56	56.000	56
area (m²)	122.90	81.08	102.41	81.08
Weight per roll	0.08	0.12	0.10	0.15
price (\$/m²)	0.28	0.41	0.64	0.94

Table C- 10. Modeling of ionization solvent evaporation using HYSYS Aspen.

Parameter	Inlet	outlet	unit
Vapor fraction	0	1	NA
Flow rate	2615.4	2615.4	kg/day
ammonia mass fraction	0.07	0.07	NA
water mass fraction	0.93	0.93	NA
temperature	50	180	$^{\circ}\mathrm{C}$
Pressure	100	1071	kPa
Molar enthalpy	-2.69E+05	-2.23E+05	kJ/kmol
Duty	6,753.82		MJ/day

**Table C-11.** Summary of equipment costs and sizing for CPBAT, CPABT-K and CPBAT-S production.

<b>Equipment item</b>	Size	Equip.	Installed	Installed	Installed	Ref.
	$(m^3)$	Cost	<b>Equip.</b> Cost	Equip. Cost	Equip. Cost	
		(\$)	(CPBAT)	(CPBAT-K)	(CPBAT-S)	
			(\$)	(\$)	(\$)	
Rotary dryer I	1.32	108,265		162,398	162,398	[11]
CSTR (PBAT-	0.29	24,228	162,398	24,228	24,228	This
diol production)						study,
						[10]
Filter	NA	3,634	24,228	3,634	3,634	[12]

Tabla		11	(acret	, J\
Table	C-	11.	(COni	$a_{I}$

CSTR (CPBAT production)	0.03	12,114	3,634	23,985	23,985	This study, [10]
CSTR (CPBAT emulsification)	0.16	18,171	3,162	18,171	18,171	This study, [10]
Furnace I	9.70		18,171			This study,
Isolated storage tank (CPBAT)	0.3	10,095	NA	10,095	10,095	This study, [10]
Coating machine (CPBAT)	NA	87,500	NA	135,625	135,625	[13]
CSTR (starch dissolution)	0.68	36,341.25	NA	NA	71,956	This study,
Furnace II	NA		NA	NA		This study,
Isolated storage tank (starch)	8	16,151.67		NA	31,173	This study,
Coating machine for starch	NA	108,265	NA	NA	162,398	[13]

**Table C- 12.** Modeling of ionization solvent condensation modeling using Aspen HYSYS (20% loss).

Parameter	Inlet	outlet	unit
Vapor fraction	1	0	NA

**Table C- 12.** (cont'd)

Flow rate	2092.3	2092.3	kg/day
Ammonia mass fraction	0.07	0.07	NA
Water mass fraction	0.93	0.93	NA
Temperature	180	25	$^{\circ}\mathrm{C}$
Pressure	1000	100	kPa
Molar enthalpy	-2.23E+05	-2.72E+05	kJ/kmol
Duty (20% material loss)	-5,23	MJ	

#### REFERENCES

- [1] S. Santra *et al.*, "Post-CMOS wafer level growth of carbon nanotubes for low-cost microsensors A proof of concept," *Nanotechnology*, vol. 21, no. 48, 2010.
- [2] D. V. Zinov'ev and P. Sole, "Quaternary codes and biphase sequences from Z8-codes," *Probl. Peredachi Informatsii*, vol. 40, no. 2, pp. 50–62, 2004.
- [3] J. Spannhake, O. Schulz, A. Helwig, A. Krenkow, G. Müller, and T. Doll, "High-temperature MEMS heater platforms: Long-term performance of metal and semiconductor heater materials," *Sensors*, vol. 6, no. 4, pp. 405–419, 2006.
- [4] T. Lafarga, A. V. Queralt, G. Bobo, M. Abadias, and I. Aguiló-Aguayo, "Thermal Processing Technologies," *Food Formul.*, pp. 165–181, 2021.
- [5] A. Goh, H.W., Salmiaton, A., Abdullah, N. and Idris, "Process Simulation of Two-stage Evaporation and Crystallization Systems for Bis(2-hydroxyethyl) terephthalate Recovery," *J. Appl. Sci.*, vol. 12, no. 15, pp. 1547–1555, 2012.
- [6] T. B. Gaur, S. and Reed, "Thermal Data for Natural and Synthetic Fuels," *Technol. Eng.*, 1998.
- [7] Z. Raheem, "POLYMER DATA," no. June, 2019.
- [8] J. A. B. Obek, D. Ó. R. A. R. I. E. T. H. Ő, É. V. A. M. Olnár, and R. Ó. B. Ocsi, "SELECTIVE HYDROGEN SULPHIDE REMOVAL FROM ACID GAS BY ALKALI CHEMISORPTION IN A JET REACTOR," vol. 44, no. 1, pp. 51–54, 2016.
- [9] R. H. Green, D. W., & Perry, *Perry's Chemical Engineers' Handbook*. McGraw-Hill Education, 2008.
- [10] M. S. Peters and K. D. Timmerhaus, *Plant design and economics for chemical engineers*. Journal of Chemical Education, 1958.
- [11] SummitSystems, "DRYPLUS DP160 Rotary Dryer Data Sheet," 2023.
- [12] "Agilent 7890B GC System." [Online]. Available: https://www.agilent.com/en/product/gas-chromatography/gc-systems/7890b-gc-system.
- [13] "Xiamen Simy Equipment Customizable Coating Line Solvent Coater Machine with Oven," 2023. [Online]. Available: https://www.alibaba.com/product-detail/Customizable-Coating-Line-Solvent-Coater-Machine\_1600795313902.html?spm=a2700.galleryofferlist.p\_offer.d\_title.17ca5608lDiV Nu&s=p.